Master's Thesis

Energy Science

Universiteit Utrecht

Modelling Future Investments in the Dutch Electricity Infrastructure

Student	-	Bart Visser
Student no.	-	6593259
Email	-	b.p.visser@students.uu.nl
Supervisor UU	-	Dr. Vinzenz Koning
Supervisors PBL	-	Dr. Paul Koutstaal & Bert Daniels
Date	-	06-04-2020

Planbureau voor de Leefomgeving

ABSTRACT

Electrification of energy demand combined with increased renewable energy generation are key drivers for reducing CO_2 emissions. However, these measures also result in increased strains on the Dutch power grid, leading to substantial infrastructure costs and posing challenges for electrical infrastructure planning. Grid simulation models are becoming increasingly relevant for forecasting grid expansion requirements. However, these models can be very complex, requiring specific expertise and data. For national strategic policy advisory bodies such as PBL Netherlands Environmental Assessment Agency, it is not feasible to build, operate and maintain such complex models. Therefore, this study makes a first step in the development of a simplified grid simulation model. To limit model complexity and data requirements, a nationally aggregated representation of the power grid is used. Power flows are simulated using nationally aggregated load and generation profiles. The power flows are used to determine the required capacity of grid assets for a reference year and a freely configurable future scenario year. This is then translated into capacity expansion requirements and eventually used to calculate infrastructure costs.

The model constructed in this study does express some important features which resemble the behavior expected from the actual power system. However, unrealistic model behavior also occurs resulting from the absence of flexibility options such as energy storage, demand response and curtailment. Furthermore, modelling results are accompanied by large uncertainties, due to unclear effects of self-consumption of decentralized generation and the lack of access to more accurate input data from grid operators. Finally, considerations for future research are presented and the inherent feasibility of the modeling approach is evaluated.

TABLE OF CONTENTS

ABBREVIATIONS

AC	:	alternating current
CHP	:	combined heat and power
COP	:	coefficient of performance
EHV	:	extra high voltage
EV	:	electric vehicle
HV	:	high voltage
LV	:	low voltage
MV	:	medium voltage
IV	:	intermediate voltage
PV	:	photovoltaic
SCOP	:	seasonal coefficient of performance
VA	:	Volt-Ampere
var	:	Volt-Ampere reactive
VRE	:	variable renewable energy

1 INTRODUCTION

To limit the adverse effects of climate change, the Paris agreement calls for a drastic reduction in global CO_2 emissions to keep global temperature rise well under 2˚C (*Paris Agreement*, 2016). In order to meet this goal, the Netherlands has enacted goals of a 49% reduction of CO_2 emissions in 2030 and 95% reduction in 2050 into law (Klimaatwet, 2019). Measures for reaching the emission reduction goals have been put together in the Dutch 'Climate Accord'. These include measures in the electricity, industry, agriculture & land use, built environment and mobility sectors (*Klimaatakkoord*, 2019). According to the Climate Accord, a major driver of decarbonisation throughout these sectors will be the transition from fossil fuel fired power generation towards renewable electricity combined with electrification of energy demand.

The primary sources of future renewable electricity generation are expected to be wind and solar energy. The intermittent nature of weather patterns and the decentralized distribution of wind turbines and photovoltaic (PV) panels pose unique challenges for electrical infrastructure planning. Furthermore, electrification of energy demand (e.g. adoption of heat pumps and electric vehicles) can result in disruptive increases in electricity consumption, also leading to some serious challenges for electrical infrastructure planning (Heres et al., 2017; van Westering et al., 2016, 2016; Veldman et al., 2013). These developments will put significant strains on power grid assets, requiring substantial investments for the reinforcement and expansion of the Dutch power grid (Netbeheer Nederland, 2019b).

The Dutch government plays a major role in guiding this transition by implementing policies and passing new legislation. To make deliberate strategic decisions they must be able to take into account the impacts on the power grid. The PBL Netherlands Environmental Assessment Agency plays an important role in advising the government on such matters. However, PBL currently has limited tools available for calculating the infrastructure costs associated with changes in renewable energy generation and electrification of energy demand.

Tools for forecasting grid expansion requirements of transmission networks often rely on grid simulation modelling (Heres et al., 2017; Medjroubi et al., 2017). Grid simulation modelling focuses on the technical and physical behavior of electrical grids by performing power flow calculations (Medjroubi et al., 2017; Stott, 1974). Power flow calculations require data regarding the network structure, grid assets and consumer and generation behavior in order to be accurately carried out (van Oirsouw, 2012). Traditionally, this approach is only applied to transmission networks and not to distribution networks as the latter are more complex, requiring significantly more data and computational power (Heres et al., 2017; van Westering et al., 2017). Instead, grid expansion planning for distribution networks was done based on assumptions regarding a steady rise in consumer load. However, due the uncertainty and disruptive changes resulting from the advent of decentralized generation and electrification, this method is starting to become increasingly inadequate. At the same time, due to the increasing availability of measurement data and computational power, power flow calculations are also starting to be applied for distribution networks (Heres et al., 2017; Veldman et al., 2013).

While PBL does require insights into the infrastructure costs on a national level associated with changes in renewable energy generation and electrification of energy demand, it does not have the expertise or data to build, operate and maintain a detailed grid simulation model of the entire Dutch power grid. However, a grid simulation model might not necessarily need to perform power flow simulations on the level individual components in order to provide insights on a national level. In several reports carried out on behalf of 'Netbeheer Nederland', national grid simulation models have been developed using highly simplified representations of the power grid, wherein power flow calculations are performed for aggregated classes of consumers and generation (Alfman & Rooijers, 2017; Blom et al., 2012; Rooijers et al., 2014; Rooijers & Leguijt, 2010). However, these reports are carried out by consultancy firms and do not strictly adhere to the scientific method. The description of the model structure is often limited, little transparency is provided regarding data input and the models are not always properly validated.

The aim of this study is to lay the foundation for the development of a simplified grid simulation model. Unlike the aforementioned reports which did not strictly adhere to the scientific method, this study will provide transparency regarding the model structure and validity as well as the input data. The purpose of this model is to provide forecasts

regarding the Dutch infrastructure costs associated with changes in renewable energy generation and electrification of energy demand. Due to the magnitude of this task it is not realistic to expect a fully finished model from this study, but rather a first step in its development. This entails development of the basic model structure, consisting of two main components; representation of the power grid structure, and the representation of load and generation connected to the power grid. The value in this is twofold. First, the uncertainties introduced by different structural and data-related modelling aspects can be charted, providing guidance for future improvements. Secondly, critical insights into the usefulness of the chosen modelling approach can be obtained.

The core purpose of the grid simulation model is to forecast required infrastructure investments for the Dutch power grid. The complexity involved in such a broad task requires clear boundaries to be drawn up, since this study will only make a first step in its development. First of all, while power generation and demand may change in myriad ways, this study only focuses on a selection of these. For power generation, only increases in wind turbines and PV panels are considered, and for demand only the adoption of electric vehicles and residential heat pumps are included. Secondly, the goal of this study is not to make predictions on how generation and demand will change, but rather how the power grid is affected if they change. In other words, the goal is not to perform a scenario analysis, but rather to develop a model that is able to perform scenario analyses. Thirdly, even though traditional infrastructure planning mainly concerns the reinforcement and expansion of grid assets, new developments regarding demand response, storage and curtailment are becoming increasingly relevant for reducing infrastructure investments and equalizing supply and demand (Esmat et al., 2018). However, these developments are not included in this study. Instead, the balance between supply and demand will be maintained through import and export. Finally, the financial consequences of infrastructure investments are not always evident. They are affected by the timing of the investment due to the time value of money, but also due to amortization of existing infrastructure and their expected end-of-life replacements. However, this study will only focus on the absolute, non-discounted investment costs.

In chapter 2, contextual information for the development of the grid simulation model is provided, consisting of relevant information regarding the power grid structure, power generation, consumer load and infrastructure planning. Then, the structure of the grid simulation model is expanded upon in chapter 3. In chapter 4, the model is validated, providing insights into the accuracy and uncertainties of the model. Then, the results are reflected upon in chapter 5 and the findings of the study are summarized in chapter 6.

2 THEORETICAL BACKGROUND

This chapter provides contextual information of the Dutch power grid. Due to the broadness of this subject, only information relevant for the development of the national grid simulation model is addressed. In section 2.1, the main structural aspects of the Dutch power grid is expanded upon. Furthermore, section 2.2 lists the different consumers and producers of electrical power. Finally, some practical information regarding infrastructure planning is described in section 2.3.

2.1 Power grid structure

Alike most power grids, the Dutch power grid has been designed to accommodate centralized power production. The first public generator of electrical power in the Netherlands was built in 1886. Since then, it has been developed and expanded by many distribution companies, resulting in varying grid structures and voltage levels across different regions within the Netherlands. After many mergers and efforts towards standardization, this regional variability has decreased considerably but some of its traces still remain today (van Oirsouw, 2012).

The Dutch power grid consists of a transmission and a distribution network. Conventionally, power is transported from the centralized generators over long distances using the transmission network. In the late 20th century an interconnection network has been added for the purpose of interconnecting large power plants and for cross-border interconnections. After being transported through the transmission network, power is delivered to consumers using regional and local distribution networks (van Oirsouw, 2012). Lately, a significant amount of decentralized generation capacity is being added to the power grid in the form of variable renewable energy (VRE) generation such as wind turbines and PV systems. In Figure 2.1, a schematic representation of the Dutch power grid is shown.

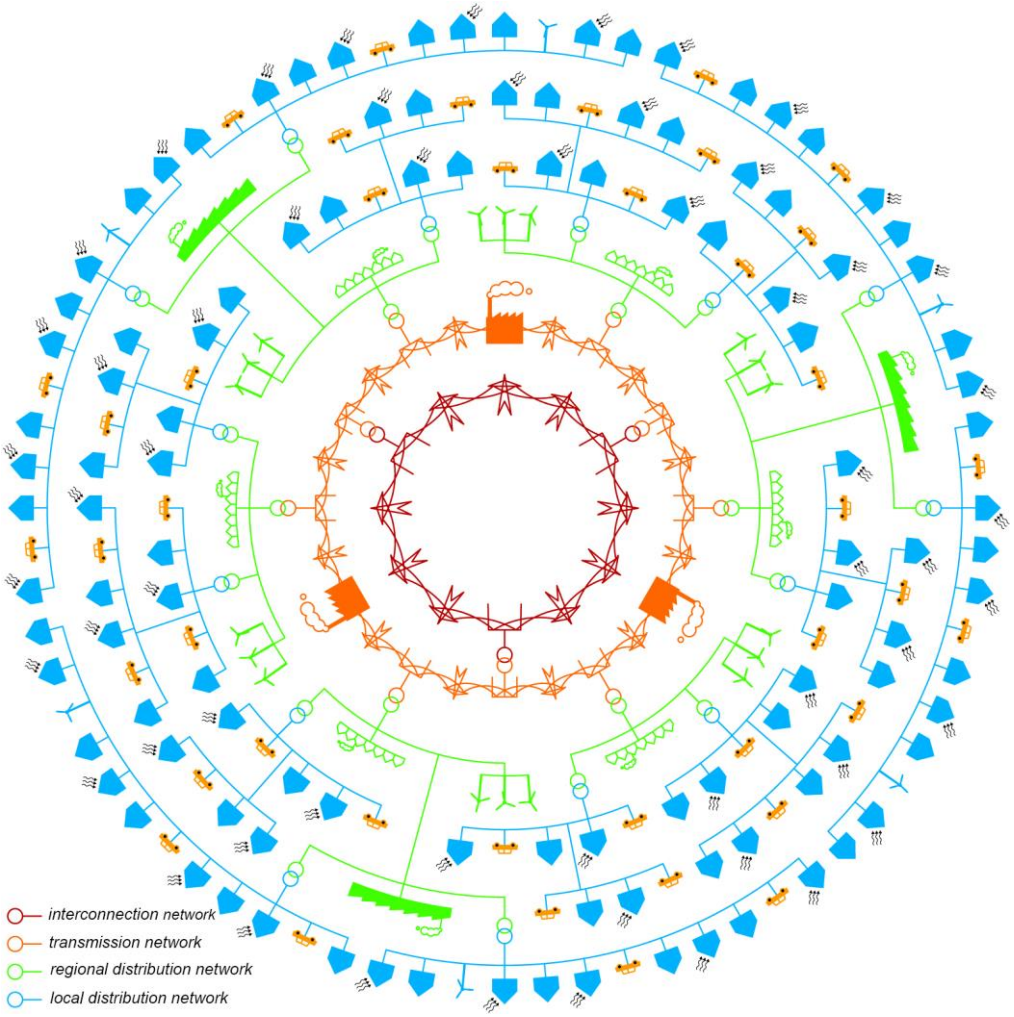

Figure 2.1: Schematic representation of the Dutch power grid (van Oirsouw, 2012)

The Dutch power grid consists of multiple voltage levels. The interconnection grid uses extra high voltage (EHV) to minimize electrical losses. Then, the voltage level is reduced in a stepwise manner to high voltage (HV), intermediate voltage (IV), medium voltage (MV) and low voltage (LV). Transformers are used to achieve these shifts in voltage levels. In Figure 2.2, an overview is provided of all voltage levels commonly occurring within the Dutch power grid. The overlapping circles represent the transformer steps in between the voltage levels.

In order to reduce the probability of a power outage, the Dutch power grid has a high degree of redundancy. There are two types of redundancy within the power grid, the first being a single fault reserve without energy interruption. This implies that for each single component malfunction, a back-up component is available to take over its function without loss of power. This requires a reserve component installed in parallel for each component,. The second type of redundancy is single fault reserve with energy interruption. This implies that for each single component malfunction, power can be rerouted automatically or manually through different components. This does not require backup components to be installed in parallel, but does lead to a brief loss of power.

In section 2.1.1 characteristics of the transformers used between each of the voltage level will be described. Then, in sections 2.1.2 to 2.1.6, a closer look will be taken at each voltage level including the types of redundancies present at each voltage level. Finally, relevant characteristics of electrical power flow are addressed in section 2.1.7.

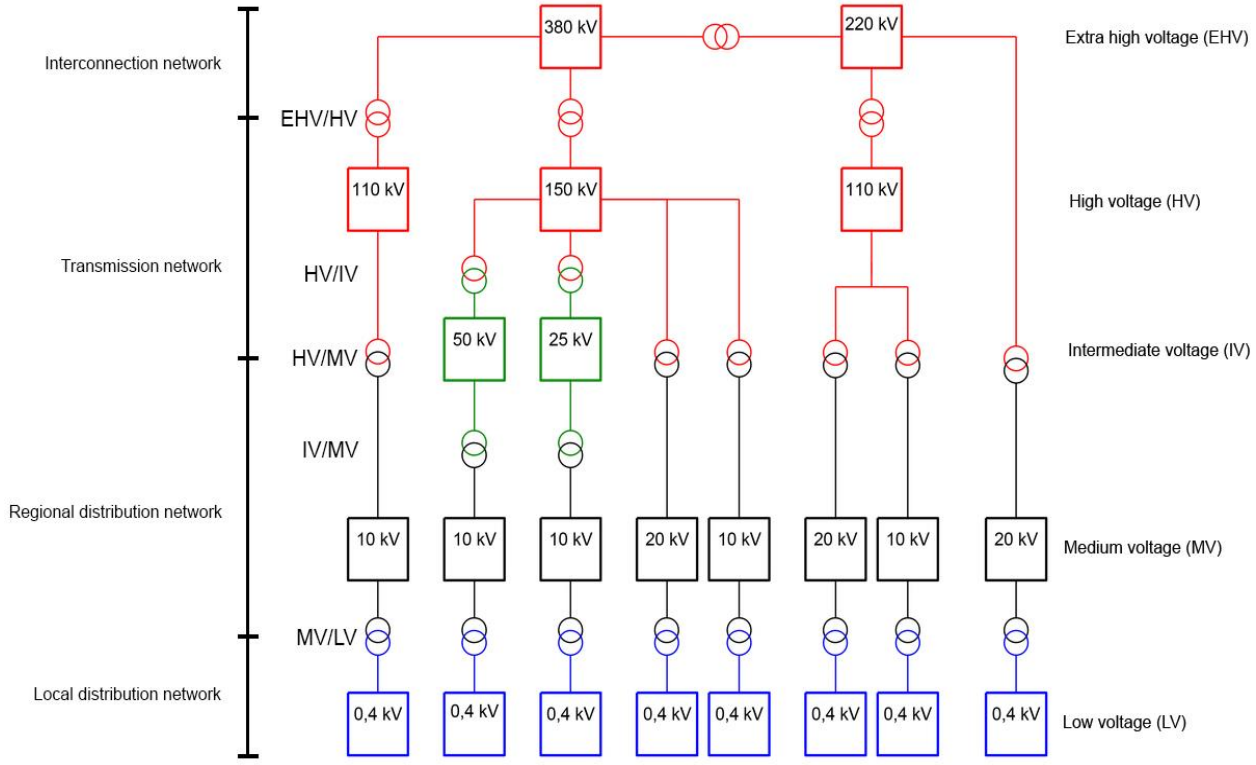

Figure 2.2: Line-to-line voltage levels, network layout and transformer steps within the Dutch power grid (van Oirsouw, 2012)

2.1.1 Transformers

Transformers are used throughout the power grid to transform power from one voltage level to another. All different types of transformers are listed in Figure 2.2. Each side of a transformers is connected to a busbar (a high and low voltage side). These busbars connect in and out going power cables to the transformer. Transformers between the interconnection, transmission and regional distribution networks are called substations. They are of substantial size requiring the space equivalent of several football fields. They contain sufficient redundant components to ensure single fault reserve without energy interruption (van Oirsouw, 2012). The distribution of substations is shown in Figure 2.3. A simplified illustration of a HV/MV substation is shown in Figure 2.5. Transformers between the regional and local distribution networks are called distribution transformers. They are much smaller and fit within a metal casing and are not equipped with redundant components and therefore have no fault reserve (van Oirsouw, 2012). In urban areas, each town district has several distribution transformers (Netbeheer Nederland, 2019a).

Figure 2.3: The Dutch (extra) high voltage grid (380, 220, 150 & 110 kV) (TenneT, 2018)

2.1.2 Extra high voltage (EHV)

EHV cables constitute the interconnection network and use voltages of 220 or 380 kV. Practically all EHV cables run above ground using large electricity pylons. The interconnection network forms the main spine of the Dutch power grid as it connects large power plants and EHV/HV substations and is used for cross-border interconnections. Because outages in the interconnection network are unacceptable due to their critical function in the power grid, EHV cables are installed with single fault reserve without energy interruption. This requires every cable and pylon to be constructed twofold (van Oirsouw, 2012). The layout of EHV cables in the Netherlands is displayed in Figure 2.3.

2.1.3 High voltage (HV)

HV cables constitute the transmission network and use voltages of 110 and 150 kV. The majority of HV cables run above ground alike the EHV cables. However, in some densely populated areas the HV cables run underground. The transmission network accommodates power transmission at a provincial level and acts as a link between the interconnection and regional distribution network. It connects HV/MV and HV/IV substations and medium sized centralized power plants as well as large industrial consumers. Alike EHV cables, HV lines are also installed with single fault reserve without energy interruption, requiring every cable and pylon to be constructed twofold (van Oirsouw, 2012). The layout of HV cables in the Netherlands is displayed in Figure 2.3.

2.1.4 Intermediate voltage (IV)

Similar to the HV cables, IV cables serve a transmission function and use voltages of 25 and 50 kV. Unlike EHV and HV cables, all IV cables run underground. They are used only in a certain part of the Dutch power grid (Figure 2.4) and are not formally part of either the transmission nor the regional distribution networks. The IV network acts as the link between these networks and connects IV/MV substations, medium sized centralized power plants and large industrial consumers (van Oirsouw, 2012).

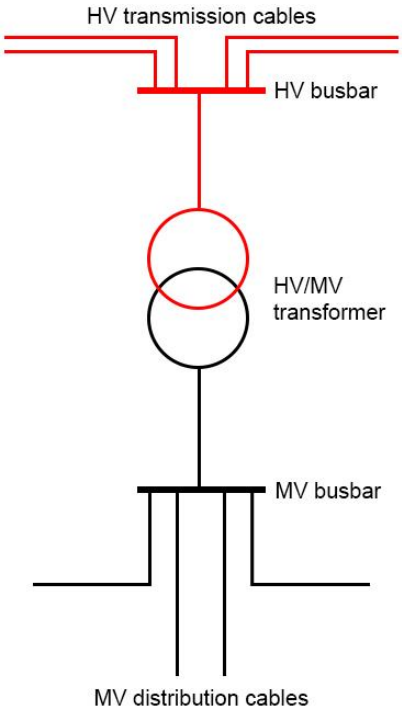

Figure 2.5: Simplified illustration of a HV/MV substation

Figure 2.4: The Dutch intermediate voltage grid (50 kV) (Hoogspanningsnet.com, n.d.)

2.1.5 Medium voltage (MV)

MV cables constitute the regional distribution networks and mainly use voltages of 10 kV. However, in some cases 20 kV cables are used instead. Practically all MV cables run underground. The regional distribution networks acts as a link between the transmission and the local distribution networks. They connect substations, distribution transformers, large decentralized generation units as well as large consumers.

The MV cables within the regional distribution networks can have a radial, annular, or meshed design (van Oirsouw, 2012). Radial designs of regional distribution networks are most straightforward. Cables run in all directions from the substation. If a cable were to fail, there is no way of restoring power without repair work. Therefore, these networks have no fault reserves. These networks are used in rural areas where consumers are relatively far apart (van Oirsouw, 2012). Instead of radial designs, most regional distribution networks have an annular design. The MV lines are structured such that the ending of each line is connected with the ending of another MV line. However, these

lines are separated with a circuit breaker. If a MV cable were to fail anywhere in a ring, proper functioning of the ring can be restored quickly by connecting the ending of the faulty line with another cable using the circuit breaker. This is a single fault reserve with energy interruption, as a short outage occurs before the power flow is switched (van Oirsouw, 2012). Some regional distribution networks have a meshed design. In these networks, the ends of cables coming from one or two different substations meet and are separated with a circuit breaker. In case of a faulty cable, power can be redirected through several other cables, increasing the robustness of the system. Using these networks can be beneficial in regions with industrial activity or large cities. Similarly to the annular networks, meshed networks have single fault reserves with energy interruption (van Oirsouw, 2012). Figure 2.6 shows a schematic illustration of each structure type of the regional distribution network. Some regional distribution networks also contain MV cables with a transmission- instead of a distribution- function (Figure 2.7). The transmission cables are used as an alternative to higher voltage transmission but is not used everywhere (van Oirsouw, 2012).

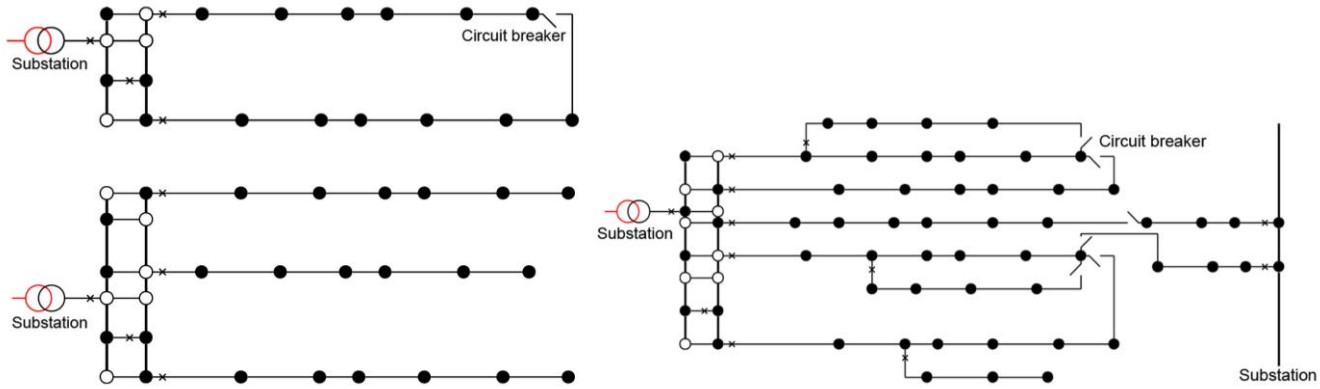

Figure 2.6: Annular (top left), radial (bottom left) and meshed (right) MV distribution network structures (van Oirsouw, 2012)

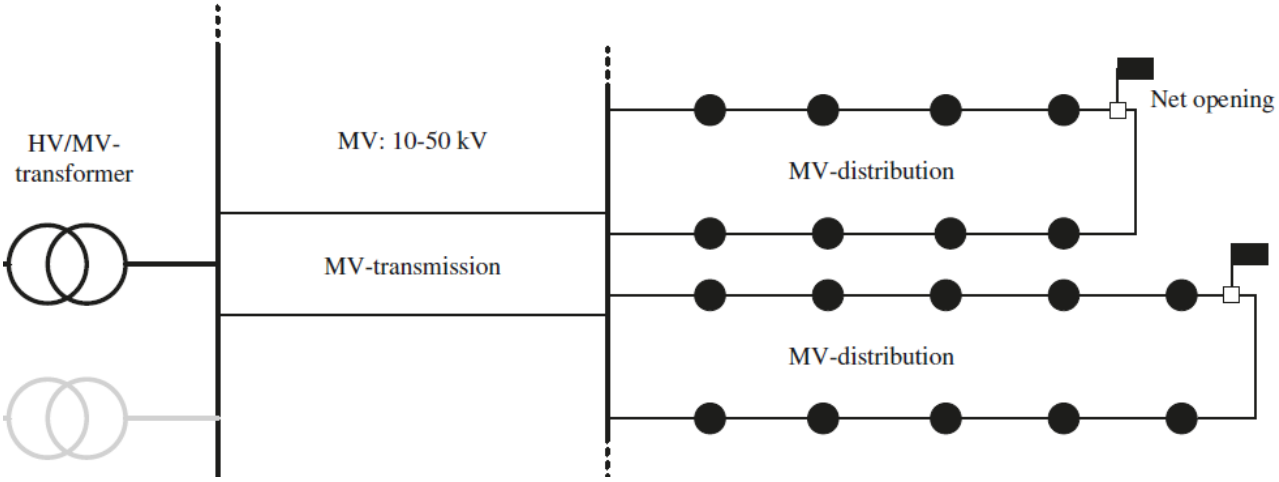

Figure 2.7: MV transmission cables within the regional distribution network (Veldman et al. 2013)

2.1.6 Low voltage (LV)

LV cables constitute the local distribution network and use a voltage of 400 V. All LV cables run underground. The local distribution network connects households and other small consumers of electricity. These networks often have a radial structure. Cables are connected to one distribution transformer and run outward in all directions without interconnecting with other LV cables. Therefore, there is no fault reserve as there is no way to reroute power when an LV cable fails (van Oirsouw, 2012). In some older urban areas, local distribution networks have a meshed structure instead of a radial structure. LV cables are sometimes connected to two distribution transformers. These networks perform better regarding voltage management and electrical losses, but experience higher short-current voltages in case of an outage. This is, among other things, the reason that new networks are built using radial structures (van Oirsouw, 2012). Figure 2.8 shows a schematic illustration of a radial and a meshed local distribution network.

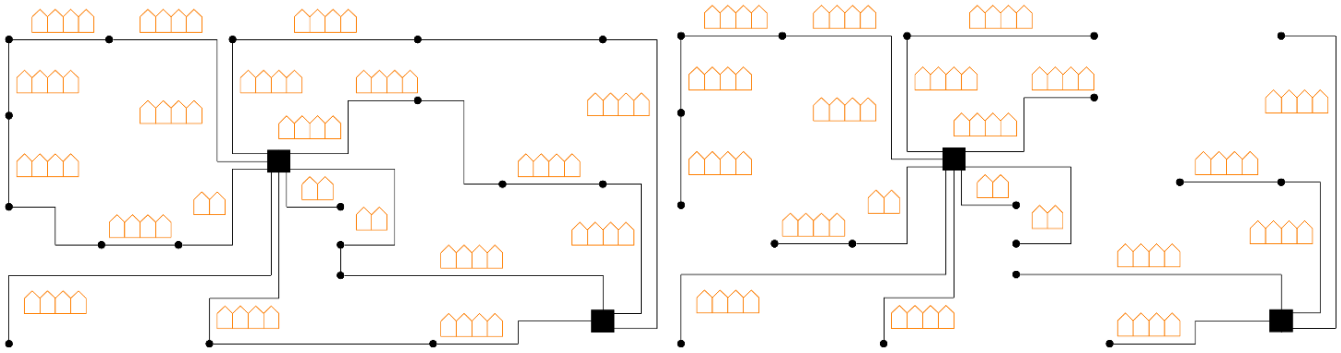

Figure 2.8: Radial (left) and meshed (right) local distribution network structures. The black squares represent distribution transformers (van Oirsouw, 2012)

2.1.7 Three-phase alternating current

The Dutch power system is a balanced three-phase alternating current (AC) system. In a balanced three-phased system, the sinusoidal voltages are shifted in phase by 120 degrees. Consequently, the line-to-neutral voltage of each voltage level is equal to the line-to-line voltage, listed in Figure 2.2, divided by √3 (Schavemaker & Van der Sluis, 2017). For example, LV cables have a 400V line-to-line voltage and therefore a 230V line-to-neutral voltage. Furthermore, in AC systems both the current and voltage alternate. The relation between current and voltage is affected by the impedance of devices in the electrical circuit. Impedance can be described as the amount of opposition resulting from a change in current or voltage, and comprises of resistance and reactance. Increased resistance leads to a decrease in current in a circuit while increased reactance leads to a phase change of the current relative to the voltage (Schavemaker & Van der Sluis, 2017).

Resistance actively dissipates electric power in Watts, called active power. Reactance changes the phase angle (Φ) between the current and the voltage, leading to less available active power without actually dissipating active power. This results in increased reactive power measured in Volt-Ampere reactive (var). The total load on grid assets is the combination of active and reactive power, called apparent power and is measured in Volt-Ampere (VA). The relation between phase angle Φ, real, reactive and- apparent power is visualized in Figure 2.9. The ratio of real power dissipated by a load and apparent power flowing through the circuit is called the power factor, and is expressed as cos(Φ) based on trigonometric identities (Schavemaker & Van der Sluis, 2017). A high power factor is often desirable as less grid asset capacity is required per unit of transported active power (van Oirsouw, 2012). Dutch regulation dictates that the power factor of electrical load must at least 0.85 (Tarievencode Elektriciteit, 2016). To increase the power factor, the reactance of an electrical load must be reduced. In practice, this often requires correction with a capacitor of the appropriate size (van Oirsouw, 2012).

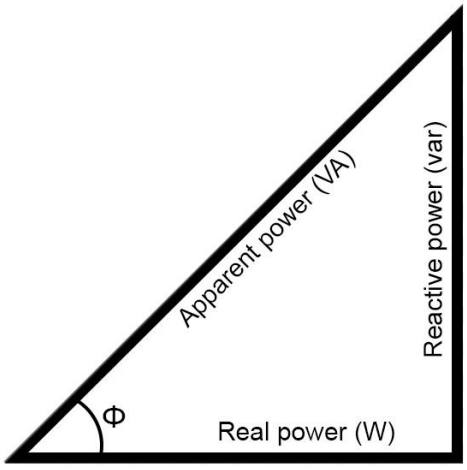

Figure 2.9: Relationship between real power, reactive power, apparent power and phase angle Φ

2.2 Grid connections

The previous section described the structure of the power grid and how the interconnection, transmission, regional distribution network and local distribution network transport and distribute power. This section will expand upon consumers (section 2.2.1) and producers (section 2.2.2) of electricity and the manner in which they are connected to the grid. A connection between a consumer or producer with the power grid will be referred to as a 'grid connection'. Grid connections are standardized and the way that producers and consumers must be connected to the grid is laid down in law (Tarievencode Elektriciteit, 2016). This law distinguishes between six types of grid connections. These are listed in Table 2.1, along with their points of connection to the power grid. Further explanation is given below.

Table 2.1: Grid connection categories and their point of connection to the power grid

Category	Connection
≤1x 6A	LV cable
>3 x 25A and ≤60 kVA	LV cable
>60 kVA and ≤300 kVA	MV/LV transformer
>0.3 MVA and ≤3 MVA	MV cable
>3 MVA and ≤10 MVA	HV/MV transformer
>10 MVA	HV/MV transformer (<100 MVA)
	HV network (>100 MVA)

≤1x 6A

Grid connections up to 1x 6 Ampere (A) are connected to an LV cable in the local distribution network (Netcode Elektriciteit, 2016). LV cables have a 400V line-to-line voltage (Figure 2.2), and thus 230V line-to-neutral voltage. Consequently, the maximum capacity of an 1x 6A connection is 1.38 kVA.

>3 x 25A and ≤60 kVA

Similar to the 1x 6A connection, grid connections from 3 x 25A up to 60 kVA are connected to an LV cable in the local distribution network. A 3 x 25A connection has a capacity of 17.25 kVA. However, connections in this category can have lower capacity by only using one of the three phases. For example, one could choose a 1 x 25A connection with a capacity of 5.75 kVA (Tarievencode Elektriciteit, 2016).

>60 kVA and ≤300 kVA

Grid connections from 60 kVA up to 300 kVA are connected directly to the busbar at the LV side of the nearest MV/LV distribution transformer using an LV cable (Tarievencode Elektriciteit, 2016).

>0.3 MVA and ≤3 MVA

Grid connections from 0.3 MVA (or 300 kVA) up to 3 MVA are connected to the regional distribution network by lacing it into the closest MVA cable (Tarievencode Elektriciteit, 2016).

>3 MVA and ≤10 MVA

The standard method for grid connections from 3 MVA up to 10 MVA is to connect them to the MV busbar of a HV/MV or IV/MV substation using two MV connection cables. This provides the grid connection with single fault reserve without energy interruption (Tarievencode Elektriciteit, 2016).

>10 MVA

Grid connections larger than 10 MVA require a custom approach, in which connection is made at the closest point in the grid with sufficient available capacity (Tarievencode Elektriciteit, 2016). In practice, grid connections up to 100 MVA are often connected to a substation of either the regional distribution network or the IV network (TenneT, 2019). Grid connections larger than 100 MVA and up to 500 MVA are normally connected to the HV transmission network and connections larger than 500 MVA are to the EHV interconnection network (van Oirsouw, 2012).

2.2.1 Power consumption

In 2018, 388.7 PJ of electrical energy was consumed in the Netherlands[1] (CBS, 2020a). This is the sum of all electricity consumption by Dutch industry, the service sector, agriculture, households and transport.

Industry

A wide range of different industries are active in the Netherlands, such as the chemical, steel and food industry. An overview of all industrial sectors and their respective electricity consumption is listed in appendix A1. The sum of all industrial electricity consumption was 129.1 PJ in 2018, which is 33% of the national consumption (CBS, 2020a). Industrial electricity consumption is expected to rise in the coming decades as a result of plans to electrify total energy consumption in a way to reduce CO_2 emissions (*Klimaatakkoord*, 2019). Industrial companies range from small businesses to large scale industrial complexes. Even though industrial activity is widely spread across the Netherlands, five main industrial clusters are responsible for a large share of the total industrial electricity consumption. These clusters consist mainly of heavy process industries such as chemical, steel and food industries (van der Linden, 2019). The locations of the industrial clusters are shown in Figure 2.10. Industrial consumers requiring grid connections larger than 100 MVA are connected directly to the HV transmission network. Connections smaller than 100 MVA are connected to a substation of either the regional distribution network or the IV network (TenneT, 2019).

Service sector

The service sector is very diverse, ranging from education and healthcare to hospitality and financial services. An overview listing each service category and their respective electricity consumption is given in appendix A1. The total electricity consumption of the Dutch service sector was 133.2 PJ in 2018, which is 34% of the national consumption (CBS, 2020a). The types of grid connections among electricity consumers in the service sector varies considerably. For instance, a small hairdresser may only need a 1 x 25A grid connection connected to an LV cable of the local distribution network, while a large University campus may need a grid connection larger than 10 MVA that is connected directly to a substation of the regional distribution network.

Agriculture

Dutch agriculture can roughly be divided into arable farming, livestock farming and (greenhouse) horticulture. The total electricity consumption of Dutch agriculture was 35.7 PJ in 2018, which is 9.2% of the national consumption (CBS, 2020a). Only a small part of this electricity consumption is due to arable farming, livestock farming and non-greenhouse horticulture (CBS, 2015). The majority is used for lighting in greenhouse-horticulture (van der Velden & Smit, 2013). The electricity demand by greenhouse-horticulture is expected to rise in the coming decades as a result of plans to electrify heat demand in a way to reduce CO_2 emissions (*Klimaatakkoord*, 2019). The distribution of greenhouses throughout the Netherlands is illustrated in Figure 2.11. For smaller greenhouses, a grid connection from 0.3 up to 3 MVA can be sufficient, directly laced in to a MV cable of the regional distribution network. However, large greenhouses may need larger grid connections up to tens of MVAs connected to a substation of either the regional distribution network or the IV network (Alfen, n.d.).

Households

The total electricity consumption of Dutch households was 82.7 PJ in 2018, which is 21% of the national consumption (CBS, 2020a). For virtually all houses a 3 x 25A grid connection provides sufficient capacity. All newly built houses come with this type of grid connection. However, the majority of existing houses use only one of three phases (1 x 25A or 1 x 35A) (Liander, 2018). The electricity demand by households is expected to rise significantly in the coming decades resulting from the adoption of heat pumps and EVs (*Klimaatakkoord*, 2019). EVs are addressed in the transport sector.

[1] This is the final consumption of electricity, excluding electricity consumption of the power sector and losses.

Figure 2.10: Locations of the five Dutch industrial clusters (Netbeheer Nederland, 2019)

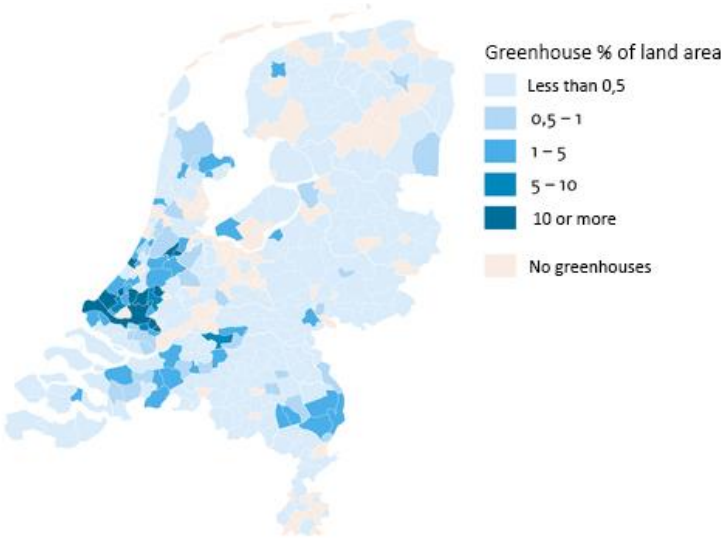

Figure 2.11: Distribution of greenhouse horticulture in 2015 (CBS, 2016)

Residential heat pumps extract heat from exterior sources such as the ground, water, or air, and transfer it to the inside. Heat pump efficiency is generally referred to as the coefficient of performance (COP) as it is higher than one (Blok & Nieuwlaar, 2016). The average COP throughout the heating season is referred to as the seasonal coefficient of performance (SCOP).

Transport

Following the segmentation of the annual energy consumption data by CBS (2020a), electricity consumption of transport includes only transport on public roads and railway. Total electricity consumption of Dutch transport was 7.6 PJ in 2018, which is 2% of the national consumption (CBS, 2020a). For rail traffic, power is supplied through MV cables of the regional distribution network.

The majority of electricity used for transport is currently used by rail traffic, while only a limited amount is used by road traffic. However, the electricity demand for road traffic is expected to rise as the number of electric vehicles is expected grow in the coming decades in order to reduce CO_2 emissions (*Klimaatakkoord*, 2019). For EVs, the type of grid connection depends on the type and location of the charging points. The Dutch EV charging infrastructure can be divided into four categories: private, public, semi-public and fast charging (Hoen et al., 2017). Private chargers are often located at households. Public chargers are places at freely accessible parking lots. Semi-public chargers are located at e.g. offices or parking garages and are not accessible 24 hours a day. Fast chargers are mostly located next to the highways (Hoen et al., 2017).

2.2.2 Power generation

To keep the power system in balance, demand must be met at all times. This is done by various types of power generators. In this study, power generation capacity is divided into four different categories: conventional power plants, decentralized combined heat and power, wind turbines, and photovoltaics.

Conventional power plants

Conventional power plants provide the majority of electrical power in the Netherlands and include gas, coal, nuclear, biomass and waste fired power plants. The installed capacity in 2018 is shown in Table 2.3. Very large conventional power plants (>500 MVA) are connected to the EHV interconnection network, while smaller power plants (<500 MVA) are connected to the HV transmission network (van Oirsouw, 2012). Starting in 2030, the Dutch government will prohibit coal fired power generation (Wet Verbod Op Kolen Bij Elektriciteitsproductie, 2019). Furthermore, the installed capacity of gas fired generation also includes decentralized combined heat and power (CHP) generators operated and used directly by consumers (CBS, 2019c). The next section will go into further detail regarding CHP generation.

Table 2.3: Installed capacity per production type in the Netherlands in 2018 (ENTSO-E, 2020)

Type	Installed capacity [GW]
Gas	18.43
Coal	4.64
Nuclear	0.49
Biomass	0.49
Waste	0.79
Wind Onshore	3.68
Wind Offshore	0.96
Photovoltaics (PV)	4.14*

*ENTSO-E includes only units larger than 1 MW. Since PV systems are often smaller, CBS data is used (CBS, 2019b)

Decentralized combined heat and power (CHP)

CHP is the cogeneration of both electric power and heat. CHP generators are used since the cogeneration of electric power and heat often requires less primary energy, produces less CO_2 emissions, and is cheaper than producing power and heat separately (Blok & Nieuwlaar, 2016). Total electrical CHP capacity in the Netherlands was 11.60 GW in 2017. CHP capacity used by energy companies for centralized power generation amounts to 4.36 GW and that of waste fired power plants amount to 0.75 GW. The remaining 6.49 GW of CHP capacity is operated and used by energy consumers (partly) for their own demand (CBS, 2019c). In this study, the latter will be addressed as decentralized CHP. The distribution of decentralized CHP capacity among consumers is listed in Table 2.2.

Table 2.2: Decentralized installed CHP capacity in the Netherlands in 2017 (CBS, 2019a)

Consumer category	Installed CHP capacity [GW]
Refineries and mining	0.29
Chemical industry	2.74
Food and stimulants industry	0.34
Paper industry	0.31
Other industries	0.12
Agriculture	2.75
Healthcare and other sectors	0.71

Due to the design of CHP generators, production of heat is linked with the production of power and vice versa. Consequently, a CHP must also generate power if there is a demand for heat (or industrial steam). These units are called ‘must-run’. However, CHP units can be made more flexible in their power generation by adding heat storage, alternative heat production (e.g. boilers), or in some cases by bypassing the turbines altogether (Danish Energy Agency, 2015).

Wind turbines

Wind turbines produce electrical power by extracting energy from wind and converting it to electricity. Dutch wind turbine generation capacity is expanded in an effort to reduce the CO_2 intensity of electricity production (*Klimaatakkoord*, 2019). Wind turbines are installed both onshore and offshore. They are often installed in proximity of other turbines, forming wind parks. In the Netherlands, onshore wind parks comprise of anywhere from a few to over a hundred wind turbines (Energiekaart, n.d.). The current generation of onshore wind turbines have capacities of more than 3 MW (Wind Europe, 2020). Wind parks or single turbines smaller than 3 MW are directly laced into an MV cable of the regional distribution network. However, the large majority of wind turbines or wind parks currently installed in the Netherlands are larger than 3 MW (RVO, 2020a). Wind parks up to 100 MW are connected to a substation of either the regional distribution network or the IV network, while larger wind parks (>100 MW) are connected to the transmission network. The distribution of onshore wind turbines is shown in Figure 2.12.

In 2018, the installed capacity of onshore and offshore wind turbines was 3.69 and 0.96 GW respectively (ENTSO-E, n.d.). 1.83 GW of onshore wind capacity comprises of wind parks larger than 100 MW (Energiekaart, n.d.). Furthermore, Figure 2.13 shows the existing and planned offshore wind parks. In 2030, there will be approximately 11 GW of offshore wind capacity (Rijksoverheid, n.d.). Most of the (future) offshore wind parks have capacities

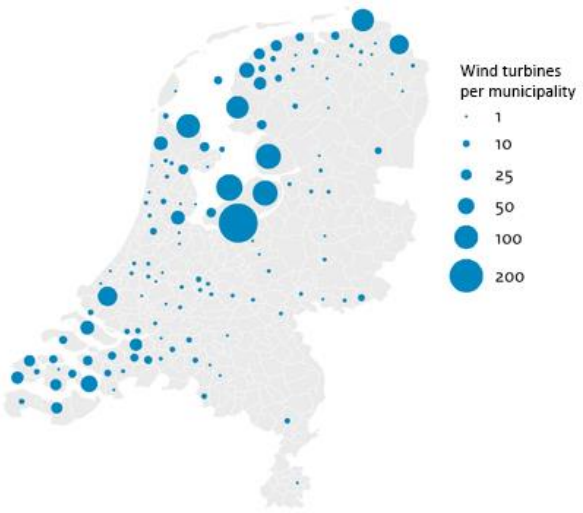

Figure 2.12: Distribution of onshore wind turbines across the Netherlands in 2017 (Windstats, 2018)

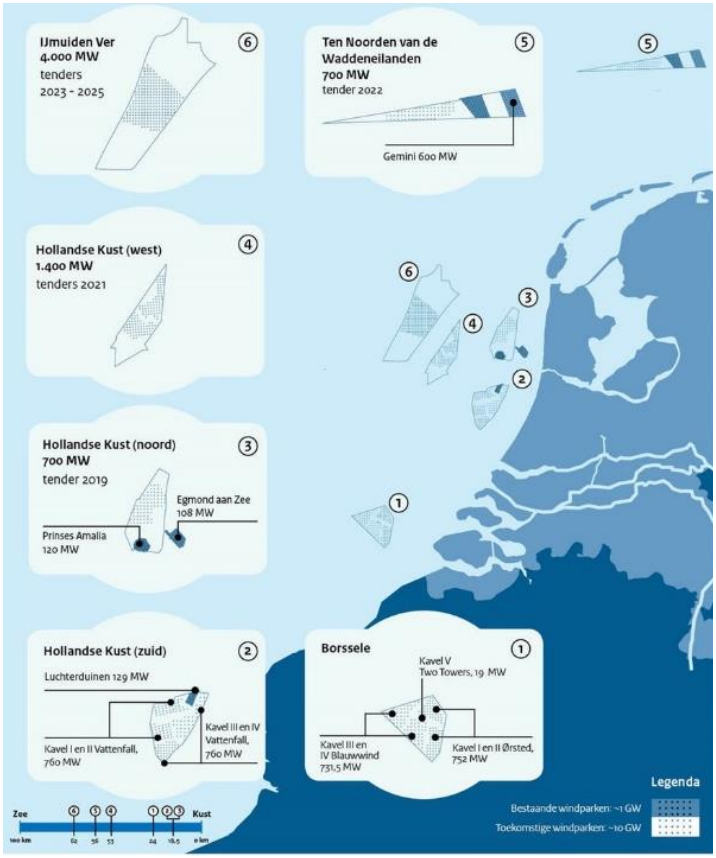

Figure 2.13: Existing and planned offshore wind parks (Rijksoverheid, n.d.)

Figure 2.14: Schematic illustration of a grid connection for an offshore wind park (Noordzeeloket, n.d.)

larger than >500 MW and are connected to the interconnection network via marine EHV cables (TenneT, n.d.-a). A schematic illustration of such a grid connection is shown in Figure 2.14. Grid connections for offshore wind parks are fully subsidized by the Dutch government (Ministerie van Economische Zaken, 2014).

Photovoltaics (PV)

PV panels generate electrical power by converting solar irradiation into electricity. Alike wind turbines, PV generation capacity is also expanded in an effort to reduce the CO_2 intensity of electricity production (*Klimaatakkoord*, 2019). In 2018, the installed PV capacity in the Netherlands was 4.14 GW, of which 2.31 GW installed on roofs of residential houses, 1.66 GW installed on roofs of buildings from the service and industrial sectors, and 0.44 GW installed as ground bound PV parks (CBS, 2019b). Figure 2.15 the distribution of PV systems larger than 1 MW and Figure 2.16 shows the distribution of residential rooftop PV.

Although roof mounted PV panels often use the grid connection of the building they are mounted on, some businesses prefer a separate grid connection for regulatory and economic considerations. In these cases, the roof mounted PV

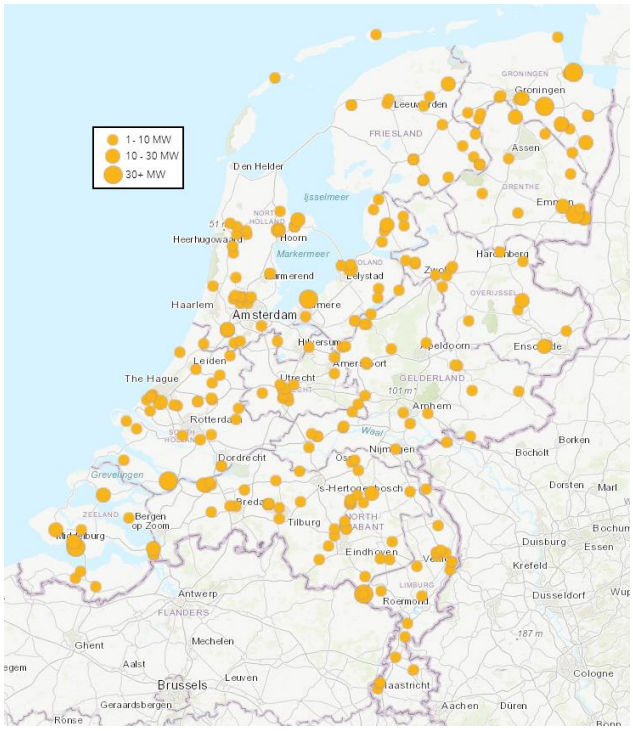

Figure 2.15: Distribution of PV installations larger than 1 MW in January 2020 (RVO, 2020b)

Figure 2.16: Distribution of residential rooftop PV panels in December 2017 (CBS, n.d.)

system can be laced directly into the MV cable of the regional distribution network as they are rarely larger than 3 MW (RVO, 2020a). Ground bound PV parks are mostly larger than 3 MW but smaller than 100 MW (RVO, 2020a). Therefore, they are connected to a substation of either the regional distribution network or the IV network.

2.3 Infrastructure planning

The Dutch power grid is owned and operated by grid operators. Grid operators manage the physical grid infrastructure and facilitate the energy market. However, they are not permitted to participate in the energy market themselves (Elektriciteitswet, 1998; Nadere Regels Omtrent Een Onafhankelijk Netbeheer, 2006). The transmission and interconnection networks are owned and operated by one transmission system operator and since 1998, this has been the responsibility of TenneT (Elektriciteitswet, 1998; TenneT, n.d.-b). TenneT also owns and operates the offshore

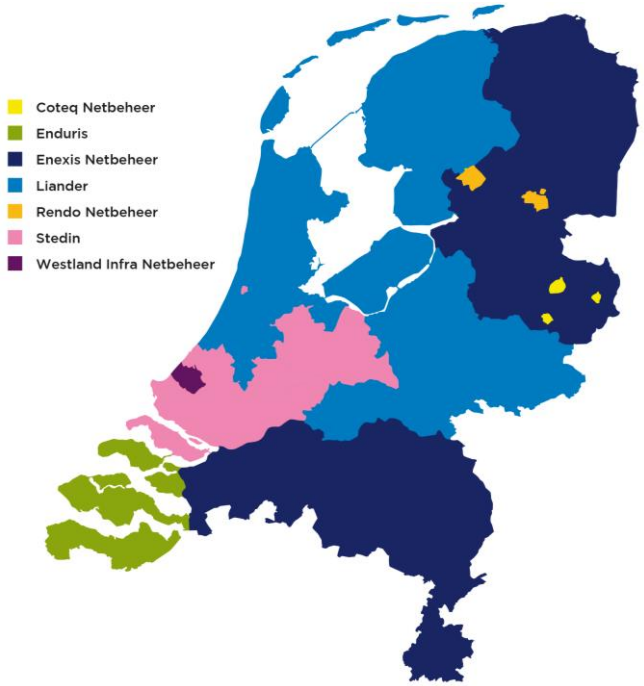

Figure 2.17: Operating areas of each distribution system operator in the Netherlands (Netbeheer Nederland, 2019a)

power grid required for connecting offshore wind parks (Tijdig Realiseren Doelstellingen Energieakkoord, 2016). Distribution networks are owned and operated by independent distribution system operators (Nadere Regels Omtrent Een Onafhankelijk Netbeheer, 2006). An overview of the different distribution system operators and their operating areas is shown in Figure 2.17.

For grid operators, managing the physical grid infrastructure requires them to install, repair, renew and expand grid assets in order to provide security of supply (Elektriciteitswet, 1998). Whether or not to expand grid assets depends on multiple factors. First, it depends on the expected electrical loads on the power grid several decades into the future, as many grid assets have lifetimes of at least 40 years. Furthermore, considerations regarding reserve capacity need to be taken into account (Elektriciteitswet, 1998; van de Sande et al., 2017). These subjects will be addressed in sections 2.3.1 and 2.3.2 respectively.

2.3.1 Electrical loads

Electrical load on the power grid refers to the current flowing through grid assets, such as cables and transformers. These assets have maximum rated capacities regarding the magnitude of current they can withstand without getting damaged due to overheating (Alvarez et al., 2019; van Oirsouw, 2012). For infrastructure planning, the most important aspect of electrical loads are moments of peak loads (Gasunie & TenneT, 2019; van de Sande et al., 2017; van Oirsouw, 2012). The grid infrastructure must be dimensioned such that the rated capacity of grid assets are, at minimum, equal to the peak loads they will be subjected to. Therefore, it is essential for effective infrastructure planning to anticipate on future changes in peak loads on grid assets (van Westering et al., 2016).

2.3.2 Reserve capacity

The term ‘reserve capacity’ describes the surplus of capacity among grid assets on top of the minimum capacity required to accommodate peak loads. For instance, if the capacity of all grid assets are exactly the same as the peak load on each grid asset, grid utilization would be 100% and the reserve capacity would be 0%. From an economic efficiency standpoint this would be desirable. However, this would make it impossible to accommodate new grid connections or a rise in electrical load without grid expansion work. For making the power grid accessible and to enable a free energy market, grid operators are required by law to have sufficient reserve capacity (Elektriciteitswet, 1998). However, grid operators must also work efficiently, without making unnecessary investments (Elektriciteitswet, 1998). Consequently, grid operators must strike a balance between reserve capacity and economic efficiency. Since the liberalization of the energy markets, grid operators are strictly regulated and inspected. This has led to a pressure for increasing economic efficiency. This increase was achieved in part by increasing the utilization of grid assets and thereby reducing reserve capacity (Algemene energieraad, 2009).

3 MODEL STRUCTURE

To achieve the research aim of this study, a grid simulation model is developed that can calculate the national grid expansion costs required for accommodating changes in electrical loads on the power grid, resulting from electrification of energy demand and increasing wind and PV generation capacity. This chapter will provide a detailed description of this model.

For calculating grid expansion costs, the model assesses changes in peak loads between a reference year and a future scenario year. For the scenario year, a freely configurable amount of wind and PV generation and EV and heat pump load is added. In all other aspects, the scenario is identical to the reference case. Incremental annual changes in consumer load are not incorporated in the model. The goal of this study is not to perform a scenario analysis, but rather to develop a model that is able to perform scenario analyses. Therefore, this chapter will not include assumptions regarding for future scenarios, but only describe the structural characteristics of the model.

In section 3.1, peak loads are calculated by combining generation- and load profiles with structural characteristics of the power grid. In section 3.2, the peak loads are converted into grid capacity requirements based on assumptions regarding reserve capacity of grid assets. Capacity requirements for the reference and scenario years are translated into the capacity expansion of grid assets. Finally, the capacity expansion is used to calculate infrastructure costs based on asset prices. A schematic overview of the model structure is illustrated in Figure 3.1.

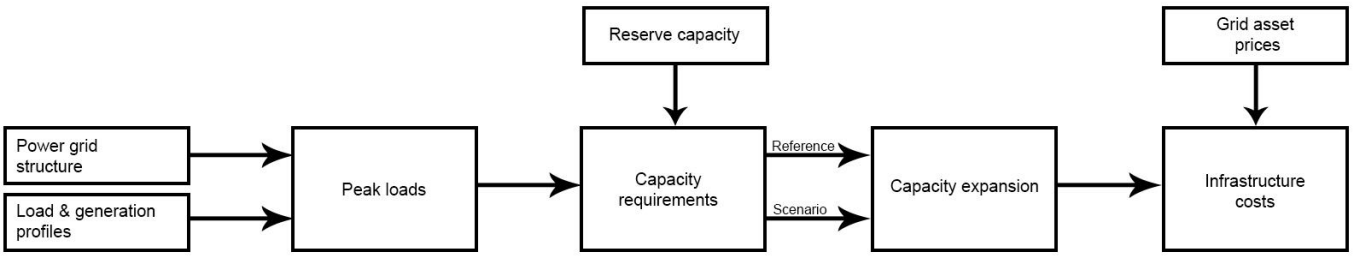

Figure 3.1: Schematic overview of the grid simulation model

3.1 Peak loads

The best way to determine peak loads on grid assets like transformers and cables is via direct measurements (Heres et al., 2017). Traditionally, grid operators extrapolate these measurements based on customer prospects and incremental autonomous growth to predict changes in peak loads (van de Sande et al., 2017). There are several reasons why this approach is not practical for this study. First of all, measuring grid assets is sometimes not feasible for technical, economic or privacy related reasons (Heres et al., 2017). In addition, the measurement data that is available often remains with grid operators who are prohibited by law from sharing them (Uitvoeringswet Algemene Verordening Gegevensbescherming, 2018). Furthermore, due to the efforts of electrifying energy demand to reduce CO_2 emissions (*Klimaatakkoord*, 2019), radical changes in electrical load on the power grid are expected which makes the traditional forecasting method using incremental autonomous growth inaccurate (Klaassen et al., 2015; van de Sande et al., 2017; van Westering et al., 2016). Consequently, a new approach is required for determining peak loads on grid assets.

An alternative approach that is suggested in literature uses bottom-up modelling for determining peak loads on grid assets (Klaassen et al., 2015; van de Sande et al., 2017; van Westering et al., 2016; Veldman et al., 2013). The basic procedure behind this type of modelling is to simulate power flows through cables and transformers by modelling the consumption and production of electrical power using load and generation profiles. With this approach, radical changes in electrical loads resulting from increasing electrification and VRE generation capacity can be taken into account (Heres et al., 2017; van de Sande et al., 2017; van Westering et al., 2016; Veldman et al., 2013). In the next sections this method will be elaborated upon.

3.1.1 Representation of the power grid structure

For the grid simulation model to make any meaningful assessments regarding peak loads on grid assets, the structure of the power grid has to be represented in a way that is both sufficiently operable and accurate. As described in section 2.1, the Dutch power grid has substantial spatial heterogeneity regarding both the distribution of power consumers and producers, as well as its topological characteristics (e.g. different voltage levels and grid structures). Including these regional differences in the grid simulation model would require very comprehensive datasets regarding structural aspects of the power grid as well as the distribution of consumers and producers and their behavior. Since the research aim of this study is to provide insights on a national level rather than on a local level, the grid simulation model uses an aggregated representation of the power grid instead.

The basic structure of this aggregated power grid representation is inspired by several reports that use a nationally aggregated approach for Dutch grid capacity assessments (Alfman & Rooijers, 2017; Blom et al., 2012; Rooijers et al., 2014; Rooijers & Leguijt, 2010). The different voltage levels (EHV, HV, IV, MV and LV) are condensed into three voltage levels (HV, MV and LV) with two intermediary transformer steps (HV/MV and MV/LV) (Figure 3.2). Figure 3.3 illustrates the resulting representation of the power grid.

This aggregation simplifies the grid structure in three ways. First, networks are merged horizontally across voltage levels, which means that for each voltage level, cables are represented as a copper plate across the entire power grid. Consequently, the power grid is assessed from a national perspective without including a spatial dimension and therefore, no conclusions can be drawn at a regional level. While the copper plate approximation may hold for a limited extent for the interconnection and transmission networks, it is certainly not an accurate representation of distribution grids. Distribution grids are more localized as the level of mutual interconnection amongst and within these grids is limited. Section 3.1.5 introduces parameters to correct for these factors. Secondly, interconnection (EHV) and transmission (HV) networks are merged vertically. This is based on the assumption that in the case of increased peak loads on the system, any necessary capacity expansion is proportional between these voltage levels. To limit the scope of this study, testing this assumption must be passed on to further research. Thirdly, the IV network as well as the HV/IV and IV/MV transformers are incorperated in the HV/MV transformation step. This is based on the assumption that the IV network acts only as an intermediate step between the transmission network (HV) and the regional distribution network (MV). While this is partly true, power producers and consumers can also be directly connected to the IV network (van Oirsouw, 2012). In the grid simulation model, these loads are divided amongst the HV and MV levels instead.

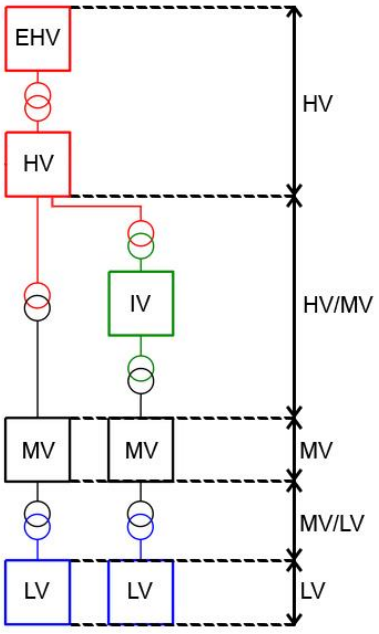

Figure 3.2: Simplified representation of voltage levels

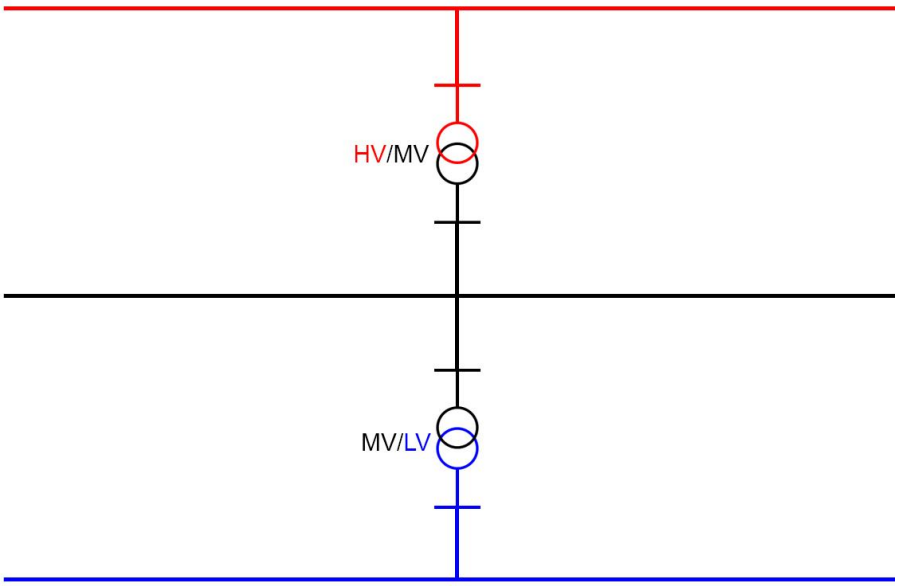

Figure 3.3: Aggregated representation of the Dutch power grid

3.1.2 Consumer and producer classes

Now that the representation of the power grid structure has been described, load and generation profiles must be added for each power consumer and producer in order to perform power flow calculations, based on the approach of Klaasen et al. (2015), van de Sande et al. (2017), van Westering et al. (2016) and Veldman et al. (2013). For each power consumer or producer, profiles will be assigned in section 3.1.3. In this section, these power consumers and producers are divided among the different voltage levels in the grid simulation model shown in Figure 3.3.

Since the grid simulation model uses a nationally aggregated representation of the power grid, power consumers and producers will also be grouped on a national level. Consequently, no conclusions can be drawn at the level of individual power consumers or producers. Section 2.2 distinguishes between the following consumer and producer categories: industry, service sector, agriculture, households, transport, conventional power plants, combined heat and power (CHP), wind turbines, and photovoltaics (PV). Power consumers or producers within one category can have different type of grid connections. For example, consumers in the service sector range from small (e.g. a local hairdresser) to large (e.g. university campus). Their grid connections therefore also range from small (e.g. 3 x 25A) to large (>10 MVA) which can be connected to either an LV cable, directly to a distribution transformer, to an MV cable or directly to a substation of the regional distribution network (Tarievencode Elektriciteit, 2016). Very little data is publicly available regarding such distributions of grid connections for most categories. Therefore, in the grid simulation model no distinction is made between grid connections connected to cables or to transformer busses. Each grid connection is connected to a voltage level that is represented by a copper plate, instead of the grid structures described in section 2.1[2].

Using the above-mentioned approach, categories listed in section 2.2 are divided among different voltage levels in the grid simulation model (HV-MV-LV). Some categories are split into subcategories (e.g. service sector consumers connected to LV). Each (sub)category will be referred to as consumer or producer classes. Figure 3.4 provides an overview of all consumer and producer classes and their respective voltage level. An elaboration behind the class division among voltage levels is provided in appendix A5.

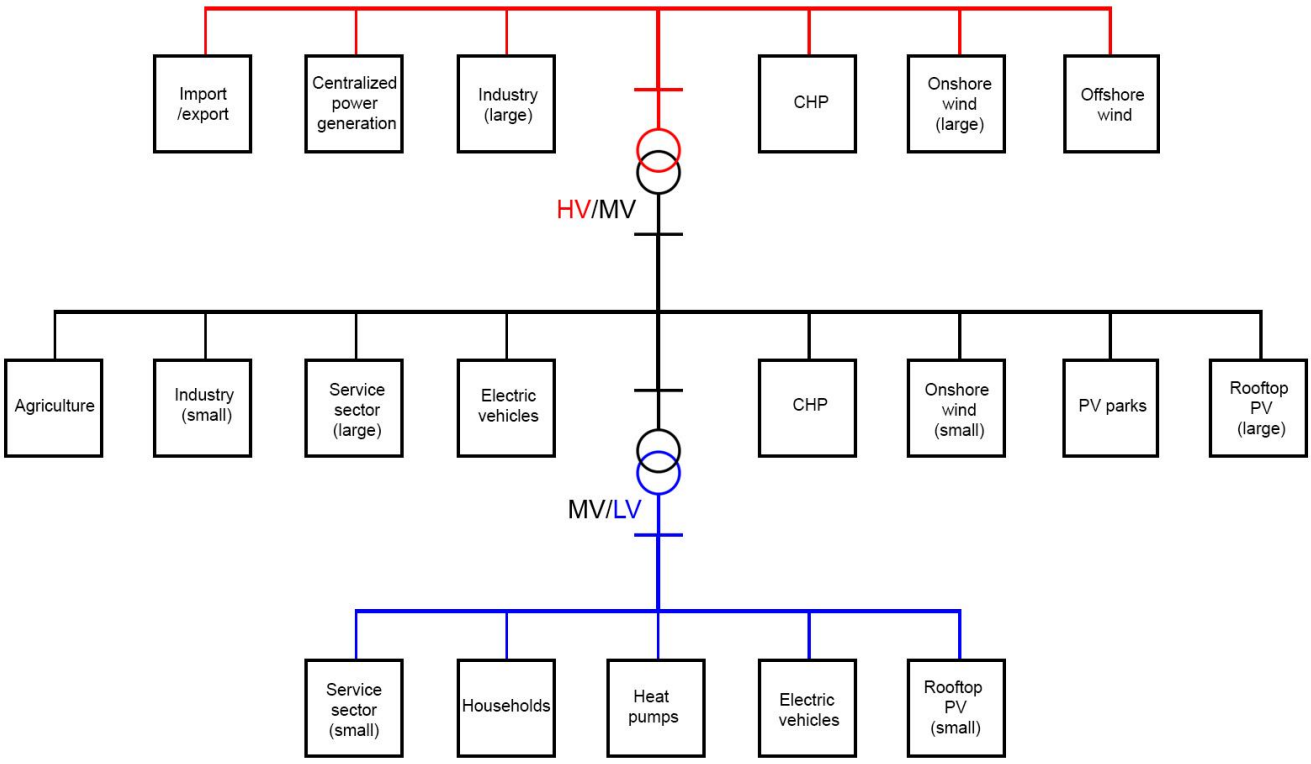

Figure 3.4: Consumer and producer classes and their division among voltage levels

[2] Exception to this rule is made for wind turbines and large PV parks, explanation is given below.

3.1.3 Load and generation profiles

Now that all consumer and producer classes have been assigned to voltage levels in the grid simulation model, load and generation profiles required for performing power flow calculations are introduced in this section. Profiles are assigned to consumer and producer classes on a national level. This implies that, for example, the load profile of households describes the combined load of all households in the Netherlands. Some classes have readily available profiles while for other classes, profiles are derived indirectly from other data sources or are built from scratch based on assumptions.

Households & the small service sector

For households and small service sector consumers, normalized profiles are used based on actual measurements (NEDU, 2019). These normalized profiles consist of energy consumption data on a quarter-hourly basis as a fraction of the annual energy consumption. There are different profiles for different types of grid connections, listed in Table 3.1. The NEDU (2019) data also includes the total annual electricity consumption per profile category, that can be used to calculate the actual load profiles.

Table 3.1: NEDU profile categories with lower (>) and upper (≤) grid connection capacity bounds and annual electricity consumption in the year 2018 per category (NEDU, 2019)

Profile	>	≤	Description	Electricity consumption [PJ/year]
E1A	-	3 x 25A	Single tariff	15.6
E1B	-	3 x 25A	Night tariff	48.8
E1C	-	3 x 25A	Evening tariff	17.7
E2A	3 x 25A	3 x 80A	Single tariff	3.1
E2B	3 x 25A	3 x 80A	Double tariff	27.1
E3A	3 x 80A	100 kVA	OT ≤ 2000 h	3.3
E3B	3 x 80A	100 kVA	OT 2000 – 3000 h	2.4
E3C	3 x 80A	100 kVA	OT 3000 – 5000 h	1.3
E3D	3 x 80A	100 kVA	OT ≥ 5000 h	0.2

NEDU (2019) only includes data for grid connections up to 100 kVA, but consumers within the small service sector can have grid connections up to 300 kVA. No data is available regarding the total annual electricity consumption of these consumers. However, data regarding the annual electricity consumption of households and service sector consumers can be used to make an estimation. The total annual electricity consumption of the NEDU profiles amount to 119.3 PJ. The annual electricity consumption of households and service sector consumers amount to 82.7 PJ and 133.2 PJ respectively (CBS, 2020a). Since virtually all households are included in the E1 categories, the remaining annual electricity consumption of service sector consumers not included in the NEDU (2019) is 96.6 PJ. This must be divided between the small service sector consumers in the 100 – 300 kVA category and large service sector consumers. A ratio of 50/50 is used, resulting in an annual electricity consumption of 48.3 PJ for small service sector consumers in the 100 – 300 kVA category. This assumption is elaborated upon in appendix A2. A load profile for the 100 – 300 kVA category is not available and therefore, a normalized load profile is constructed using the average of the four E3 profiles (E3A – E3D). To calculate the actual load profiles for each profile category, the normalized profiles are multiplied with the annual electricity consumption per category. Figure 3.5 provides an illustration of four of the resulting load profiles.

Large industry

Large industrial consumers mainly comprise of large process industries such as the chemical-, food- and steel industries (Lieshout, 2017). Many of these industries use continuous (production) processes in order to maximize production volumes (Kallrath, 2002). Since continuous processes also tend to require continuous energy input, a flat load profile is assigned to large industrial consumers based on the assumption that the majority use continuous processes. A similar approach is used by Hers et al. (2016). Using this profile, the power demand is constant year-round. The magnitude of the power demand therefore depends only on the annual electricity consumption.

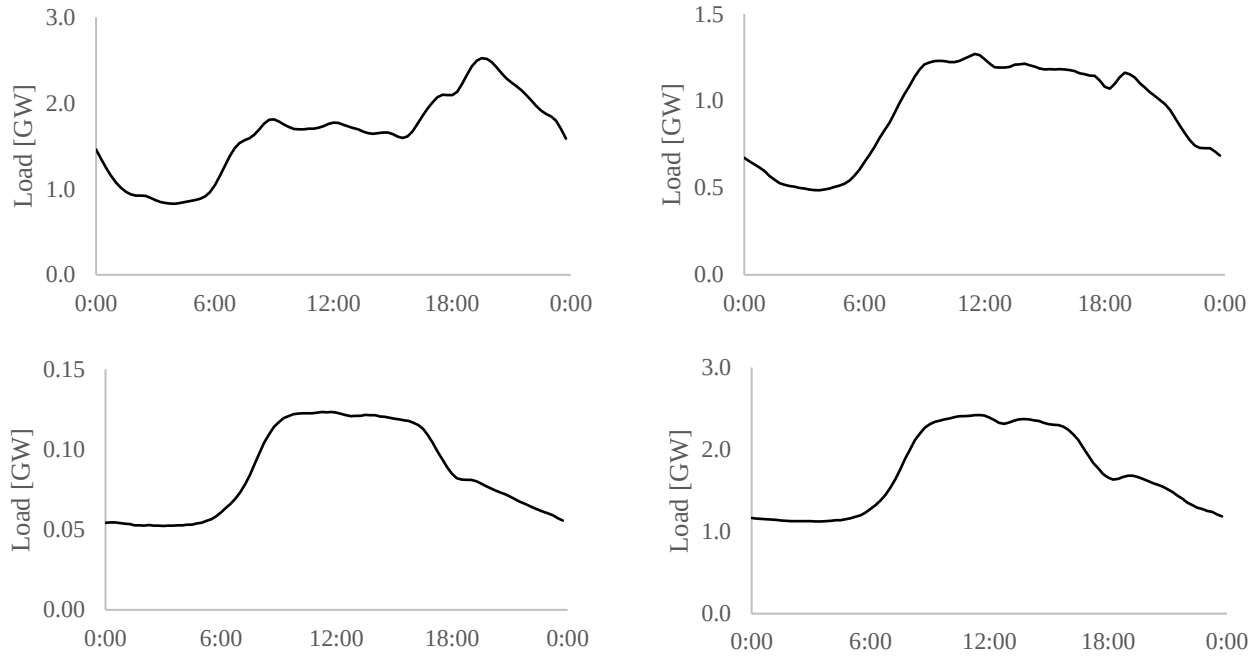

Figure 3.5: NEDU load profiles E1B (top left), E2B (top right), E3B (bottom left) and 100 – 300 kVA (bottom right) for Wednesday the 14th of March 2018 (NEDU, 2019)

Total industrial electricity consumption was 129.1 PJ in 2018 (CBS, 2020a). For the grid simulation model, large industrial consumers are assumed to use 77.5% of the total industrial consumption. This assumption is further elaborated in appendix A2. This results in a constant load profile of 3.2 GW.

Large service sector, agriculture & small industry

There is no data available regarding load profiles of large service sector-, agricultural- and small industrial consumers. Constructing load profiles using a bottom-up approach would be challenging due to the large variety within these consumer classes. Instead, a top-down approach is used to create a residual load profile using the national load profile.

The combined load profile of large service sector-, agricultural- and small industrial consumers can be obtained by subtracting the load profiles of households, small service sector consumers and large industrial consumers from the national load profile[3]. The national load profile of 2018 is based on data from ENTSO-E (n.d.). The residual load profile is shown in Figure 3.6.

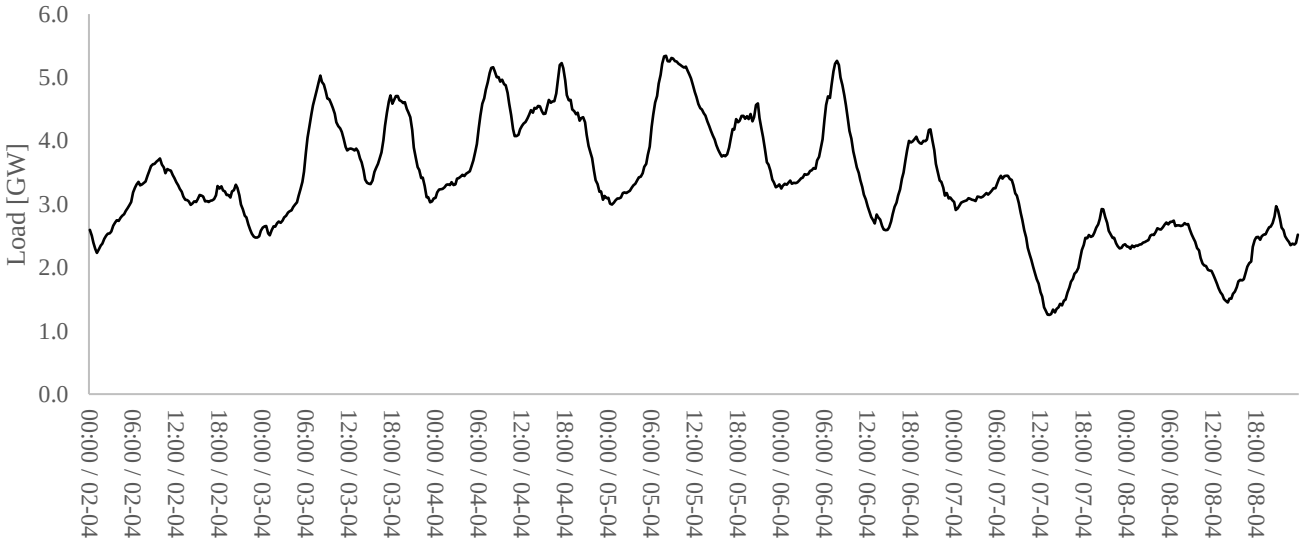

Figure 3.6: Residual profile of the large service sector, agriculture and small industry based on the national load profile. First week of April 2018, starting on a Monday

[3] 5% grid losses are subtracted from the national load first (Aalberts et al., 2011)

Heat pumps

For heat pumps, no load profiles are available. Therefore, a heat pump profile is developed using an approach based on the work of Veldman et al. (2010), which uses residential natural gas consumption as a proxy for residential heat demand. A normalized natural gas demand profile for households is used based on the G1A profile from NEDU (2019). This profile consists of two components; a temperature-dependent and a temperature-independent component. The temperature-independent component is a fixed normalized profile on an hourly basis. The temperature-dependent component consists of a maximum outside temperature above which there is no temperature dependent gas consumption, as well as a normalized profile of extra gas consumption per degree Celsius below this maximum temperature. Using a KNMI dataset with outside temperatures on an hourly basis measured in 'de Bilt' (KNMI, n.d.), the normalized temperature dependent profile can be calculated. To calculate the total gas consumption profile, the temperature-independent profile is added to the temperature-dependent profile and then multiplied by the annual gas consumption of Dutch households of 286.4 PJ in 2018 (CBS, 2020a).

The gas consumption profile is multiplied by 0.8 as only 80% of the gas consumption is used for space heating (Tigchelaar, 2013). To convert this natural gas profile into a heat demand profile, it is multiplied with the typical efficiency of a gas boiler of 95% (Blok & Nieuwlaar, 2016). Then, the heat demand profile is converted into a heat pump load profile by dividing it by a seasonal coefficient of performance (SCOP). The grid simulation model includes an air source heat pump profile and a ground source heat pump profile using a SCOP of 2.6 and 3.5 respectively. These values are based on the minimum performance thresholds set by the European Commission (2013). The actual SCOPs may deviate from these values, but cannot be lower than 1 due to the first law of thermodynamics, and are practically never larger than 5 (Blok & Nieuwlaar, 2016).

Because not all households may have adopted heat pumps in any given year, the natural gas consumption for space heating is multiplied with a heat pump adoption level (between 0 and 100%). Figure 3.7 provides an example of a ground source heat pump load profile using an adoption level of 50%.

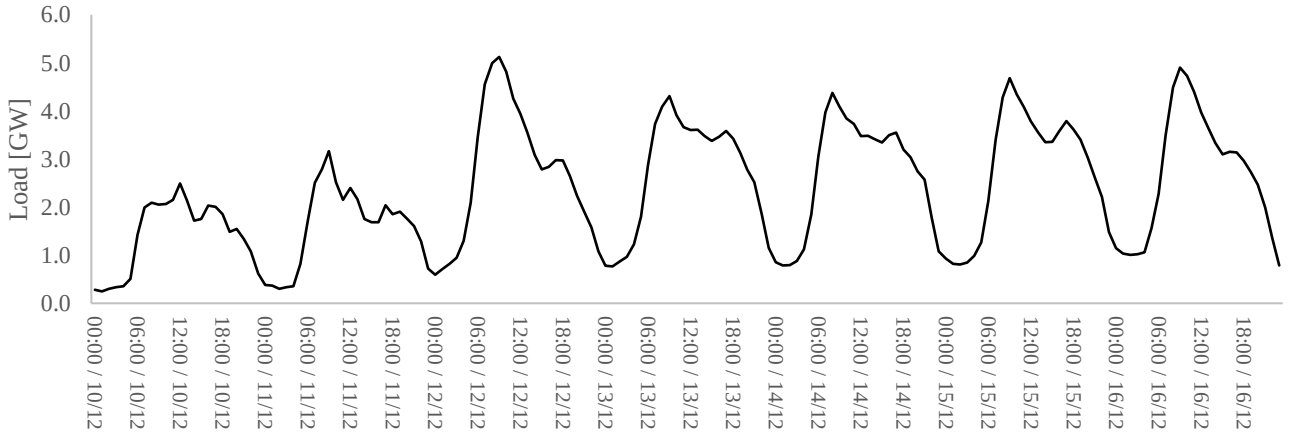

Figure 3.7: Ground source heat pump load profile with an adoption level of 50% and a SCOP of 3.5 for the second week of December 2018, starting on a Monday (KNMI, n.d.; NEDU, 2019)

Electric vehicles (EVs)

Electric vehicle charging profiles are constructed using the approach of Verzijlbergh et al. (2011) and Visser et al. (2013), based on a large dataset of personal transportation data named 'ODiN' (CBS, 2019a). This dataset contains nearly 60,000 transportation movements by car of more than 20,000 individuals. Each individual has reported their transportation movements by car for a single day. Using weighting factors, the sample has been expanded such that it is considered to be representative of the Dutch transportation behaviour for the year 2018. Figure 3.8 shows the distribution of arrival times during a day, distinguishing between residential and non-residential destinations.

Charging profiles are constructed using the arrival time, departure time, driving distance and destination of each transportation movement by car. However, the charging profiles do not just depend on transportation behaviour by car, but also on the availability of charging infrastructure. It is uncertain how charging infrastructure will develop into the future and therefore, two type of charging scenario's are used, from now on referred as the 'residential' and

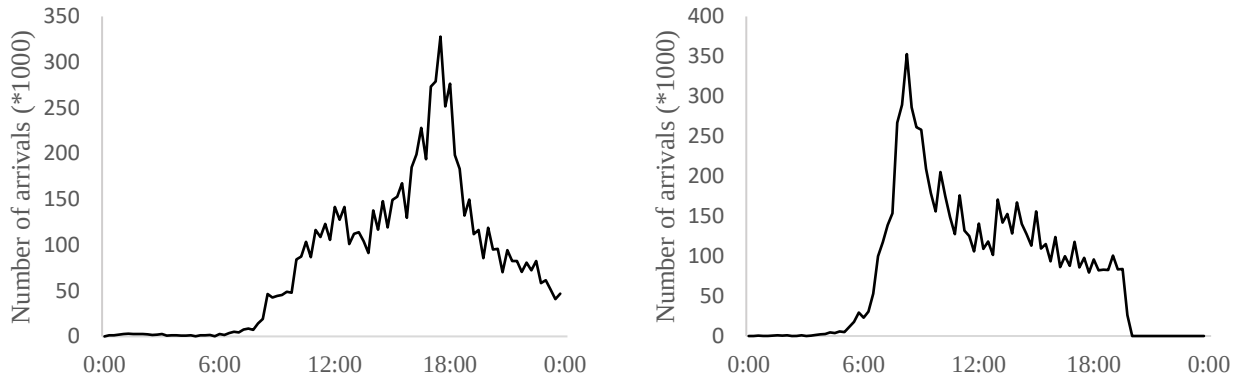

Figure 3.8: Arrivals on an average day at residential (left) and non-residential (right) destinations in 2018 (CBS, 2019a)

'everywhere' scenarios. The 'residential' scenario assumes that charging infrastructure will be predominantly developed in residential areas. The 'everywhere' scenario assumes that charging infrastructure will be widespread, with virtually every parking place having access to EV chargers.

The 'residential' charging profile is constructed based on the approach of Verzijlbergh et al. (2011) and assumes that charging only takes place after the last arrival at home. The amount of energy that is charged depends on the total daily driving distance, the energy use per driven kilometer, and the average EV battery capacity. The charging duration depends on the average residential charger capacity. The residential charging profile is assigned to the LV level of the grid simulation model. The 'everywhere' charging profile is constructed based on the approach of Visser et al. (2013) and charging takes place after every transportation movement. The amount of energy that is charged after each transportation movement depends on the driving distance, the energy use per driven kilometer, and the average EV battery capacity. The charging duration depends on the average residential or non-residential charger capacity. If the charging duration would be longer than the interval between arrival and the departure of the next transportation movement, the charging session is stopped at the moment of departure. Any uncharged battery capacity is added to the next charging session. The 'everywhere' scenario results in two distinct charging profiles, a residential and a non-residential profile. The residential and non-residential profiles are assigned to the LV and MV level of the grid simulation model respectively.

For the EV load profiles, the energy use per driven kilometer is assumed to be 0.2 kWh/km (Grahn et al., 2013; Verzijlbergh et al., 2011). An average battery capacity of 50 kWh is assumed, which provides sufficient range for nearly 98% of the daily driven distances (CBS, 2019a). For the sake of simplicity, these values are assumed to remain constant in future scenarios. Commonly used residential charging capacities range between 3.7 and 11 kW, while non-residential charging capacities are often 11 or 22 kW (Gerritsma et al., 2019; Transport & Environment, 2020). For both scenario's, weekly averaged charging profiles are created. These profiles are then normalized by dividing the charging loads by the number of driven kilometers in the ODiN dataset. The national charging profiles are then obtained by multiplying the charging loads with the total distance driven by cars in the Netherlands per year, which amounted to 121.4 billion km in 2018 (CBS, 2019d). Because not all cars may be electric in any given year, the total driven distance is multiplied with an EV adoption level (between 0 and 100%). Figure 3.9 provides an illustration of the EV load profiles for each scenario using an EV adoption level of 50% as well as residential and non-residential charging capacities of 3.7 and 11 kW respectively.

PV & Wind

PV and wind generation profiles are based on generation data from ENTSO-E (n.d.) of the year 2018. The data distinguishes between PV panels, onshore wind turbines and offshore wind turbines in the Netherlands. It consists of actual power generation per production type on a quarter-hourly basis. However, normalized generation profiles are required, as generation capacity should be freely adjustable in order to perform scenario analyses. Normalized generation profiles are calculated by dividing the power generation by the installed capacity for the year 2018, on a quarter-hourly basis. The PV generation profile is used for both rooftop PV as for PV parks.

In power systems with installed PV and wind capacity, electrical loads on grid assets depend on both the power demand and PV and wind generation. PV and wind power generation depends on weather conditions which are

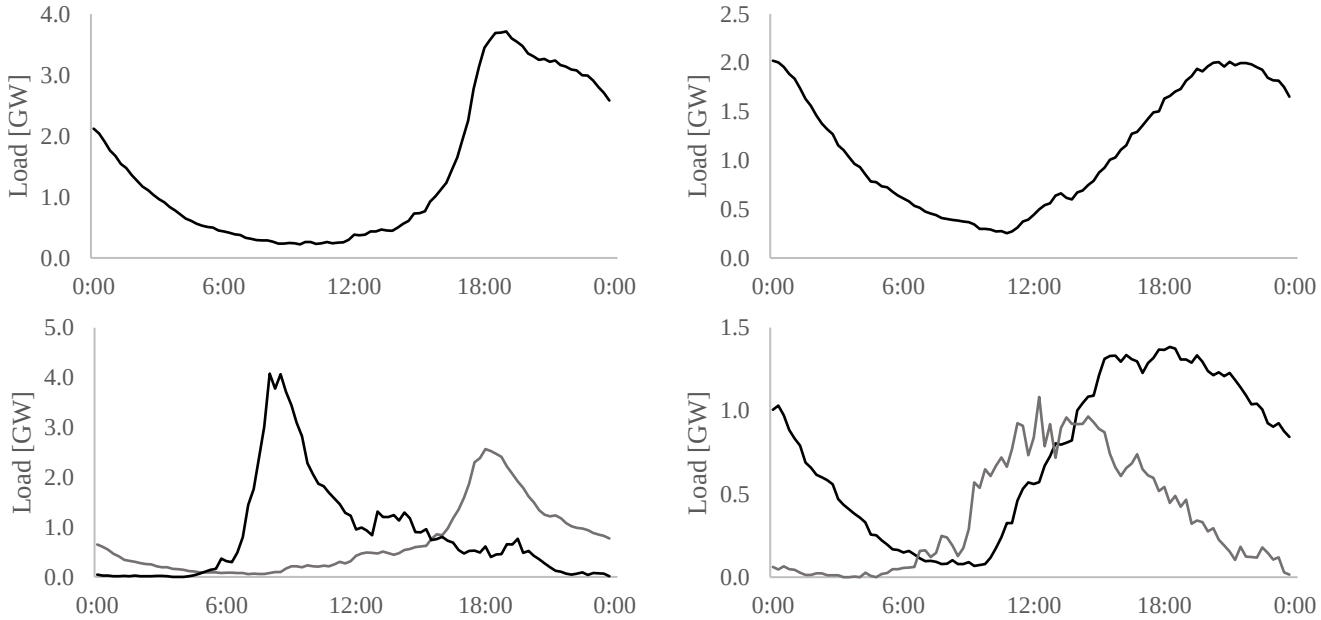

Figure 3.9: Examples of national EV charging profiles with an EV adoption level of 50%, based on the 'residential' scenario for a Tuesday (top left) and a Sunday (top right), and the 'everywhere' scenario for a Tuesday (bottom left) and a Sunday (bottom right) with both residential (grey) and non-residential (black) charging profiles

stochastic in nature. Furthermore, grid assets are built to last many decades and must therefore be able to handle worst-case scenario electrical loads (Aien et al., 2014). Worst-case scenario electrical loads on grid assets can occur when extreme weather conditions coincide with moments of exceptionally high or low power demand. It may therefore not be sufficient to use a generation profile based on one year, as it may not capture the worst-case scenario. Ideally, many years of PV and wind generation data should be used in order to maximize the probability of capturing the worst-case weather conditions. However, due to the recent growth of especially PV capacity in the Netherlands, insufficient generation data is available.

Instead of using many years of generation data, an alternative approach is used. The generation profiles based on one year are split into two separate versions, named 'minimum' and 'maximum'. For the 'maximum' profile, power generation data at each time of the day is replaced with the maximum value that occurs during that time of day across the entire month. This is done for each month, resulting in daily reoccurring generation profiles which are different for each month of the year. The same is done for 'minimum' profile, but then using the minimum value that occurs each month. The grid simulation model calculates the load on each voltage level and transformer separately for the minimum and maximum profiles. From the resulting peak loads for each of the two profiles, the largest peak load is used for capacity expansion calculations. This way, the probability of capturing a worst-case scenario of coinciding extremes in power demand and generation is increased while the correlations between weather patterns and the time-of-year and time-of-day remain in place. Examples of the 'minimum', 'maximum' and 'regular' generation profiles are shown in Figure 3.10.

CHP

For must-run CHP capacity, the generation profile depends on the demand for heat (or industrial steam), as power production is linked with heat production. However, there are several ways to make CHP generation more flexible (section 2.2.2). For flexible CHP, the electricity market often has a stronger influence on generation profile, as it will only generate power if it is economically viable to do so. However, predicting electricity prices for a specific scenario would be very difficult to do accurately. Therefore, an alternative approach is used instead.

Since for the grid simulation model only worst-case scenarios are relevant as only the peak loads eventually determine capacity expansion, the behavior of CHP generation only has to be modelled for these worst-case scenarios. Intuitively, two types of worst-case scenarios can be thought of: high renewable generation + low consumer loads and vice versa. At moments of high renewable energy generation and low consumer loads, electricity prices are relatively low, resulting in decreasing flexible CHP power generation. Therefore, flexible CHP is not likely to increase the peak loads on grid assets during such moments. Furthermore, moments of high consumer loads and low

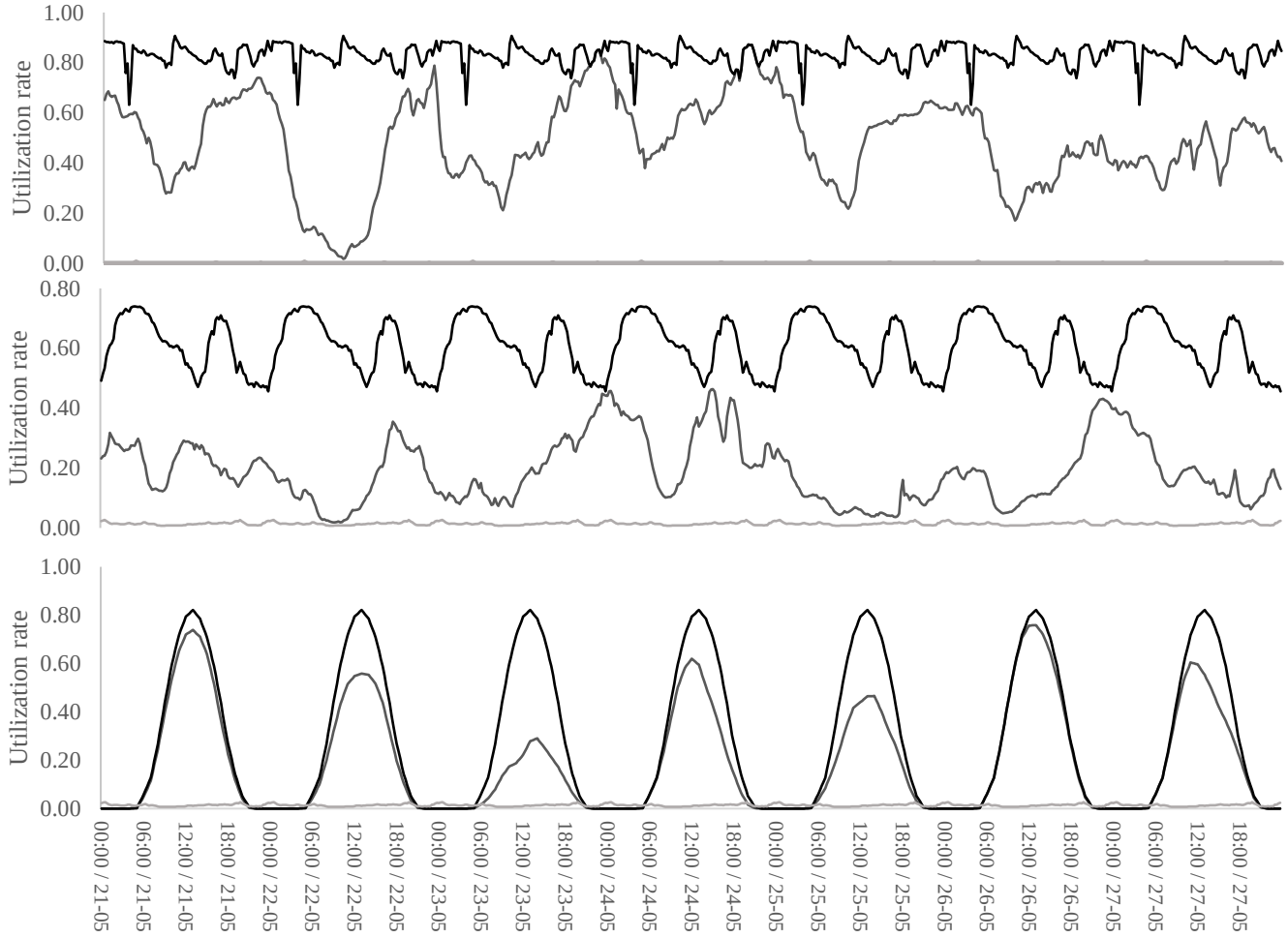

Figure 3.10: 'Maximum' (black), 'regular' (grey) and 'minimum' (light grey) generation profiles with utilization rates of offshore wind (top), onshore wind (middle) and PV panels (bottom) for a week in May, 2018.

renewable generation are likely to result in higher electricity prices, resulting in increasing flexible CHP power generation. In these situations, flexible CHP might even decrease peak loads on grid assets as CHP is decentralized, enabling local generation and reducing strains on the interconnection and transmission networks.

Based on this interplay between peak loads and flexible CHP behavior, CHP generation is modelled by using two flat profiles, named 'minimum' and 'maximum'. The 'minimum' profile is based on the minimum must-run CHP generation that may be active at any given time, and is expressed using a unit commitment rate between 0 and 1. The 'maximum' profile is based on the maximum amount of CHP generation (both must-run and flexible) that can realistically run at any given moment, also expressed as a unit commitment rate. The grid simulation model calculates the peak loads on each voltage level and transformer separately using both the minimum and maximum profile. Then, the smallest peak load is used for capacity expansion calculations.

While total installed decentralized CHP capacity was 7.26 GW in 2017 (Table 2.2), just over 6 GW of this installed capacity was operational in 2018, based on the SAVE model of 'PBL Netherlands Environmental Assessment Agency' (van Hout et al., 2019). The minimum and maximum CHP generation occurring throughout the year was roughly 1 and 4.25 GW respectively (M. van Hout, PBL, personal communication, January 16, 2020). This translates to unit commitment rates of 0.14 and 0.59 for the 'minimum' and 'maximum' profiles respectively.

Conventional power plants & import/export

The development of conventional power generation capacity and international interconnection capacity falls outside the scope of this study. In the grid simulation model, conventional power plants and import/export are used for equalizing supply and demand of electrical power. Ramp-rates are assumed to play no limiting role. Furthermore, no distinction is made between conventional power plant power generation and import as they are functionally identical within this framework.

3.1.4 Power flow

Power flow modelling of three-phase AC systems is often performed by iterative modelling methods such as the Gauss-Seidel or Newton-Raphson methods. These methods are used to model active and reactive power flows on the level of individual cables and transformers (Chatterjee & Mandal, 2017; Schavemaker & Van der Sluis, 2017). This requires both resistive and reactive characteristics of individual grid components as well as individual power consumers and producers. These modelling methods are not suited for the grid simulation model for two reasons. First, the grid simulation model does not include individual grid assets but rather a nationally aggregated power grid representation. Secondly, the load and generation profiles of the consumer and producer classes only include active power consumption and generation. Consequently, no information regarding the reactive characteristics of is available.

In light of these limitations, only active power flow is simulated in the grid simulation model, ignoring reactive power flow characteristics. This simplification leads to several inaccuracies. First, cable and transformer resistances are neglected (Schavemaker & Van der Sluis, 2017). A way to correct for this is to manually add grid losses based on AC estimations instead (Overbye et al., 2004). Section 3.1.5 explains how this correction is implemented in the grid simulation model.

Secondly, power factors and voltage levels are assumed to be constant throughout the power grid (Schavemaker & Van der Sluis, 2017). However, in reality the power factors are not constant throughout the power grid as voltage phase shifts occur due to the reactance and capacitance of the power cables and consumer loads (van Oirsouw, 2012). Furthermore, voltage levels are not always constant as they can increase or drop across power cables. Ohmic losses caused by the resistance of power cables can cause significant voltage drops, while distributed generation like PV panels can cause a voltage rise (Petinrin & Shaabanb, 2016; van Oirsouw, 2012). If changing power factors or voltage fluctuations would lead to the overcharging of grid assets, capacity expansion of those assets is not necessarily the best solution. There are various methods for voltage control such as energy storage, demand side integration, reactive power control by PV inverters or phase shifting transformers that would solve overcharging issues without capacity expansion (Demirok et al., 2011; Hertem et al., 2006; Petinrin & Shaabanb, 2016). Since power quality falls outside the scope of this study, these extra costs associated with voltage control are not relevant for this study. Therefore, errors resulting from the inaccurate representation of power factors and voltage variations are expected to be limited in the context of this study.

3.1.5 Correction parameters

The use of a simplified power grid representation and aggregated consumer classes leads to a drastic reduction in data requirement and model complexity. However, these simplifications also lead to the disappearance of a number of important structural characteristics of the power grid that can potentially have substantial influences on the modelling results. This section will elaborate on these characteristics and introduce parameters to correct for them.

Stochastic coincidence factors

The load profiles from section 3.1.3 describe the loads of consumer classes on a national level, representing the average behavior of these consumers. However, these profiles do not provide information regarding momentary load fluctuations of individual consumers. Rusck (1956) proposed that these momentary load fluctuations can behave stochastically and that, following the Central Limit Theorem, groups of stochastic fluctuations are normally distributed. This is relevant for groups of consumers that share the same load profiles and are connected to the same grid asset (cable or transformer). As the number of consumers in a group increases, it becomes increasingly unlikely that their individual peak loads occur simultaneously. This phenomenon is referred to as ‘noncoincidence’. Due to the noncoincidence of peak loads, the sum of peak loads of individual consumers is always larger than the peak load of these consumers as a group. As the group size increases, the variance decreases and therefore, the peak load approaches the average load profile. The ratio between individual peak load and the average load is referred to as the ‘coincidence factor’. This relation is shown in equation 3.1.

$$c_{\infty} = \frac{P_{av,1}}{P_{max,1}} \qquad 3.1$$

In equation 3.1, c_∞ is the coincidence factor for an infinite number of consumers, $P_{av,1}$ the average load of one consumer and $P_{max,1}$ the maximum load of one consumer. The coincidence factor of groups with an infinite number of consumers converges to the average load profiles described in section 3.1.3. To describe the load behavior of smaller groups, Rusck's interpretation of stochastic loads results in equation 3.2 (van Oirsouw, 2012).

$$P_{max,group} = c_\infty \cdot P_{max,1} \cdot n_{group} + (1 - c_\infty) \cdot P_{max,1} \cdot \sqrt{n_{group}} \quad 3.2$$

In equation 3.2, $P_{max,group}$ is the maximum load per consumer group and n_{group} is the average number of consumers sharing the same load profile that are connected to the same cable or transformer. The total peak load on grid assets induced by each load profile (e.g. E1A) is the sum of the peak loads of all groups ($P_{max,group}$) that share that load profile. This relation is expressed in equation 3.3.

$$P_{max,type} = P_{max,group} \cdot \frac{n_{type}}{n_{group}} \quad 3.3$$

In equation 3.3, $P_{max,type}$ is the peak load induced by all consumers that share a specific profile type (e.g. E1A) and n_{type} is the total number of consumers per profile type. This equation is applied for translating the total load profile peak loads to the physical peak loads on actual grid assets. This relation will be referred to as the 'asset/profile peak load ratio'. For this, $P_{max,type}$ is divided by the national load of that profile type (equation 3.4).

$$\frac{asset\ peak\ load}{profile\ peak\ load} = \frac{P_{max,type}}{P_{max,1} \cdot c_\infty \cdot n_{type}} \quad 3.4$$

Equation 3.4 can then be simplified into equation 3.5, which is illustrated in Figure 3.11.

$$\frac{asset\ peak\ load}{profile\ peak\ load} = 1 + \frac{\sqrt{n_{group}}}{n_{group}} \cdot \left(\frac{1}{c_\infty} - 1\right) \quad 3.5$$

The framework of Rusck (1956) described in this section has traditionally been used by grid operators for designing distribution networks (Heres et al., 2017). However, in this study, this method is only applied for the local distribution networks as there are no individual load profiles available for the consumer categories connected to the regional distribution networks. Therefore, an alternative approach will be used which is described later in this chapter. For the local distribution network, load profiles are available for households and small service sector consumers (NEDU profiles E1A up to E3D), electric vehicles and heat pumps. Based on these load profiles, the peak loads on grid assets can be calculated using only the variables n_{group} and c_∞ (equation 3.5). For each consumer type connected to the local distribution network, the coincidence factors, group sizes and peak load ratios are listed in Table 3.2. Appendix A4 elaborates on how these coincidence factors and group sizes have been determined. Textbox 3.1 provides further explanation on how coincidence factors and group sizes affect asset peak loads based on an example.

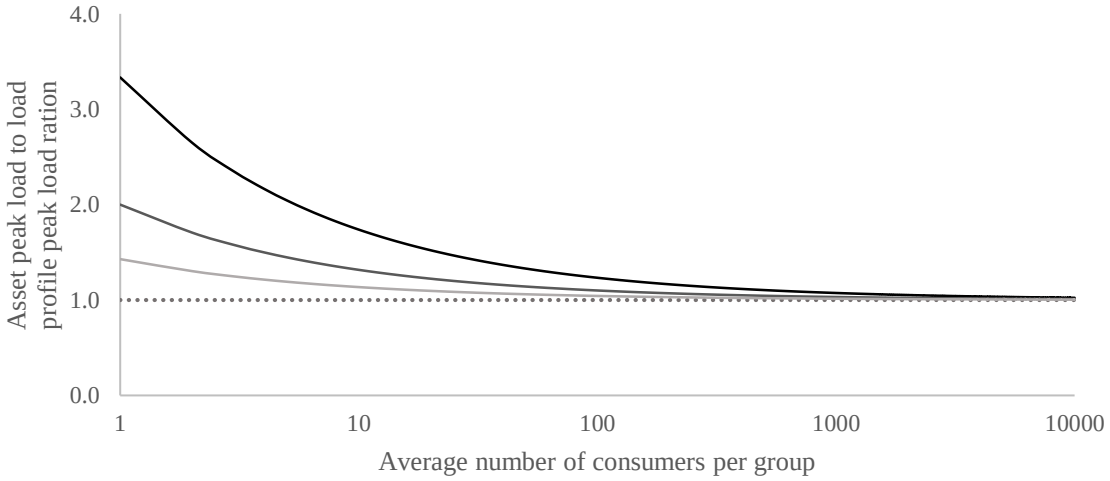

Figure 3.11: Peak load contribution per consumer with a coincidence factor of 0.3 (black), 0.5 (dark grey) and 0.7 (light grey)

Textbox 3.1: Practical example regarding the effects of coincidence factors and group sizes on peak loads on grid assets

If the total peak load of profile E1A is 1.0 GW for a total of 1500,000 houses, the average peak load per house ($P_{av,1}$) would be 0.67 kW. Then, if the typical peak load of an individual house ($P_{max,1}$) would be 6.7 kW, the coincidence factor (c_∞) becomes 0.1 (equation 3.1). If, on average, 20 houses are connected to a single LV cable (n_{group}), the asset/profile peak load ratio becomes 3 (equation 3.5). This means that, instead of a peak load of 1.0 GW for load profile E1A, the combined load of all E1A consumers ($P_{max,type}$) leads to a peak load of 3 GW on LV cables.

Table 3.2: Peak load contribution per consumer with a coincidence factor of 0.3 (black), 0.5 (dark grey) and 0.7 (light grey)

Consumer type	c_∞	n_{group} Cable	n_{group} Distribution transformer	Cable/profile peak load ratio	Transformer/profile peak load ratio
E1A	0.08	21	82	3.4	2.2
E1B	0.08	21	82	3.6	2.3
E1C	0.09	21	82	3.2	2.1
E2A	0.15	5	19	3.6	2.3
E2B	0.13	5	19	4.1	2.6
E3A	0.23	1	3	4.4	3.0
E3B	0.28	1	3	3.5	2.5
E3C	0.46	1	3	2.2	1.7
E3D	0.37	1	3	2.7	2.0
100 – 300 kVA	0.36	1	3	2.8	2.0
EV ‘residential’	0.24	1 – 21	1 – 82	4.2 - 1.7	4.2 - 1.3
EV ‘everywhere’ – residential	0.17	1 – 21	1 – 82	6.3 - 2.1	6.3 - 1.6
Heat pump	0.53	1 – 21	1 – 82	1.9 - 1.2	1.9 - 1.1

Intergroup coincidence factor

The load on the regional distribution network comprises of the residual load profile (large service sector-, agricultural- and small industrial consumers) and the combined load profile of the distribution transformers (combined load of the local distribution network). For the residual load profile, no individual load profiles are available. Consequently, the method of using coincidence factors to calculate peak loads on grid assets for consumers within each class cannot be applied. However, when groups of loads with different load profiles are combined in a specific area of a distribution network, intergroup coincidence factors become relevant (Bary, 1945; Guyer, 2017). An intergroup coincidence factor describes the ratio of the coincident peak load of a group of consumer classes divided by the individual peak loads of each consumer class (Bary, 1945). This relation is expressed in equation 3.6.

$$Intergroup\ coincidence\ factor = \frac{coincident\ peak\ load}{\sum class\ peak\ loads} \qquad 3.6$$

In other words, if the peak load of the individual consumer classes do not coincide with the peak load of the combined load profile, the intergroup coincidence factor is lower than one. Because the load profiles per consumer class are not available, the intergroup coincidence factor cannot be calculated accurately. However, the combined load profile of the local distribution grid is available. If, for the sake of calculation, the residual load profile is considered as one consumer class, equation 3.6 can be used to calculate the upper bound for the intergroup coincidence factor. The combined peak load of the local distribution grid is 8.7 GW and the peak load of the residual profile is 7.8 GW. The coincident peak load of both profiles is 15.7 GW. Following equation 3.6, the intergroup coincidence factor then becomes 0.95. However, because the sum of peak loads of the consumer classes making up the residual profile is larger than its coincident peak, the actual intergroup coincidence factor must be lower than 0.95. Furthermore, intergroup coincidence factors of distribution networks are rarely lower than 0.7 (Guyer, 2017).

An intergroup coincidence factor lower than one implies that the peak loads of consumer classes occur non-simultaneously. If consumer classes are not evenly spread across the regional distribution networks, the sum of peak loads on individual grid assets must be larger than the peak load of the aggregated residual load profile. Since there

is significant clustering in industrial and agricultural load (Figure 2.10 and Figure 2.11) within the Netherlands, the intergroup coincidence factor must be taken into account.

Self-consumption

When decentralized generation is installed at or near power consumers, some power can be consumed directly while making little or no use of the power grid. In the grid simulation model, two types of self-consumption that are relevant in the actual power system are not taken into account; direct self-consumption and local self-consumption.

Direct self-consumption occurs when decentralized generation shares the same grid connection as the consumer (rooftop PV and CHP). In this case, generated power can be consumed directly without using the power grid (Luthander et al., 2015). The simplified power grid representation does not account for direct self-consumption, because consumer and producer classes are all separately connected to the power grid. Therefore, a 'direct self-consumption factor' is introduced for distributed generation (rooftop PV and CHP). This factor is further elaborated upon in appendix A6.

Local self-consumption occurs when decentralized power generation (rooftop PV, PV parks, CHP and small onshore wind) is consumed in a local- or regional distribution network, without needing to be transported via parent voltage levels. Because the simplified power grid representation merges the voltage levels horizontally, they are represented as a copper plates. Consequently, if there is sufficient demand on a specific voltage level, all decentralized power generation can be consumed on that voltage level without needing transportation via parent voltage levels (full local self-consumption). In reality, there may be sufficient demand on a voltage level on a national level, but on a local level generation could be higher than demand. In this scenario, power must be transported via the parent voltage level(s), putting additional strains on these grid assets. An example for this would be a high penetration of rooftop PV in one neighborhood, but a lower penetration of rooftop PV on a national level. If, during a sunny afternoon, this neighborhood has a surplus of PV generation, while other neighborhoods do not, power must be transported via the regional distribution network. In short, the grid simulation model assumes 100% local self-consumption. To correct for this, a 'local self-consumption factor' is introduced for distributed generation (PV, CHP and onshore wind). This factor is further elaborated upon in appendix A6.

Grid losses

Because a simplified DC power flow method is used in the grid simulation model, grid losses cannot be calculated directly from power flows through grid assets. Instead, grid losses are estimated based on measurement data and added to the grid simulation model as separate consumers.

Table 3.3 lists the total grid losses per voltage level, based on measurements of grid operators as well as the total power flow per voltage level (Aalberts et al., 2011; Rooijers & Leguijt, 2010). Based on these numbers, grid losses are determined as a percentage of the total power flow for each voltage level (HV, HV/MV, MV, MV/LV and LV).

Table 3.3: Grid losses per voltage level

Voltage level	Grid losses in 2008 [TWh] (Aalberts et al., 2011)	Annual power flow [TWh] (Rooijers & Leguijt, 2010)	Grid losses [% of power flow]
HV	1.00	90	1.1%
HV/MV	0.71	65	1.1%
MV	1.08	90	1.2%
MV/LV	0.46	45	1.0%
LV	0.60	45	1.3%

3.1.6 Peak load calculation

The loads on grid assets are based on load and generation profiles, peak load ratios, self-consumption, and grid losses described in this chapter. Power flows through transformers (HV/MV and MV/LV) are such that the power in- and outflow is equal for each voltage level. Loads are determined per voltage level (HV, MV and LV) and transformer step (HV/MV and MV/LV) using equations 3.7 to 3.11.

$$Load_{LV} = \sum_i (p_{load,i} \cdot r_{cable,i}) + p_{gen} - 2 \cdot p_{sc-direct} - p_{sc-local} + p_{losses} \quad 3.7$$

$$Load_{MV} = \sum_i (p_{load,i}) \cdot r_{intergroup} + \sum_j p_{gen,j} - 2 \cdot p_{sc-direct} - p_{sc-local} + p_{losses} \quad 3.8$$

$$Load_{HV} = \sum_i (p_{load,i}) + p_{losses} = \sum_j p_{gen,j} \quad 3.9$$

$$Load_{MV/LV} = \sum_i (p_{load,i} \cdot r_{trans,i}) + p_{gen} - 2 \cdot (p_{sc-direct} + p_{sc-local}) + p_{losses} \quad 3.10$$

$$Load_{HV/MV} = \sum_i (p_{load,i}) \cdot r_{intergroup} + \sum_j p_{gen,j} - 2 \cdot (p_{sc-direct} + p_{sc-local}) + p_{losses} \quad 3.11$$

In equations 3.7 to 3.11, p_{load} is a consumer load (e.g. E1A residential consumers or heat pumps) on the specified voltage level, r_{cable} the cable/profile peak load ratio of the corresponding consumer load, r_{trans} the transformer/profile peak load ratio of the corresponding consumer load, $r_{intergroup}$ the intergroup peak load ratio, p_{gen} the power generation (e.g. rooftop PV or centralized power generation), $p_{sc\text{-}direct}$ the total direct self-consumption on a specific voltage level, $p_{sc\text{-}local}$ the total local self-consumption on a specific voltage level and p_{losses} the grid losses at a specific voltage level. For the transformer steps, p_{load} and p_{gen} in equations 3.10 and 3.11 refer to the underlying voltage level[4]. Using equations 3.7 to 3.11, the loads on each voltage level and transformer step can be calculated for each moment in time. The peak loads are simply the maximum values of these loads throughout the year.

[4]For instance, the MV/LV load only depends on generation and demand on the MV level.

3.2 Infrastructure investments

This section will describe the method used for calculating the power grid infrastructure investments required for accommodating increasing peak loads on power grid assets. The method is inspired by research reports of Rooijers & Leguijt (2010) and Alfman & Rooijers (2017), which were written on behalf of 'Netbeheer Nederland'. The basic principle behind this method relies on extrapolating the reinvestment value of power grid assets based on increases in required grid capacity. This approach is based on the assumption that the structure of the power grid remains the same when grid capacity increases. Furthermore, it assumes that doubling the capacity of a grid asset (transformer or cable) costs the same as installing an additional asset with the same capacity. Capacity requirements depend on peak loads on grid assets as well as assumptions regarding reserve capacity. This method does not consider the time value of money and end-of-life replacements of grid assets.

3.2.1 Reinvestment value of the power grid

The reinvestment value of the power grid does not resemble the total capital expenditures that have been spent on grid assets, but instead refers to the replacement value of the sum of all grid assets. Calculating the reinvestment value requires data on the number of currently installed grid assets and their respective investment costs.

Grid assets mainly consist of substations, distribution transformers and power cables. Table 3.6 lists the quantities of all substations and distribution transformers, based on data from Hoogspanningsnet.com (n.d.) and Netbeheer Nederland (n.d.). Table 3.5 lists the total cable length per voltage level, based on data from Netbeheer Nederland (n.d.). Both data sources are regularly updated based on public data and expert judgement (A. van Geest, Netbeheer Nederland, personal communication, February 20, 2020; *Hoogspanningsnet.com*, n.d.). Note that only the publicly owned transformers are included and not the transformers used in the privately owned grid connections.

The investment costs per substation, distribution transformer and power cable are listed in Table 3.4. Three different data sources are compared. Because the cost data from Netbeheer Nederland (2019a) is most complete, this data will

Table 3.4: Investment costs per grid asset

Substation type	Costs [k€] (Rooijers & Leguijt, 2010)	Costs [k€] (Alfman & Rooijers, 2017)	Costs [k€] (Netbeheer Nederland, 2019b)
EHV/HV	30,000	15,000	> 100,000
HV/IV	-	-	> 25,000
HV/MV	15,000	15,000	> 25,000
IV/MV	-	-	1,500 – 10,000
MV/MV	-	-	1,300 – 6,500
MV/LV*	38	38	35 – 250
Cable type	[k€/km]		[k€/km]
EHV	625	408	-
HV	300	408	1,000 – 5,000
IV	-	-	300 – 1000
MV	100	100	100 – 400
LV	50	80	70 – 150

*(Netbeheer Nederland, n.d.)

Table 3.5: Cable lengths per voltage level (Netbeheer Nederland, n.d.)

Cable type	Total cable length [km]
EHV	2873
HV	6035
IV	4677
MV	103738
LV	220629

Table 3.6: Number of substations and distribution transformers (*Hoogspanningsnet.com*, n.d.)

Substation type	Number of substations
EHV/HV	36
HV/IV	48
HV/MV	198
IV/MV	192
MV/MV	111
MV/LV*	97,000*

*(W. van Westering, Alliander, personal communication, February 5, 2020)

Table 3.7: Reinvestment value of the Dutch power grid

Substation type	Reinvestment value [M€]
HV	12,508
HV/MV	7,841
MV	10,518,
MV/LV	3,395
LV	15,444
Total	49,706

be used. The data consists of cost ranges, often higher than the cost data from Rooijers & Leguijt (2010) and Alfman & Rooijers (2017). Therefore, the lower limit of the cost data of Netbeheer Nederland (2019a) is used[5]. Following the simplification of voltage levels illustrated in Figure 3.2, the total reinvestment value can be calculted based asset and cost data listed in Table 3.4, Table 3.5, Table 3.6. The resulting reinvestment values per voltage and transofmer level is listed in Table 3.7.

3.2.2 Infrastructure investments

Following a similar approach as Rooijers & Leguijt (2010) and Alfman & Rooijers (2017), infrastructure investments are estimated by linearly extrapolating the reinvestment value of the power grid (section 3.2.1) in proportion to increases in peak loads on grid assets (section 3.1). Equation 3.12 provides a mathematical description of the relation between peak load, reinvestment value and infrastructure investments.

$$Investments_l = RV_l \cdot \left(\frac{Load_{peak,scenario,l}}{Load_{peak,reference,l}} - 1 \right) \quad 3.12$$

In equation 3.12, $Investments_l$ are the infrastructure investments required for voltage level or transformer step l. RV_l is the reinvestment value for voltage level or transformer step l (Table 3.7). $Load_{peak,reference,l}$ and $Load_{peak,scenario,l}$ are the peak loads on voltage level or transformer step l for the reference- and scenario year.

The main underlying assumptions behind this approach are that the available cable length per unit of peak load and the distribution of transformers remain constant, and that the capital expenditures for installing new grid assets are the same in every situation. A constant cable length per unit of peak load implies that the structure of the power grid remains roughly the same. Furthermore, while it is evident that in some situations (e.g. old city centres or rural areas with long distribution cables) capacity expansion can be more expensive than other situations, it is assumed that on a national level these differences average out. Without making such an assumption, it would be very difficult to use a greatly simplified power grid representation without a spatial dimension (section 3.1.1). Finally, this method does not take into account the possibility of allowing short moments of transformer overload to reduce the need for capacity expansion.

Reserve capacity

Equation 3.12 does not take into account reserve capacity of grid assets. Although grid operators are required by law to keep some amount of reserve capacity, there are no rules regarding how much (Elektriciteitswet, 1998). The reserve capacity of a grid asset (e.g. cable) is the difference between the peak loads it is exposed to and its capacity. For example, if a cable has a capacity of 120 kVA and the peak load is 100 kVA, the reserve capacity is 20%. Consequently, grid assets with reserve capacity can accommodate increases in peak loads without requiring capacity expansion. However, if a grid operator wants to retain a certain amount of reserve capacity, capacity expansion is required nonetheless. Therefore, reserve capacity can only be used for accommodating peak loads if it is the desire of grid operators to have a lower reserve capacity in the future. This effect of reserve capacity on the relation between peak loads and infrastructure investments is illustrated in Figure 3.12. Equation 3.13 provides a mathematical description of the relation between infrastructure investments, peak load, reinvestment value, and reserve capacity.

$$Investments_l = RV_l \cdot \left(\frac{Load_{peak,scenario,l} \cdot R_{scenario,l}}{Load_{peak,reference,l} \cdot R_{reference,l}} - 1 \right) \quad 3.13$$

In equation 3.13, $R_{reference,l}$ and $R_{scenario,l}$ are the reserve capacities on voltage level or transformer step l for the reference- and scenario year. For the reserve capacities in the reference year (2018), little data is publicly available. The best available data comes from expert judgement from Enexis in 2010 and is listed in Table 3.8 (Rooijers & Leguijt, 2010). Since 2010, peak loads on grid assets have been increasing as a result of increased electrification and VRE generation capacity and grid operators have been struggling to keep up (Topsector Energie, n.d.). It is therefore reasonable to assume that reserve capacities have not increased since 2010.

[5] The costs of EHV cable is assumed to be equal to the costs of HV cable.

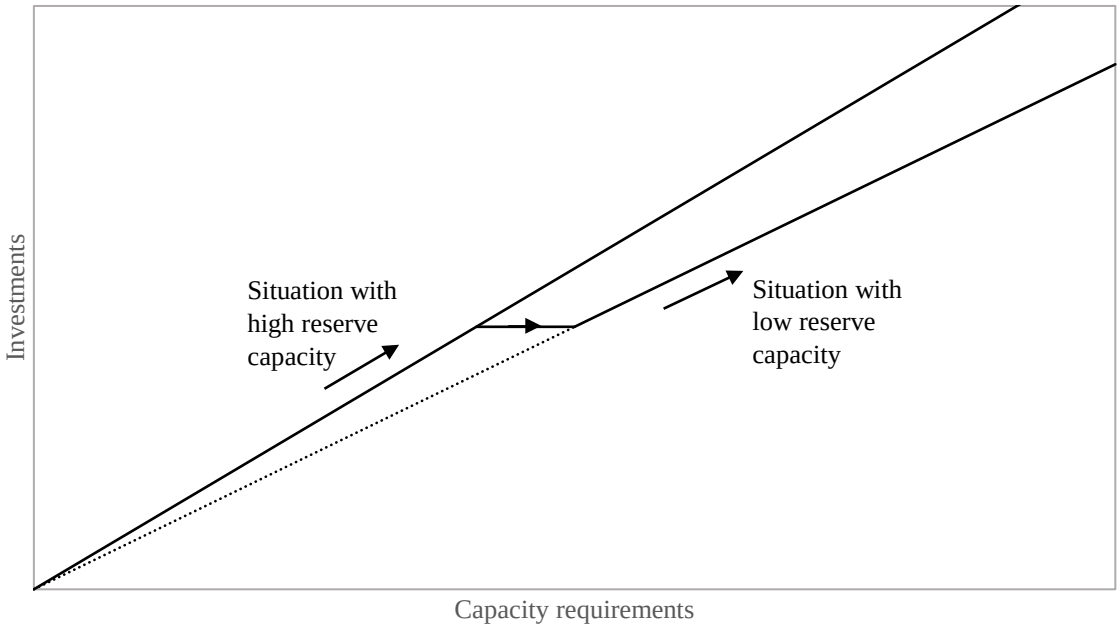

Figure 3.12, the effect of reserve capacity on the relationship between peak loads and infrastructure investments

Table 3.8: Reserve capacity of grid assets for the reference year

	Reserve capacity 2010 (Rooijers & Leguijt, 2010)	Reserve capacity 2018
HV	67%	≤ 67%
HV/MV	25%	≤ 25%
MV	25%	≤ 25%
MV/LV	67%	≤ 67%
LV	17.5%	≤ 17.5%

Offshore wind

For offshore wind parks, costs for transport cables towards the closest substation are added to the grid investments separately. These do not meet the assumption of an constant power grid structure, as they require extensions to the power grid. Offshore wind parks are connected to the interconnection network via marine EHV cables. For the 9.6 GW offshore wind capacity that is planned up to 2030, the costs of connections are expected to be approximately €10 billion (Rijksoverheid, n.d.; Wind op zee, n.d.). Even though the actual grid connections fall outside the scope of this study, an exception is made for offshore wind as these grid connection costs are socialized. Therefore, €1.04 billion is added to the total investment costs calculated using equation 3.13, for each GW of additional offshore capacity since the reference year. A similar methodology could be applied for wind and PV parks. However, these investement costs are neglected as they are deemed insignificant[6] and would only lead to unessecary model complexity.

[6] PV parks are connected to substations of the regional distribution grid via MV transport cables. For PV parks, an average distance to the substation of 2.5 km is assumed, based on an estimate of Lensink et al. (2019). Assuming an MV cable cost of 100 k€/km (Table 3.4), a non-redundant grid connection (Lensink et al., 2019), an average capacity per PV park of 14.5 MW (RVO, 2020a), and an average DC/AC ratio of 1.33 (Abd El-Aal et al., 2006), the grid infrastructure investment costs for PV parks are approximately €0.023 billion per GW. It is slightly different for wind parks, but presumably in the same order of magnitude.

4 MODEL VALIDATION

The goal of model validation is to determine whether a simulation model accurately represents a given system (Law, 2008). However, no model can have absolute validity. Therefore, model validity should always be evaluated in light of its application (Martis, 2006). Following the research aim formulated in chapter 1, the application of the grid simulation model is twofold. Its first application is to chart uncertainties introduced by input parameters, for which a sensitivity analysis is performed in section 4.1. Its second application is to provide insights into the usefulness of the chosen modelling approach, for which peak load and profile analyses are performed in sections 4.2 and 4.3 respectively. The peak load analysis assesses whether peak loads of the reference and scenario years are realistic, while the profile analysis assesses whether the synthetic load profiles of heat pumps and EVs are accurate.

4.1 Sensitivity analysis

In chapter 3, many input parameters have been introduced, often not with one certain value but with a range of plausible values. These parameters and their respective ranges have been summarized in appendix A3. In this section, the uncertainties introduced by these parameter ranges are quantified by performing a sensitivity analysis.

Two types of parameters can be distinguished; scenario parameters and structural parameters. Scenario parameters are scenario-dependent (e.g. EV adoption level), while structural parameters do not depend on the chosen scenario (e.g. intercategorical coincidence factor). These parameters are separately assessed in sections 4.1.1 and 4.1.2 respectively. However, some structural parameters are specific to a scenario parameter (e.g. EV charging capacity) and are therefore assessed alongside the scenario parameters in section 4.1.1.

4.1.1 Scenario parameters

The figures below display the infrastructure investments required to accommodate changes in peak loads resulting from changes in scenario parameters. In each figure, one structural parameter that is directly related to the scenario parameter is also varied to show its effect on the required infrastructure investments. The values of all other structural parameters are held equal to the base values listed in appendix A3. The values of the other scenario parameters are held constant, equal to the values of the reference scenario, also listed in appendix A3. This implies that reserve capacities are also held constant, which can have significant impacts on required capital investments. The magnitude of this effect is assessed in the section 4.1.2.

In Figure 4.1, the effects of an increasing heat pump adoption level are shown with varying heat pump coincidence factors and varying SCOPs. First of all, effect of heat pumps on infrastructure investments is significant. The coincidence factor has very little influence on the capital investments while the SCOP has a major impact.

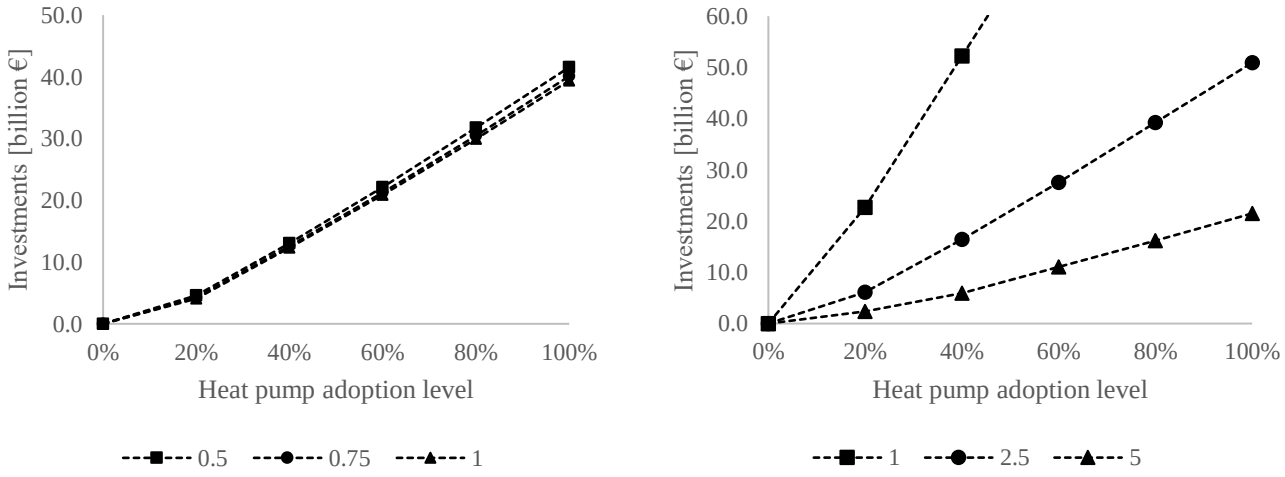

Figure 4.1: Infrastructure investments for increasing heat pump adoption levels with different heat pump coincidence factors (left) and different SCOPs (right)

Figure 4.2 shows the effects of an increasing EV adoption level with varying charging speeds. Although less than for heat pumps, EV adoption also results in large infrastructure investments. The effect of average charging capacity for non-residential charging is limited and substantial for residential charging.

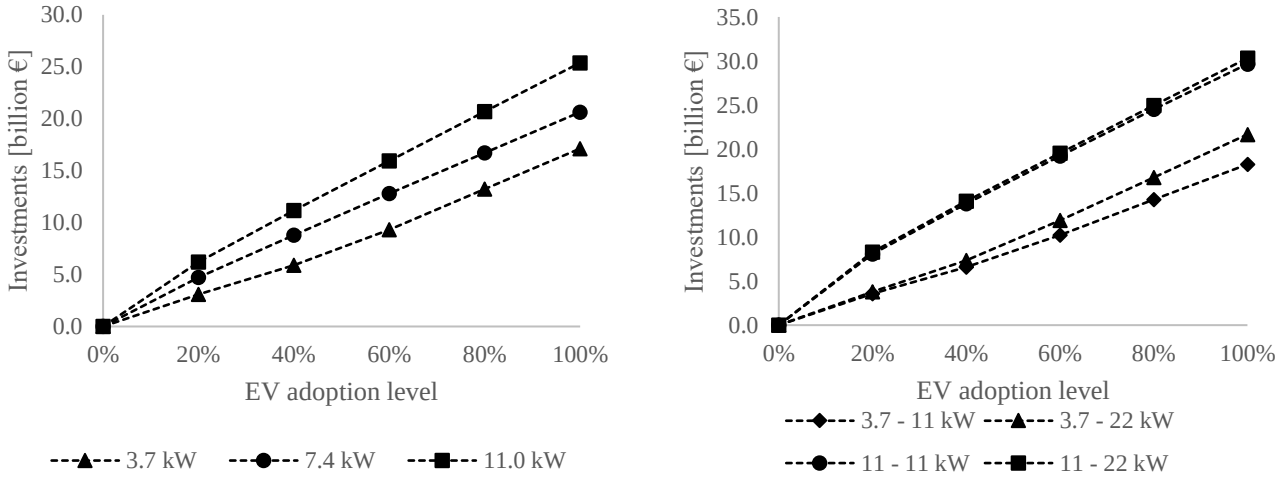

Figure 4.2: Infrastructure investments for increasing EV adoption levels with different charging capacities for the 'residential' scenario (left) and the 'everywhere' scenario (right)

Figure 4.3 shows the effect of increasing the small rooftop PV installed capacity with varying rates of direct and local self-consumption. For each graph, one self-consumption parameter is varied while the other is kept at a value of 0. Even though the parameter for local- and direct self-consumption in appendix A3 ranges between 0 and 1, self-consumption is not increased above 0.5 as for this value the infrastructure investments already approach 0.

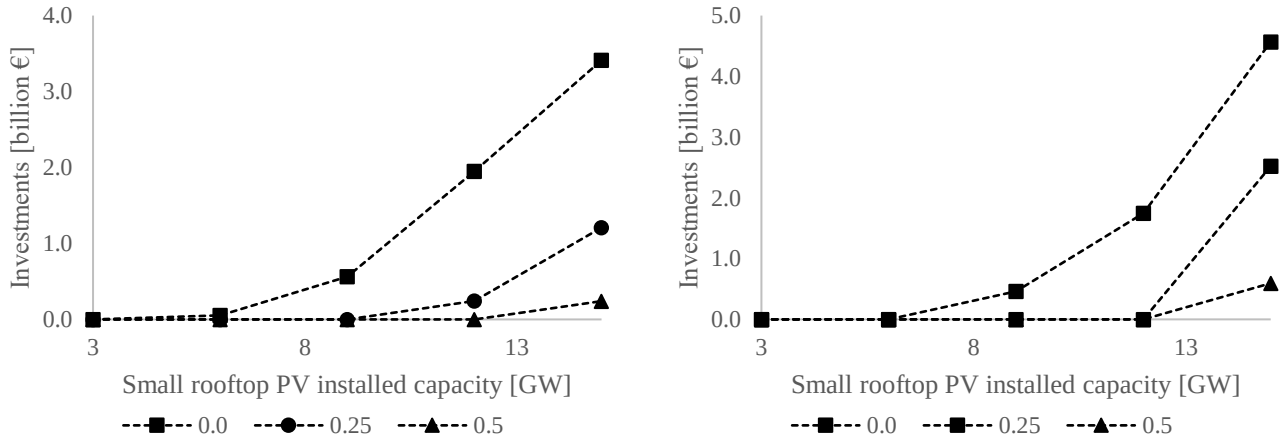

Figure 4.3: Infrastructure investments for increasing small rooftop PV capacities with different direct (left) and local (right) self-consumption rates

In Figure 4.4, the effect of increasing large rooftop PV capacity is shown with varying rates of direct self-consumption. Figure 4.5 shows the effect of increasing onshore wind and large PV installations (rooftop and parks) generation with varying rates of local self-consumption. Instead of installed capacity, the annual generation is varied as wind turbines and PV systems each operate with different load hours. The share of the annual generation by PV and wind is assumed to be 50% each. Based on load hours of 854 and 3327 hours for PV and onshore wind respectively[7], each TWh of generation results in 0.59 GW PV and 0.15 GW onshore wind capacity. Varying one value of self-consumption is done with the other values kept at 0. For both direct and local self-consumption, the marginal effect of increasing self-consumption is substantial at low values, but decreases at higher values. At 12 TWh the investments are 0 as this describes the situation in the reference year.

[7]Load hours used in the Dutch climate agreement (*Klimaatakkoord*, 2019)

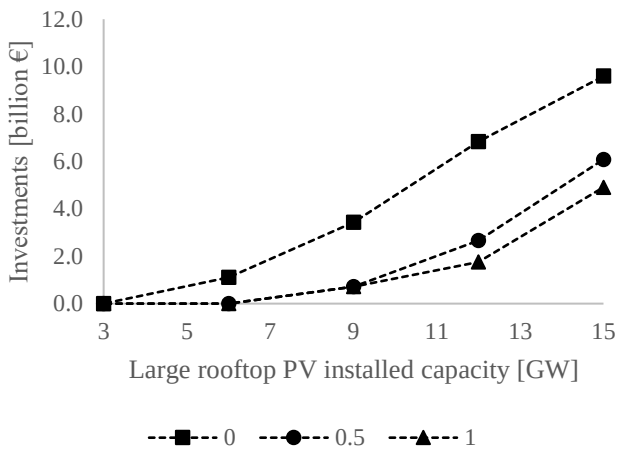

Figure 4.4: Infrastructure investments for increasing large rooftop PV capacities with different direct self-consumption rates

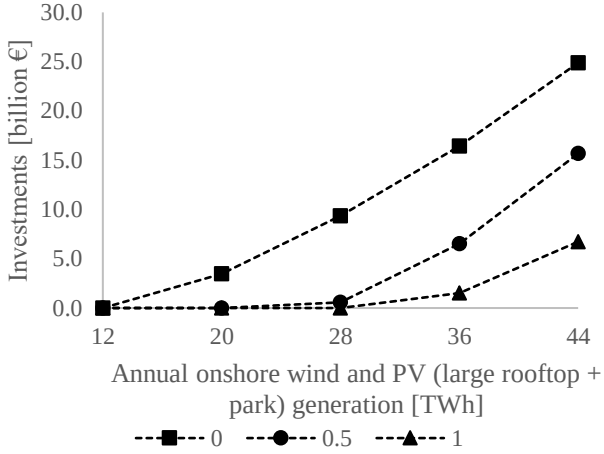

Figure 4.5: Infrastructure investments for increasing onshore wind and large PV generation with different local self-consumption rates

Finally, Figure 4.6 shows the effect of increasing offshore wind capacity. No other structural parameters are directly relevant for offshore wind. However, a distinction is made between investments required for the offshore grid extensions and infrastructure investments of current infrastructure.

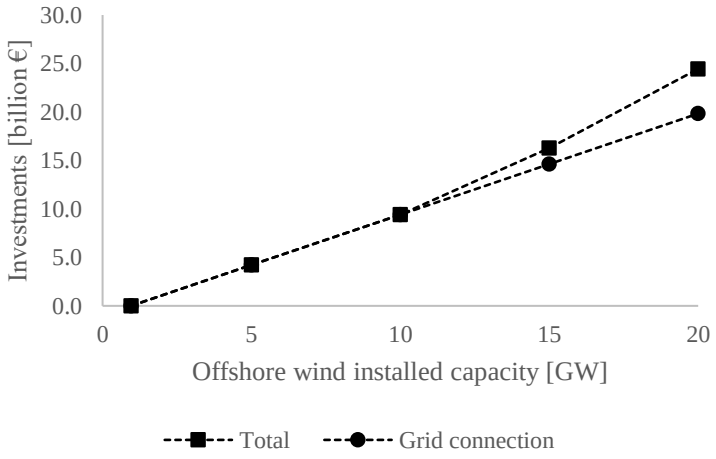

Figure 4.6: Capital investments for increasing offshore wind capacity, distinguishing between grid connection costs and capacity expansion costs of the existing infrastructure

4.1.2 Structural parameters

Structural parameters are not linked to any specific scenario parameter, but to the main structure of the model itself. To assess the effect of their uncertainties on the infrastructure investments a sensitivity analysis is performed. For the sensitivity analysis, one scenario is selected which corresponds with the targets that are set in the Dutch climate agreement for 2030 (*Klimaatakkoord*, 2019). The values of each scenario parameter is listed in appendix A3. The resulting infrastructure investments per voltage level are shown in Figure 4.7. The structural parameters are varied within the uncertainty ranges listed in appendix A3.

Figure 4.7: Infrastructure investments for the 2030 scenario, totalling € 37.1 billion

Figure 4.8 shows the relation between the average stochastic coincidence factor of consumers connected to the LV level and the infrastructure investments. The coincidence factor is varied by changing average grid connection capacities between the minimum and maximum values listed in Table 3.1. This factor is directly related to the stochastic coincidence factors. Figure 4.9 shows the relation between the intercategorical coincidence factor and the infrastructure investments.

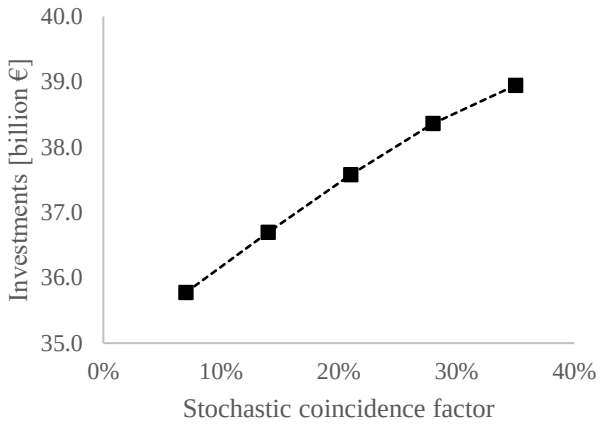

Figure 4.8: The effect of the average stochastic coincidence factor on infrastructure investments

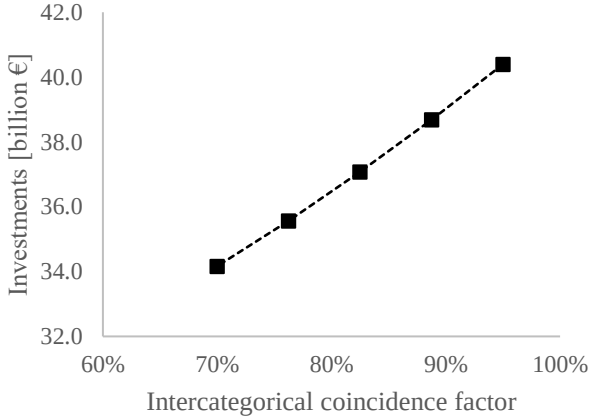

Figure 4.9: The effect of the intercategorical coincidence factor on infrastructure investments

Figure 4.10 shows the effects of changing the division of annual electricity consumption between small/large service sector and industrial consumers. A share of 20% refers to a division of 20/80 between small and large consumers.

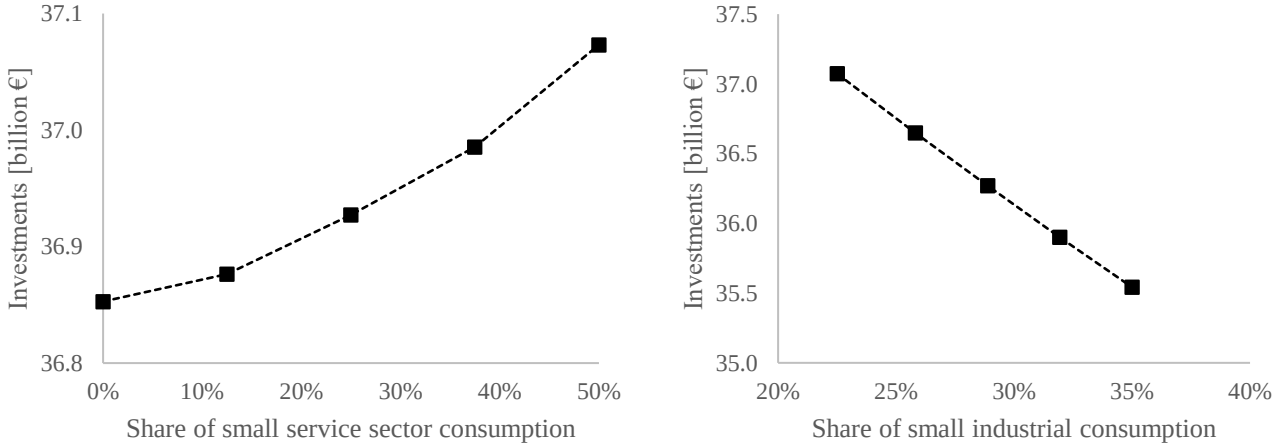

Figure 4.10: The effects of the division of annual electricity consumption between small/large service sector (left) and industrial (right) consumers

The effect of different combinations of minimum and maximum CHP commitment for the reference and scenario years is assessed in Figure 4.11. Furthermore, the effects of varying the reinvestment value listed in Table 3.7 is shown in Figure 4.12. Finally, Figure 4.13 shows the effects of lowering reserve capacities in the 2030 scenario year, while the reserve capacity for the reference year is held constant.

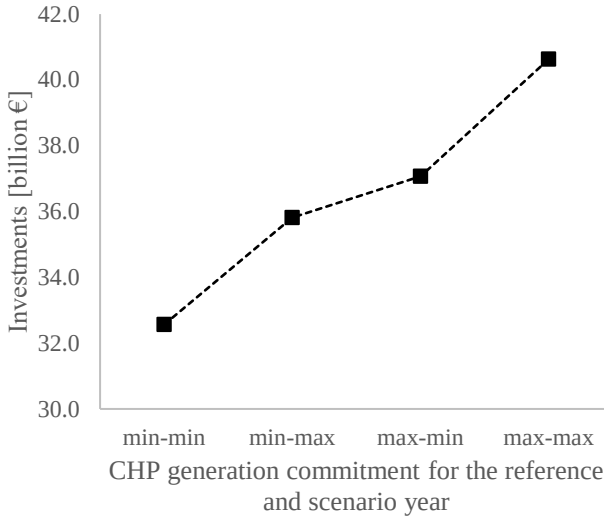

Figure 4.11: The effects of varying the minimum and maximum CHP generation commitment for the reference and scenario years respectively

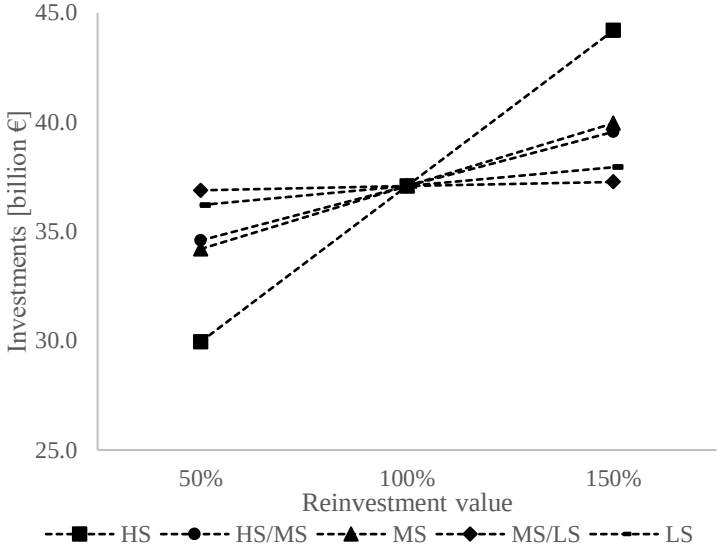

Figure 4.12: The effects of varying the reinvestment value per voltage level and transformer step

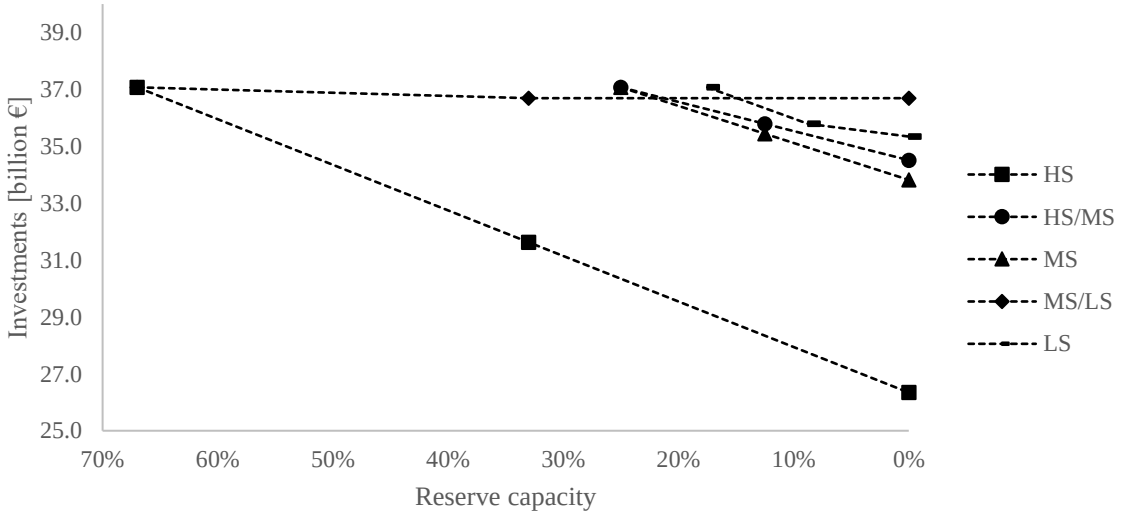

Figure 4.13: The effect of lowering reserve capacity for the future scenario year

4.2 Peak load analysis

While the previous section assessed the grid simulation model with respect to the infrastructure investments, this section will focus on the peak loads on grid assets. Section 4.2.1 will compare modelled peak loads on substations and distribution transformers from the reference scenario with data obtained from grid operators. In section 0, the changes in peak loads resulting from altering scenario parameters will be assessed regarding its logical consistency.

4.2.1 Transformer peak load validity

Substations

The peak loads on all HV/MV substations were measured by the regional grid operators and reported to TenneT. Based on these measurements, the sum of all peak loads on the HV/MV substations were expected to be just over 20 GW for 2018 (TenneT, 2017).

For the reference scenario of the grid simulation model, substation (HV/MV) peak loads depend mainly on three parameters: the division of electricity consumption between small and large industrial consumers, the intercategorical coincidence factor and the generation commitment of CHP. The uncertainty ranges of these parameters are listed in appendix A3. The scenario parameters of the reference scenario are also listed in appendix A3. The resulting

substation peak loads within these uncertainty ranges are shown in Figure 4.14. The measured peak load of 20 GW falls within the modeled uncertainty range.

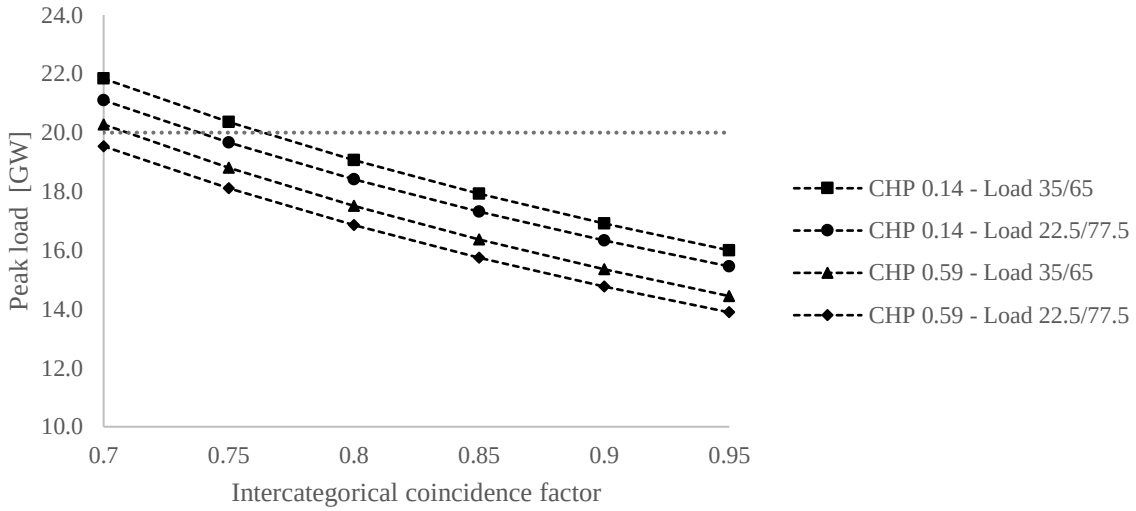

Figure 4.14: Peak load on HV/MV substations for the reference scenario for various combinations of intercategorical coincidence factors, CHP generation commitment and large/small industry division, in comparison to grid operator estimations

Distribution transformers

For distribution transformers, no measured peak load data is available. However, the total capacity can be estimated based on the total number of distribution transformers of 97k (Table 3.6) and the average transformer capacity of approximately 400 kVA (W. van Westering, Alliander, personal communication, February 5, 2020). This results in a total capacity of 38.8 GVA, or 38.8 GW when a power factor of 1 is assumed.

For the reference scenario of the grid simulation model, the installed MV/LV capacity depends on two parameters: the average maximum loads of LV consumers and the reserve capacity of MV/LV distribution transformers. The uncertainty ranges of these parameters are listed in appendix A3. The scenario parameters of the reference scenario are also listed in appendix A3. The resulting distribution transformer peak loads are shown in Figure 4.15. The estimated capacity of 38.8 GW falls within the modeled uncertainty range.

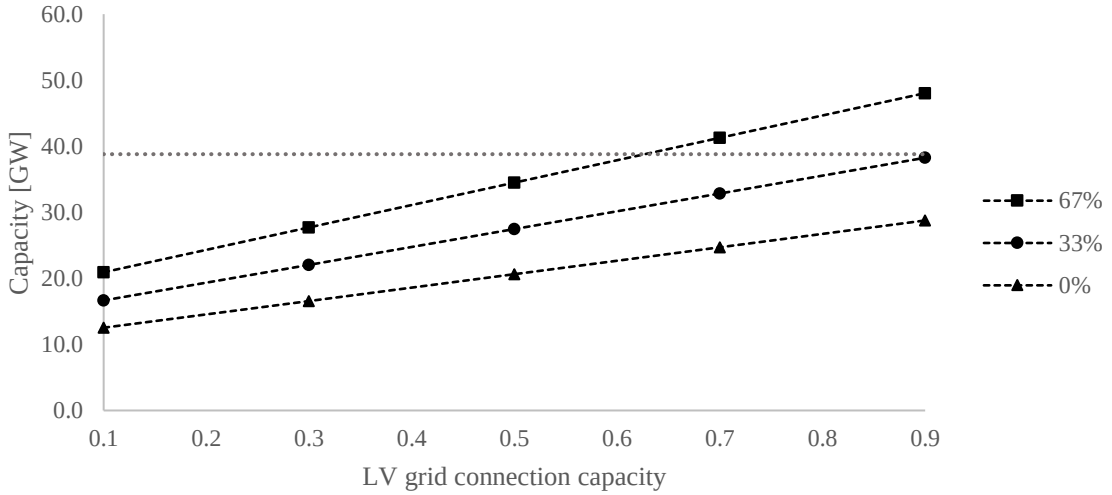

Figure 4.15: Peak load on MV/LV distribution transformers for the reference scenario for various combinations of average maximum loads of LV consumers and the reserve capacities of MV/LV distribution transformers, in comparison to the estimated transformer capacity

4.2.2 Peak load behavior

Peak loads on grid assets depend on both the generation and load (equations 3.7 up to 3.11). The effect of increasing VRE generation capacity on peak loads is shown in Figure 4.16. The total VRE generation capacity (0 – 60 GW) displayed on the x-axis is divided 50/50 between wind and PV capacity. The wind capacity is divided 25/25/50 between small onshore, large onshore and offshore wind parks respectively. PV capacity is divided 25/25/50 between large rooftop PV, PV parks and small rooftop PV respectively. For all other parameters, the base values (structural parameters) and reference values (scenario parameters) in appendix A3 are used. Figure 4.16 shows that the peak loads increase quicker for higher voltage levels than for lower voltage levels. On moments of surplus generation, all excess power is exported via the HV level.

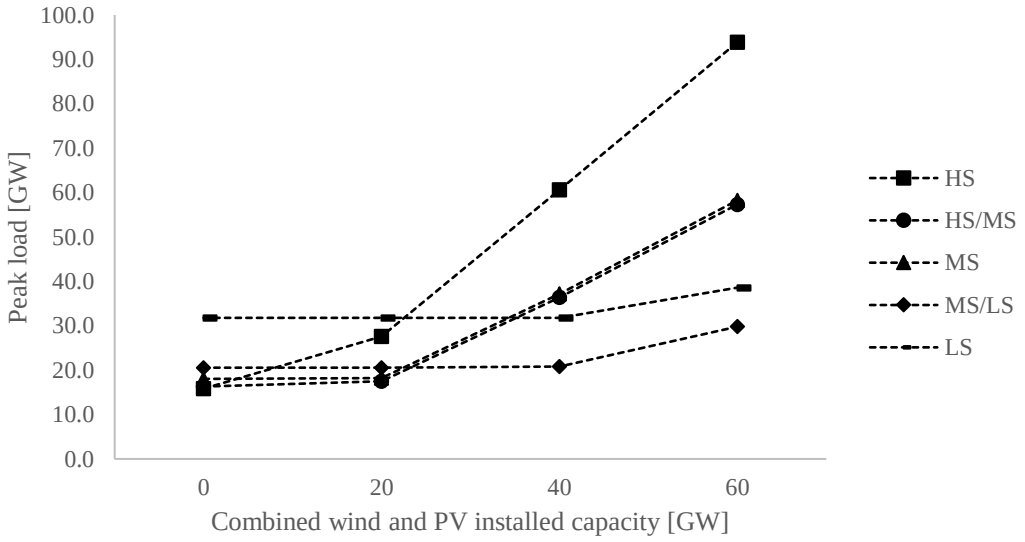

Figure 4.16: The effect of increasing VRE generation capacity on peak loads

The effect of increasing EV and heat pump adoption is shown in Figure 4.17. The adoption level of heat pumps is divided evenly between ground and air source heat pumps. For all other parameters, the base values (structural parameters) and reference values (scenario parameters) in appendix A3 are used. Figure 4.17 shows that the peak loads on each voltage level increase at a similar pace.

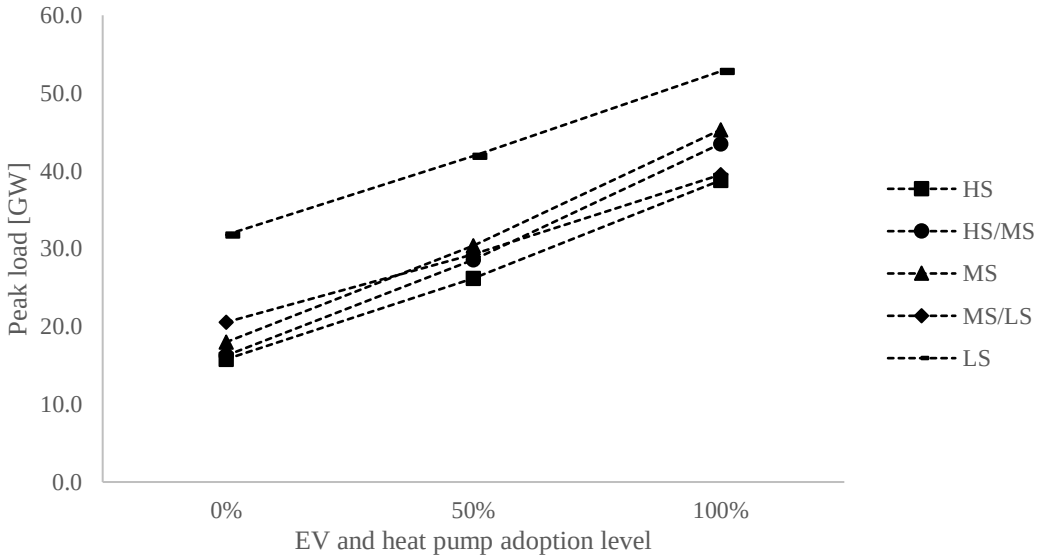

Figure 4.17: The effect of increasing EV and heat pump adoption level on peak loads

4.3 Profile analysis

Heat pump load profile

The heat pump profile generated based on household natural gas demand (section 3.1.3) is compared with a heat pump profile based on actual measurement data from household heat pumps in the United Kingdom (Love et al., 2017). An average measured heat pump profile for a winter weekday with an external temperature of 5.0 ˚C is shown in Figure 4.18. The heat pump profile used in the grid simulation model for a similar winter weekday with an external temperature of 4.8 ˚C is shown in Figure 4.19. The heat pump profiles do share similarities. Both have a morning peak and an evening peak at roughly the same times. However, for the natural gas based heat pump profile the difference between the highest and lowest power is much larger than for the actual heat pump profile.

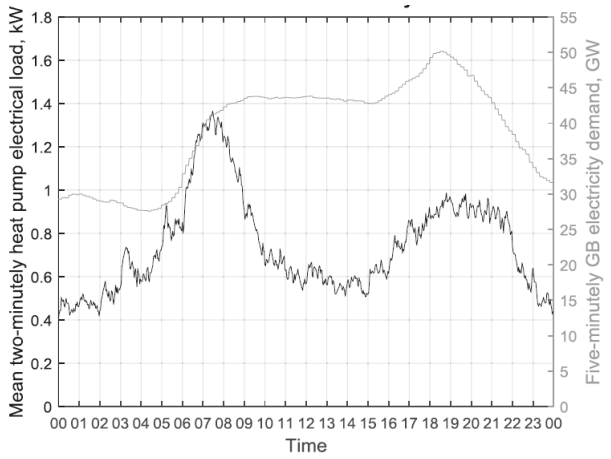

Figure 4.18: Average heat pump profile of a winter weekday in the United Kingdom with an external temperature of 5.0 ˚C (Love et al., 2017)

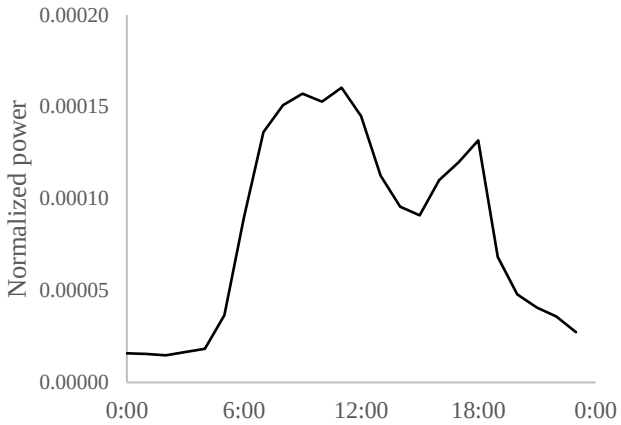

Figure 4.19: Normalized heat pump profile from the grid simulation model of a winter weekday in the Netherlands with an external temperature of 4.8 ˚C

To assess differences regarding impacts on peak loads, Figure 4.20 and Figure 4.21 show the national peak loads including a 20% heat pump adoption level. Figure 4.20 shows the heat pump profile with the national load profile of the United Kingdom based on Love et al. (2017). Figure 4.21 shows the profile of the Netherlands based on the grid simulation model.

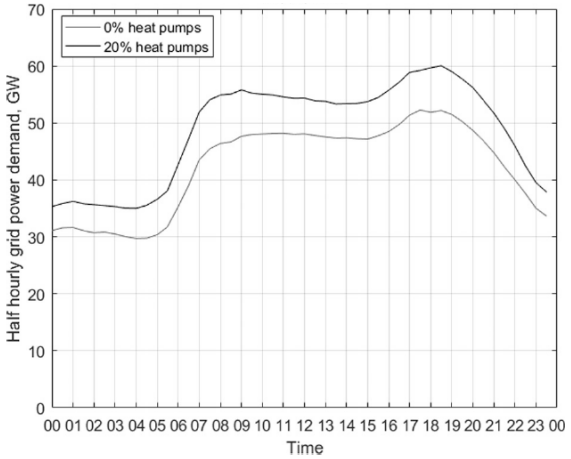

Figure 4.20: National load at the day of maximum demand for the United Kingdom with a 20% heat pump adoption level (Love et al., 2017)

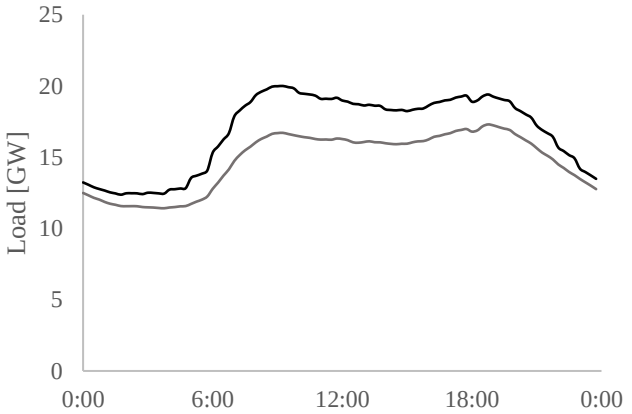

Figure 4.21: National load at the day of maximum demand for the Netherlands with a 20% heat pump adoption level (black) and without (grey) based on the grid simulation model

Love et al. (2017) report a 14.3% increase in annual maximum demand resulting from 20% heat pump adoption. In the grid simulation model, maximum demand increases with 8.3% based on 10% ground source and 10% air source heat pumps with SCOPs of 3.5 and 2.6 respectively (section 3.1.3). However, the increase in maximum national demand changes substantially for different SCOPs (Figure 4.22).

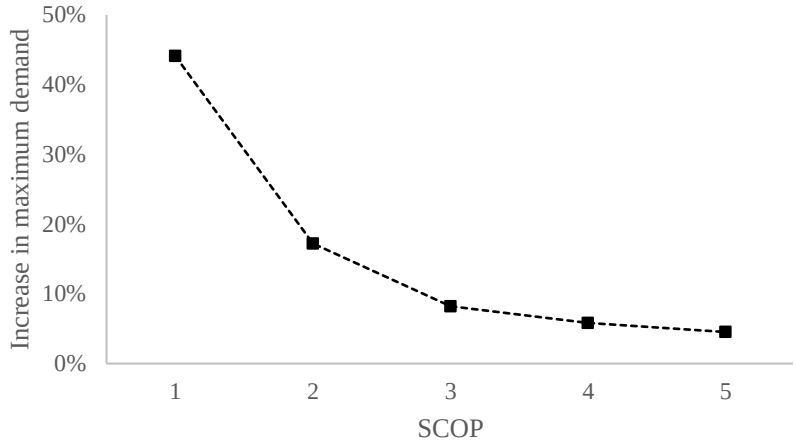

Figure 4.22: Relation between heat pump SCOP and increase of maximum national demand

Electric vehicle load profile

The EV load profile generated based on Dutch transport data (section 3.1.3) is compared with the EV load profiles drafted in a report carried out on behalf of 'Netbeheer Nederland' (Visser et al., 2013). Similar to the grid simulation model, the report distinguishes between a 'charging everywhere' scenario and a 'residential charging' scenario, using similar charging speeds (3.7 kW residential and 11 kW non-residential). The national load profiles for a fully electrified car fleet are shown in Figure 4.24. The EV load profiles used in the grid simulation model are shown in Figure 4.23.

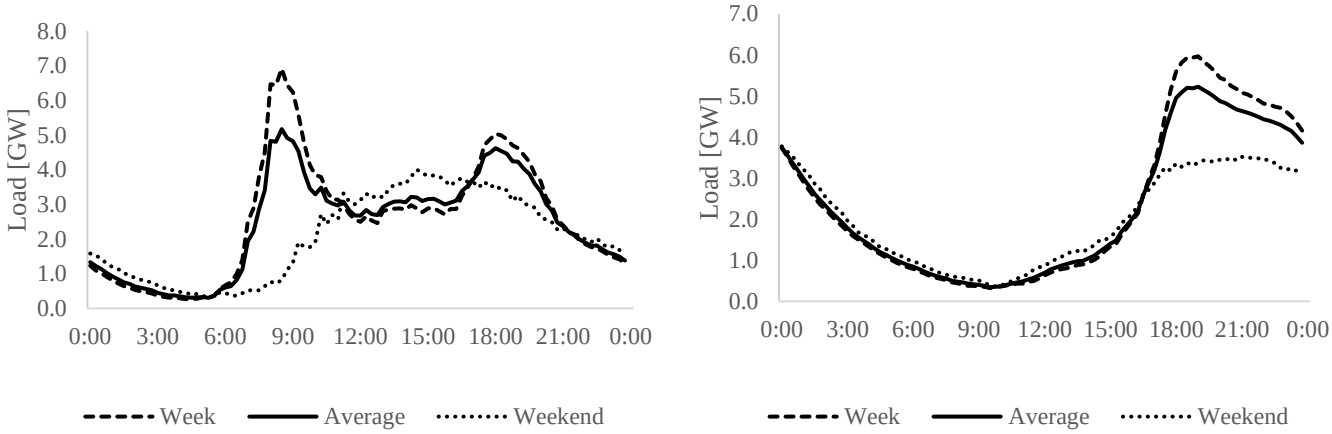

Figure 4.23: Modelled national EV load profiles used in the grid simulation model for with 100% EV adoption for the 'charging everywhere' scenario (left) and the 'residential charging' scenario (right)

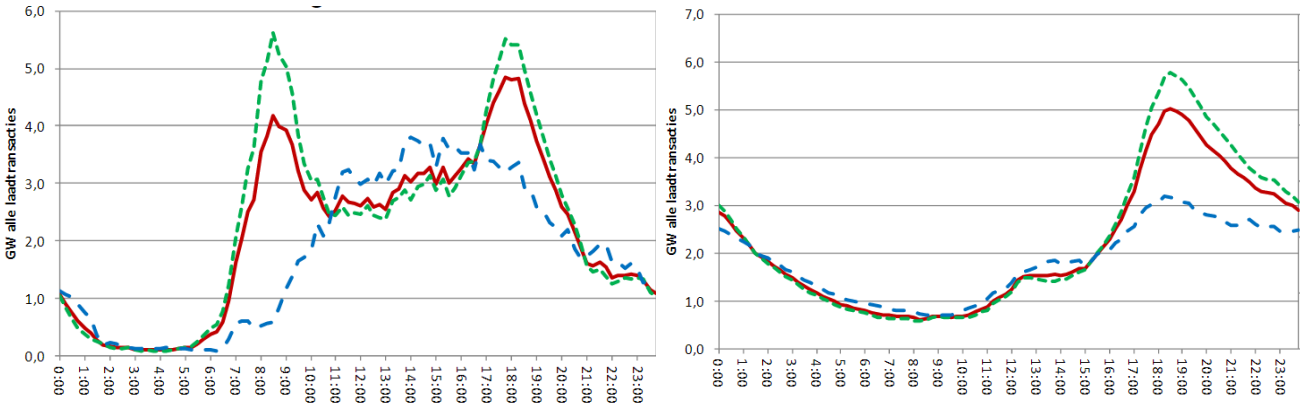

Figure 4.24: Modelled EV load profiles for a fully electrified car fleet for the 'charging everywhere' scenario (left) and the 'residential charging' scenario (right), for a weekday (green), weekend day (blue) and the weekly average (red) by Visser et al. (2013)

The load profiles from Visser et al. (2013) are very similar to the load profiles used in the grid simulation model. Both have clear morning and evening peaks for the ‘charging everywhere’ scenario which correspond to morning and evening commutes. Both profiles also share similar evening peaks for the ‘residential charging’ scenario. However, the magnitude in morning and evening peaks differ by roughly 10% with the EV profiles from Visser et al. (2013). This could be explained by the 6.7% increase in driven kilometres by passenger cars since 2013 (CBS, 2019d) and perhaps by changes in the distribution of transport movements over the day between 2013 and 2018.

5 DISCUSSION

Sophisticated grid simulation models are complex, requiring a lot of data and computing power. For PBL Netherlands Environmental Assessment Agency, building, operating and maintaining such a model for the entire Dutch power grid may not be feasible. This study set out to make a first step in developing a simplified grid simulation model, with the aim of forecasting infrastructure costs associated with changes in renewable energy generation and electrification of energy demand. The model developed in this study represents the Dutch power system using nationally aggregated consumer and producer classes. These exchange power via a nationally aggregated representation of the power grid split in a high-, medium- and low voltage level. In this chapter, the modelling results are discussed in light of relevant literature to identify strengths and limitations of the model, and to obtain novel insights and ideas for future research.

5.1.1 Discussion of results

The analyses show that more PV and wind generation leads to a small increase in peak loads and infrastructure investments at first, but a larger increase as generation capacity grows further. This is in line with the findings by Lemmens et al. (2017), who concluded that up to a certain point, installed rooftop PV capacity would not lead to increased peak loads on grid assets. This result is expected as the power flows induced by load and generation are not cumulative. Consequently, generation induced peak loads only start to affect annual peak loads when they become larger than peak loads induced by power consumption. Furthermore, as the adoption level of EVs and heat pumps rise, peak loads and infrastructure investments start to increase directly. When following the same line of reasoning, this result is also expected as the additionally induced peak loads and the peak loads of conventional load are cumulative.

Furthermore, the increase in peak loads at higher penetrations of wind and PV generation are substantially higher for the high voltage infrastructure than for the low voltage infrastructure. However, this contradicts the findings by Netbeheer Nederland (2017). In this report, large amounts of decentralized PV and wind capacity did not lead to a disproportional increase in peak loads on HV infrastructure. The reason for this disparity lies in the differences in flexibility options. Netbeheer Nederland (2017) incorporated substantial amounts of storage, flexible demand as well as some curtailment, which balances supply and demand on a local level. In the grid simulation model, no flexibility measures were included as this falls outside the scope of the research. Consequently, at moments of surplus PV and wind generation, all excess power is transferred to the HV level to be exported for preserving the balance between supply and demand. However, if neighboring countries also have substantial wind and PV generation capacity, it is not realistic to expect power can be exported. Therefore, some form of flexibility is required regardless, resulting in lower peak loads on HV infrastructure. In short, the grid simulation model simulates peak loads on the higher voltage levels that are unrealistically high for moments of excess wind and PV generation, leading to overestimation of required infrastructure investments. It is therefore important that flexibility options are included in novel grid simulation models, as peak loads apparently cannot be assessed without also taking into account realistic supply and demand balancing. In order to assess the costs associated with the implementation of flexibility options, the frequency and volume with which flexibility are to be applied must be known. This requires realistic real-time profiles for combined heat and power (CHP)-, wind- and PV generation, instead of the alternatives used in this study. To preserve the ability of a grid simulation model to include extreme weather events, wind and PV generation could be simulated using probability density functions (Borowy & Salameh, 1996).

For self-consumption, the analyses show that increased direct and local self-consumption substantially reduce the infrastructure costs resulting from increased wind and PV generation. Other studies have not directly reported the effects of self-consumption independent from other input variables and therefore these results cannot be compared. However, it is evident that increased rates of self-consumption should lead to reduced electrical loads on grid assets. Realistic behavior of local and direct self-consumption are intrinsic features of grid simulation models using a bottom-up approach, such as the models developed by Veldman et al. (2013) and van Westering et al. (2016). However, this is not the case for models using aggregated representations of the power grid and its consumers, such as the models developed by Rooijers & Leguijt (2010), Blom et al. (2012), Rooijers et al. (2014), and Alfman &

Rooijers (2017). Although these models did include a parameter for direct self-consumption, local self-consumption was not addressed. The copper plate representation of each voltage levels in these models intrinsically assumes maximum local self-consumption, resulting in an underestimation of the impact of increasing decentralized wind and PV generation on infrastructure investments. In short, addressing direct and local self-consumption for simplified grid simulation models is crucial. This study has made an attempt of incorporating these factors, but more research is required to represent the behavior of self-consumption of decentralized generation more accurately.

The analyses also indicate that increased coincidence factors of conventional consumer loads result in higher infrastructure investments. The reasoning behind this may seem counterintuitive, but is logically consistent. If all individual load patterns fully coincide, the average load profile is equal to the load profile of an individual consumer. Consequently, peak loads on grid assets decrease as the coincidence factor increases. Lower asset peak loads from conventional loads result in larger increases in peak loads, in percentage terms, from additional consumer load (EVs or heat pumps) or additional generation capacity (wind or PV). A larger increase in peak loads lead to a larger increase in additional capacity requirements and therefore lead to higher infrastructure investments. This is an interesting result since an increased coincidence factor is normally associated with increased asset peak loads (Bary, 1945). The apparent contradiction stems from the fact that the conventional use of coincidence factors is to describe the combined load profile, starting from individual consumer load. In this study it is used the other way around, with the combined load profile already available. To more accurately determine coincidence factors, it is important to get more accurate data regarding structural characteristics of the power grid. Examples for this would be the average number of households connected to a single LV cable or distribution transformer, or the load profiles of agricultural, service sector and industrial consumers. Since these data are currently only available to grid operators, it is crucial to intensify the level of data exchange between PBL and grid operators. The same holds for other parameters such as the investment costs of grid assets, current and future reserve capacity and the division of consumer load among the different voltage levels.

For heat pumps and EVs, there are a few notable findings regarding their effect on infrastructure investments. First of all, a heat pump profile based on household gas consumption is not a fully accurate representation of the actual national heat pump load. However, this inaccuracy is overshadowed by the uncertainty introduced by the average seasonal coefficient of performance (SCOP). A way to address this would be to replace the SCOP by a variable coefficient of performance based on real-time outside temperatures (air and soil) and performance characteristics of frequently used heat pumps. Secondly, for EVs the main source of uncertainty stems from the average charging capacity on the low voltage level. Therefore, forecasts regarding the development of residential charging infrastructure requires extra attention.

5.1.2 Reflection on modelling approach

As discussed in the previous section, the nationally aggregated grid simulation model does express some important features which resemble the behavior expected from the actual power system. However, the uncertainties of the modelling outcomes are of such magnitudes that no meaningful validation of the resulting infrastructure costs can yet be performed. Therefore, only interim results have yet been assessed, such as the model sensitivity to individual input parameters, peak loads and individual load profiles. Based on the insights acquired in the previous section, there are four ways in which the accuracy of the model can be improved. First, flexibility options must be added to the model. Secondly, additional research into parameters regarding self-consumption is required. Thirdly, additional load and generation profiles can be included, such as CHP generation profiles or agricultural, service sector and industrial load profiles. Finally, better input data is required regarding structural characteristics of the power grid as well as the investment costs and reserve capacities of grid assets. After these improvements have been implemented, the external validity of the model should be assessed. For this, infrastructure costs forecasted by the model can be compared to cost assessments made by the distribution- and transmission system operators. If the improvements do not lead to sufficient external validity of the grid simulation model, some of its core assumptions may need to be addressed in future research.

The main pillar on which the grid simulation model is based is its nationally aggregated representation of the power grid. Even though parameters are introduced to take into account structural characteristics that would otherwise get

lost in this simplification (coincidence factors and self-consumption rates), some factors are not accounted for. For example, the distribution of new large scale power producers or consumers can affect the peak loads on high voltage grid assets, capacity expansion costs may be different for different regions or adoption of heat pumps or EVs may differ per region. These regional differences are assumed to average out at a national level. If this assumption does not hold, the model should differentiate between different regions. These could either be based on geographical location or on other characteristics such as population density (e.g. urban vs rural). Another key assumption is that changes in power quality will not have a large influence on the infrastructure costs. If this assumption does not hold, parameters should be introduced that correct for this. Furthermore, no temporary overcharging of grid assets is allowed in the power grid model. In practice, grid operators may allow this in certain situations, reducing the requirement for capacity expansion. If the effect of this discrepancy is significant, it must also be corrected for.

Addressing these assumptions used for simplifying the power system inherently leads to increased levels model complexity. Since the primary goal is to develop a simplified grid simulation model, too much complexity can result in a model that is inoperable for PBL Netherlands Environmental Assessment Agency. Therefore, future research should always carefully consider the complexity of the model while trying to improve its accuracy. However, one should take into consideration that there is a possibility that it might not be feasible for a model of the Dutch power grid to be both highly simplified and sufficiently accurate.

6 CONCLUSION

A first step is made in the development of a simplified grid simulation model, used for forecasting Dutch infrastructure costs associated with increased renewable energy generation and electrification of energy demand. A nationally aggregated representation of the power grid is used in which power flows are simulated using nationally aggregated load and generation profiles. Based on the power flow simulation, required capacity of grid assets for a reference year and a freely configurable future scenario year are determined. This is then translated into capacity expansion requirements and eventually used to calculate infrastructure costs.

Effects of different structural and data-related modelling aspects on the modelling results have been charted. First of all, the simplified grid simulation model did express some important features which resemble the behavior expected from the actual power system. However, unrealistic model behavior also occurred resulting from the absence of flexibility options such as energy storage, demand response and curtailment. Furthermore, modelling results are accompanied by large uncertainties, requiring further research into the role of self-consumption for decentralized generation and more access to accurate input data from grid operators. Before these data improvements and structural changes have been implemented in the model, the model cannot be externally validated in a way that could confirm its overall accuracy. Therefore, it is too early to deliver a final verdict regarding the overall usefulness of the chosen modelling approach. However, if after implementation of the aforementioned improvements, the external validity of the model is not sufficient, some of the core assumptions used for simplifying the power system might need to be addressed. Because this inevitably leads to increased model complexity, future research should carefully consider the drawback of reducing model simplicity for increasing its accuracy, as this could defeat the purpose of using a simplified grid simulation model in the first place.

REFERENCES

Aalberts, A., Dekker, G., Jaarsma, S., Tieben, B., & Vlug, N. (2011). Onderzoek naar de methodologie voor de verdeling van de kosten van netverliezen. *KEMA, NMa, SEO*. https://zoek.officielebekendmakingen.nl/blg-114695.pdf

Abd El-Aal, A. E.-M. M., Schmid, J., Bard, J., & Caselitz, P. (2006). *Modeling and optimizing the size of the power conditioning unit for photovoltaic systems*.

Aien, M., Khajeh, M. G., Rashidinejad, M., & Fotuhi-Firuzabad, M. (2014). Probabilistic power flow of correlated hybrid wind-photovoltaic power systems. *IET Renewable Power Generation*, *8*(6), 649–658.

Alfen. (n.d.). *Complete energieoplossingen voor de tuinbouw*. https://alfen.com/sites/alfen.com/files/downloads/Brochure%20Complete%20oplossing%20voor%20glastuinbouw%20NL.pdf

Alfman, M., & Rooijers, F. J. (2017). *Net voor de toekomst—Achtergrondrapport* (17.3L53.170). https://www.netbeheernederland.nl/_upload/Files/Achtergrondrapport_Net_voor_de_toekomst_113.pdf

Algemene energieraad. (2009). *De ruggengraat van de energievoorziening*. https://zoek.officielebekendmakingen.nl/blg-42516

Alvarez, D. L., Rivera, S. R., & Mombello, E. E. (2019). Transformer Thermal Capacity Estimation and Prediction Using Dynamic Rating Monitoring. *IEEE Transactions on Power Delivery*, *34*(4), 1695–1705.

Bary, C. (1945). Coincidence-factor reationships of electric-service-load characteristics. *Transactions of the American Institute of Electrical Engineers*, *64*(9), 623–629.

Blok, K., & Nieuwlaar, E. (2016). *Introduction to energy analysis*. Taylor & Francis.

Blom, M. J., Bles, M., Leguijt, C., Rooijers, F. J., van Gerwen, R. J. F., van Hameren, D., & Verheij, F. (2012). *Maatschappelijke kosten en baten van Intelligente Netten* (12.3435.10). KEMA & DNV GL. https://www.ce.nl/publicaties/download/1271

Borowy, B. S., & Salameh, Z. M. (1996). Methodology for optimally sizing the combination of a battery bank and PV array in a wind/PV hybrid system. *IEEE Transactions on Energy Conversion*, *11*(2), 367–375.

CBS. (n.d.). *Slim zonnestroom in kaart brengen* [Webpagina]. Centraal Bureau voor de Statistiek. Retrieved April 11, 2020, from https://www.cbs.nl/nl-nl/onze-diensten/innovatie/project/slim-zonnestroom-in-kaart-brengen

CBS. (2015). *Energieverbruik in de landbouw*. Centraal Bureau voor de Statistiek. https://www.cbs.nl/nl-nl/onze-diensten/methoden/onderzoeksomschrijvingen/korte-onderzoeksbeschrijvingen/energieverbruik-in-de-landbouw

CBS. (2019a). *Onderweg in Nederland (ODiN)*. https://easy.dans.knaw.nl/ui/datasets/id/easy-dataset:73441/tab/2

CBS. (2019b). *Opgesteld vermogen zonnepanelen*. Centraal Bureau voor de Statistiek. https://www.cbs.nl/nl-nl/nieuws/2019/17/vermogen-zonnepanelen-meer-dan-de-helft-toegenomen

CBS. (2019c). *Opgesteld warmtekrachtvermogen, 1998-2017*. Centraal Bureau Voor de Statistiek. https://www.clo.nl/indicatoren/nl0387-warmtekracht-vermogen

CBS. (2019d). *Verkeersprestaties personenauto's; kilometers, brandstofsoort, grondgebied*. Centraal Bureau voor de Statistiek. https://opendata.cbs.nl/statline/#/CBS/nl/dataset/80428NED/table?dl=25AB8

CBS. (2020a). *Energiebalans; aanbod en verbruik, sector*. Centraal Bureau voor de Statistiek. https://opendata.cbs.nl/statline/#/CBS/nl/dataset/83989NED/table?ts=1584532424170

CBS. (2020b). *Personenauto's; voertuigkenmerken, regio's, 1 januari*. Centraal Bureau voor de Statistiek. https://opendata.cbs.nl/statline/#/CBS/nl/dataset/71405NED/table?fromstatweb

Chatterjee, S., & Mandal, S. (2017). *A novel comparison of gauss-seidel and newton-raphson methods for load flow analysis*. 1–7.

Danish Energy Agency. (2015). *Flexibility in the Power System—Danish and European experiences*. https://ens.dk/sites/ens.dk/files/Globalcooperation/flexibility_in_the_power_system_v23-lri.pdf

Demirok, E., Gonzalez, P. C., Frederiksen, K. H., Sera, D., Rodriguez, P., & Teodorescu, R. (2011). Local reactive power control methods for overvoltage prevention of distributed solar inverters in low-voltage grids. *IEEE Journal of Photovoltaics*, *1*(2), 174–182.

Elektriciteitswet, Pub. L. No. BWBR0009755 (1998). https://wetten.overheid.nl/BWBR0009755/2020-02-01

Energiekaart. (n.d.). Overzicht Nederlandse Windparken. *Kennisplatform Energiesystemen*. Retrieved March 22, 2020, from https://www.energiekaart.net/overzicht-nederlandse-windparken/

ENTSO-E. (n.d.). *ENTSO-E Transparency Platform*. Retrieved March 19, 2020, from https://transparency.entsoe.eu/

Esmat, A., Usaola, J., & Moreno, M. Á. (2018). Distribution-level flexibility market for congestion management. *Energies*, *11*(5), 1056.

European Comission. (2013). *2013/114/EU: Commission Decision of 1 March 2013 establishing the guidelines for Member States on calculating renewable energy from heat pumps from different heat pump technologies pursuant to Article 5 of Directive 2009/28/EC of the European Parliament and of the Council*. http://data.europa.eu/eli/dec/2013/114(1)/oj

Gasunie, & TenneT. (2019). *Infrastructure Outlook 2050*. https://www.tennet.eu/fileadmin/user_upload/Company/News/Dutch/2019/Infrastructure_Outlook_2050_appendices_190214.pdf

Gerritsma, M. K., AlSkaif, T. A., Fidder, H. A., & van Sark, W. G. (2019). Flexibility of electric vehicle demand: Analysis of measured charging data and simulation for the future. *World Electric Vehicle Journal*, *10*(1), 14.

Grahn, P., Munkhammar, J., Widén, J., Alvehag, K., & Söder, L. (2013). PHEV home-charging model based on residential activity patterns. *IEEE Transactions on Power Systems*, *28*(3), 2507–2515.

Guyer, J. P. (2017). *An Introduction to Electric Power Distribution*. Guyer Partners.

Heres, J., van Westering, W., van der Lubbe, G., & Janssen, D. (2017). Stochastic effects of customer behaviour on bottom-up load estimations. *CIRED-Open Access Proceedings Journal*, *2017*(1), 2543–2547.

Hers, S., Rooijers, F., Afman, M., Croezen, H., & Cherif, S. (2016). *Markt en flexibiliteit—Achtergrondrapport* (16.3E90.36). CE Delft. https://www.ce.nl/publicaties/download/2110

Hertem, D. V., Verboomen, J., Purchala, K., Belmans, R., & Kling, W. L. (2006). *Usefulness of DC power flow for active power flow analysis with flow controlling devices*. 58–62. https://doi.org/10.1049/cp:20060013

Hoen, A., Afman, M., & van Grinsven, A. (2017). *Uitbreiding publieke laadinfrastructuur to 2020* (16.4J72.119). CE Delft. https://www.rvo.nl/sites/default/files/2017/03/Rapport%20-%20Uitbreiding%20publieke%20laadinfrastructuur%20tot%202020.pdf

Hoogspanningsnet.com. (n.d.). Retrieved March 11, 2020, from https://www.hoogspanningsnet.com/

Kallrath, J. (2002). Planning and scheduling in the process industry. *OR Spectrum*, *24*(3), 219–250.

Klaassen, E., Frunt, J., & Slootweg, H. (2015). *Assessing the impact of distributed energy resources on lv grids using practical measurements*. *2015*, 5.

Klimaatakkoord. (2019). Ministry of Economic Affairs and Climate Policy.

Klimaatwet, Pub. L. No. BWBR0042394 (2019).

KNMI. (n.d.). *Uurgegevens van het weer in Nederland*. Retrieved March 31, 2020, from https://projects.knmi.nl/klimatologie/uurgegevens/selectie.cgi

Law, A. M. (2008). *How to build valid and credible simulation models*. 39–47.

Lemmens, J., van der Burgt, J., Bosma, T., van den Wijngaart, van B. B., & Koelemeijer, R. (2017). *Het potentieel van zonnestroom in de gebouwde omgeving van Nederland. Planbureau voor de Leefomgeving*. PBL. https://www.pbl.nl/sites/default/files/downloads/pbl-2014-dnv-gl-het-potentieel-van-zonnestroom-in-de-gebouwde-omgeving-van-nederland_01400.pdf

Lensink, S., Pişc, I., Strengers, B., Cleijne, H., Boots, M., Cremers, M., in 't Groen, B., Lemmens, J., Mast, E., Beurskens, L., Daey Ouwens, J., Smekens, K., Uslu, A., & Mijnlieff, H. (2019). *Eindadvies basisbedragen SDE+ 2019* (No. 3342). PBL. https://www.pbl.nl/sites/default/files/downloads/pbl-2018-eindadvies-basisbedragen-SDE-plus-2019_3342.pdf

Liander. (n.d.). *Liggingsgegevens elektriciteitsnetten*. Retrieved March 31, 2020, from https://www.liander.nl/partners/datadiensten/open-data/data/liggingsgegevens-elektriciteitsnetten

Liander. (2018). *Kleinverbruiksdata per jaar*. https://www.liander.nl/sites/default/files/Liander_kleinverbruiksgegevens_01012018.zip

Lieshout, M. (2017). *Visie op de toekomst van de Nederlandse procesindustrie: En de rol van het lectoraat Procesoptimalisatie en-intensificatie bij de realisatie daarvan*. Hogeschool Rotterdam.

Love, J., Smith, A. Z., Watson, S., Oikonomou, E., Summerfield, A., Gleeson, C., Biddulph, P., Chiu, L. F., Wingfield, J., & Martin, C. (2017). The addition of heat pump electricity load profiles to GB electricity demand: Evidence from a heat pump field trial. *Applied Energy*, *204*, 332–342.

Luthander, R., Widén, J., Nilsson, D., & Palm, J. (2015). Photovoltaic self-consumption in buildings: A review. *Applied Energy*, *142*, 80–94.

Martis, M. S. (2006). Validation of simulation based models: A theoretical outlook. *The Electronic Journal of Business Research Methods*, *4*(1), 39–46.

Medjroubi, W., Müller, U. P., Scharf, M., Matke, C., & Kleinhans, D. (2017). Open Data in Power Grid Modelling: New Approaches Towards Transparent Grid Models. *Energy Reports*, *3*, 14–21. https://doi.org/10.1016/j.egyr.2016.12.001

Ministerie van Economische Zaken. (2014). *Technische, ruimtelijke en organisatorische aspecten van het elektriciteitsnet voor de verbinding van windparken op zee op het landelijke hoogspanningsnet*. zoek.officielebekendmakingen.nl › blg-348049

Nadere regels omtrent een onafhankelijk netbeheer, Pub. L. No. BWBR0020608 (2006). https://wetten.overheid.nl/BWBR0020608/2014-08-01

Nederland, N. (2017). *Net voor de toekomst*. https://www.netbeheernederland.nl/_upload/Files/Achtergrondrapport_Net_voor_de_toekomst_113.pdf

NEDU. (2019). *Verbruiksprofielen*. https://www.nedu.nl/documenten/verbruiksprofielen/

Netbeheer Nederland. (n.d.). *Energiecijfers*. Retrieved April 6, 2020, from https://energiecijfers.info/hoofdstuk-1/

Netbeheer Nederland. (2019a). *Basisinformatie over energie-infrastructuur*. Netbeheer Nederland. https://www.netbeheernederland.nl/_upload/Files/Basisdocument_over_energie-infrastructuur_(oktober_2019)_161.pdf

Netbeheer Nederland. (2019b). *Position Paper voor het Rondetafelgesprek over Netcapaciteit*. https://www.netbeheernederland.nl/_upload/Files/Postition_paper_rondetafel_netcapaciteit_28_november_2019_162.pdf

Netcode elektriciteit, Pub. L. No. BWBR0037940 (2016). https://wetten.overheid.nl/BWBR0037940/2017-01-01

Nijland, H., Geilenkirchen, G., & Hilbers, H. (2019). *Achtergrondrapport bij effectschattingen mobiliteits-maatregelen klimaatakkoord*. Planbureau voor de Leefomgeving. https://www.pbl.nl/sites/default/files/downloads/pbl-2019-achtergronddocument-effecten-ontwerp-klimaatakkoord-mobiliteit-3703.pdf

Overbye, T. J., Cheng, X., & Sun, Y. (2004). *A comparison of the AC and DC power flow models for LMP calculations*. 9-pp.

Paris Agreement (No. 54113). (2016). UNFCCC.

Petinrin, J., & Shaabanb, M. (2016). Impact of renewable generation on voltage control in distribution systems. *Renewable and Sustainable Energy Reviews*, *65*, 770–783.

Rijksoverheid. (n.d.). *Windenergie op zee*. Ministerie van Algemene Zaken. Retrieved March 22, 2020, from https://www.rijksoverheid.nl/onderwerpen/duurzame-energie/windenergie-op-zee

Rooijers, F. J., & Leguijt, C. (2010). *Achtergrondrapportage bij NET-document Netbeheer Nederland* (10.3861.51). CE Delft. https://www.ce.nl/publicaties/1192/net-voor-de-toekomst-2010-studie

Rooijers, F. J., Schepers, B. L., van Gerwen, R. J. F., van der Veen, W., Verheij, F., de Buck, A., & Kampman, B. E. (2014). *Scenario-ontwikkeling energievoorziening 2030* (14.3C93.34). CE Delft & DNV GL. https://www.ce.nl/publicaties/1490/scenario-ontwikkeling-energievoorziening-2030

Rusck, S. (1956). The simultaneous demand in distribution network supplying domestic consumers. *ASEA Journal*, *10*(11), 59–61.

RVO. (2020a). *SDE (+) Projecten in beheer (januari 2020)*. https://www.rvo.nl/subsidie-en-financieringswijzer/stimulering-duurzame-energieproductie-sde/feiten-en-cijfers/feiten-en-cijfers-sde-algemeen

RVO. (2020b). *SDE viewer*. https://ez.maps.arcgis.com/apps/webappviewer/index.html?id=6185c5a3392e457491b65e962a37431c

Schavemaker, P., & Van der Sluis, L. (2017). *Electrical power system essentials*. John Wiley & Sons.

Stott, B. (1974). Review of load-flow calculation methods. *Proceedings of the IEEE*, *62*(7), 916–929.

Tarievencode elektriciteit, Pub. L. No. BWBR0037951 (2016). https://wetten.overheid.nl/BWBR0037951/2019-07-10#Hoofdstuk2

TenneT. (n.d.-a). *Net op zee Nederland*. Retrieved March 22, 2020, from https://www.tennet.eu/nl/ons-hoogspanningsnet/net-op-zee-projecten-nl/net-op-zee-nederland/

TenneT. (n.d.-b). *Our story*. Retrieved March 24, 2020, from https://www.tennet.eu/company/profile/our-story/

TenneT. (2017). *Kwaliteits- enCapaciteitsdocument 2017, Deel II: Investeringen Net op Land 2018—2027*. https://www.tennet.eu/fileadmin/user_upload/Company/Publications/Technical_Publications/Dutch/TenneT_KCD2017_Deel_II.pdf

TenneT. (2019). *Aansluiten op het Nederlandse hoogspanningsnet*. https://www.tennet.eu/fileadmin/user_upload/The_Electricity_Market/Dutch_Market/Digi_brochure_customersmarket_NLi_18JUNI2019.pdf

Tigchelaar, C. (2013). *Methodiek voor opslitsing CBS statistiek huishoudelijk gas- en elektriciteitsverbruik* (ECN-E--13-075). ECN. http://publications.tno.nl/publication/34629245/45C6Dl/e13075.pdf

Tijdig realiseren doelstellingen Energieakkoord, Pub. L. No. BWBR0037771 (2016). https://wetten.overheid.nl/BWBR0037771/2016-04-01

Topsector Energie. (n.d.). *Netcongestie blokkeert de energietransitie*. Retrieved April 9, 2020, from https://www.topsectorenergie.nl/spotlight/netcongestie-blokkeert-de-energietransitie

Transport & Environment. (2020). *Recharge EU: how many charge points will Europe and its Member States need in the 2020s*. European Federation for Transport and Environment AISBL. https://www.transportenvironment.org/sites/te/files/publications/01%202020%20Draft%20TE%20Infrastructure%20Report%20Final.pdf

Uitvoeringswet Algemene verordening gegevensbescherming, Pub. L. No. BWBR0040940 (2018). https://wetten.overheid.nl/BWBR0040940/2020-01-01/0/informatie

van de Sande, P., Danes, M., & Dekker, T. (2017). ANDES: grid capacity planning using a bottom-up, profile-based load forecasting approach. *CIRED-Open Access Proceedings Journal*, *2017*(1), 2097–2100.

van der Linden, N. H. (2019). *Inventarisatie van de behoefte van de industrieclusters aan grootschalige infrastructuur voor transport van elektriciteit, waterstof, warmte en CO2 nodig voor het realiseren van klimaatdoelstellingen* (TNO 2019 P10550). TNO. http://publications.tno.nl/publication/34634705/qMQ39W/TNO-2019-P10550.pdf

van der Velden, N. J. A., & Smit, P. X. (2013). *Groei elektriciteitsconsumptie glastuinbouw: Hoe verder?* LEI, onderdeel van Wageningen UR.

van Hout, M., Wetzels, W., & Daniëls, B. (2019). *Korte modelbeschrijving SAVE-Productie*. https://www.pbl.nl/sites/default/files/downloads/pbl-2019-korte-modelbeschrijving-save-productie_4033.pdf

van Melle, T., Menkveld, M., Oude Lohuis, J., de Smidt, R., & Terlouw, W. (2015). *De systeemkosten van warmte voor woningen*. Ecofys. https://repository.tudelft.nl/view/tno/uuid%3A9d49b1d3-107b-4f49-a36c-b606786bc207

van Oirsouw, P. (2012). *Netten voor distributie van elektriciteit*. Phase to Phase B.V. https://phasetophase.nl/boek/

van Westering, W., Heres, J., Dekker, T., Danes, M., & Hellendoorn, H. (2017). Assessing the Voltages and Currents in a large Dutch Regional Power Distribution Grid. *Energy-Open*, 53.

van Westering, W., Zondervan, A., Bakkeren, A., Mijnhardt, F., & van der Els, J. (2016). *Assessing and mitigating the impact of the energy demand in 2030 on the dutch regional power distribution grid*. 1–6.

Veldman, E., Gaillard, M., Gibescu, M., Slootweg, J., & Kling, W. (2010). *Modelling future residential load profiles*.

Veldman, E., Gibescu, M., Slootweg, H. J. G., & Kling, W. L. (2013). Scenario-based modelling of future residential electricity demands and assessing their impact on distribution grids. *Energy Policy*, *56*, 233–247.

Verzijlbergh, R., Lukszo, Z., Veldman, E., Slootweg, J., & Ilic, M. (2011). *Deriving electric vehicle charge profiles from driving statistics*. 1–6. https://doi.org/10.1109/PES.2011.6039609

Visser, R., Chang, M., Groenewoud, P., Duffhues, J., & Wolse, H. (2013). *Laadstrategie Elektrisch Wegvervoer* (EN-RL-120022359). Movares. https://www.netbeheernederland.nl/_upload/Files/Elektrisch_vervoer_11_ccede3d2ae.pdf

Wet verbod op kolen bij elektriciteitsproductie, Pub. L. No. BWBR0042905, Staatsbladvan het Koninkrijk der Nederlanden (2019).

Wind Europe. (2020). *Wind energy in Europe in 2019*. https://windeurope.org/wp-content/uploads/files/about-wind/statistics/WindEurope-Annual-Statistics-2019.pdf

Wind op zee. (n.d.). *Wat kost het net op zee?* [Overzichtspagina]. Retrieved April 10, 2020, from https://windopzee.nl/onderwerpen-0/wind-zee/kosten/kosten-net-zee/

APPENDICES

A1. Annual energy consumption per sector

Table A1.1, annual electricity consumption per sector

Industry	[PJ]	Service sector	[PJ]	Other	[PJ]
Paper	6.4	Water and waste management	8	Households	82.7
Graphical	1.7	Trade	31.1	Agriculture	35.7
Chemical	44.8	Transport and storage	13.1	Others	0.4
Pharmaceutical	1.7	Hospitality	11.5	Other	
Rubber and plastic	6.1	Information and communication	11.6		
Building materials	4.8	Financial services	5.3		
Basic metals	17	Rental and trade of real estate	4.6		
Metal products and machines	11.3	Specialized business services	4.6		
Transportation	2.6	Rental and other business services	2.6		
Furniture	0.7	Public administration and other government services	11.5		
Construction	3.7	Education	5.4		
Other	0.5	Healthcare	12.3		
		Culture, recreation and sports	5.4		
		Extraterritorial organizations	0.2		
		Repair and installation of machines	0.7		
		Other services	2.3		
Total	129.1	Total	133.2	Total	126.4

A2. Load division between large and small consumers

In the grid simulation model, service sector and industrial consumers are divided into small and large classes. However, because CBS (2020a) data does not discriminate between small and large consumers for the service sector and industry, the electricity consumption per class must be estimated. This is done by choosing a distributions such that the consumer peak load per voltage level (HV, MV and LV) match the consumer loads as modelled in a study by 'Netbeheer Nederland' (Rooijers & Leguijt, 2010). In this study, consumer peak loads were 3.1, 6,4 and 9,0 GW for the HV, MV and LV levels respectively, resulting in a national peak load of 18.5 GW (Rooijers & Leguijt, 2010).

For small and large industrial consumers, the total electricity consumption is 129.1 PJ (CBS, 2020a). For service sector consumers, the combined electricity consumption of the 100 – 300 kW small service sector and the large service sector consumers is 96.6 PJ (section 3.1.3). With a division of 22.5/77.5 between small and large industrial consumers and a division of 50/50 between 100 – 300 kW small service sector consumers and large service sector consumers, the consumer peak loads on the HV, MV and LV levels are 3.2, 6.5 and 9.1 GW respectively with a national peak load of 18.75 GW in 2018 (ENTSO-E, n.d.).

These numbers are calculated based on the consumer profiles described in section 3.1.3. Inaccuracies in these profiles could lead to under or overestimation of electricity consumption of either the large or small service sector/industrial consumer classes. For instance, if the load profile of large industrial consumers is not flat, peak loads increase. Therefore, a lower consumption of large industry would then result in the same peak load. However, the large industrial electricity is at least 85 PJ, or 65% of total industrial load. This is equal to electricity consumption of the chemical, food and steel industries, which are considered heavy industrial consumers (Lieshout, 2017).

For the uncertainty regarding the large and small service sector consumers, no well substantiated assessment can be made. However, it is deemed unlikely that the consumption of the category of 100 – 300 kW is larger than the combined consumption of all large service sector consumers. A lower consumption seems more plausible, but any specific estimate cannot be granted.

A3. Input parameters

Table A.3.1: Base values and ranges of structural parameters

Parameter	Base value	Range	Further elaboration
LV grid connection capacities	0.5	0.1 – 1	Section 3.1.5
Intercategorical coincidence factor	0.825	0.7 – 0.95	Section 3.1.5
Division small/large service sector	50/50	0/100 – 50/50	Appendix A2
Division small/large industry	22.5/77.5	22.5//77.5 – 35/65	Appendix A2
Heat pump coincidence factor	0.53	0.5 – 1	Section 3.1.5
SCOP – Ground source heat pump	3.5	1 – 5	Section 3.1.3
SCOP – Air source heat pump	2.6	1 – 5	Section 3.1.3
Average residential EV charging capacity	3.7 kW	3.7 – 11 kW	Section 3.1.3
Average non-residential EV charging capacity	11 kW	11 – 22 kW	Section 3.1.3
PV direct self-consumption (LV)	Relative	0 – 1	Appendix 58A6
PV direct self-consumption (MV)	Relative	0 – 1	Appendix 58A6
PV local self-consumption (LV)	Relative	0 – 1	Appendix 58A6
Combined local self-consumption (MV)	0.5	0.2 – 0.8	Appendix 58A6
CHP direct self-consumption (MV)	0.30	0.13 – 0.30	Appendix 58A6
CHP direct self-consumption (HV)	0.76	0.76 – 0.90	Appendix 58A6
CHP generation commitment	-	0.14 – 0.59	Section 3.1.3
Reinvestment value HV cables	€12.5 billion	50 – 150%	Section 3.2.1
Reinvestment value HV/MV transformers	€7.8 billion	50 – 150%	Section 3.2.1
Reinvestment value MV cables	€10.5 billion	50 – 150%	Section 3.2.1
Reinvestment value MV/LV transformers	€3.4 billion	50 – 150%	Section 3.2.1
Reinvestment value LV cables	€15.4 billion	50 – 150%	Section 3.2.1

Table A.3.2: Scenario parameters for the reference year

Parameter	Value	Voltage level	Further elaboration
Heat pump adoption level	0%	LV	Negligible and already included
EV adoption level	0%	LV-MV	in conventional profiles
Rooftop PV (small)	3.05 GW	LV	Section 2.2.2
Rooftop PV (large)	0.92 GW	MV	Section 2.2.2
PV parks	0.44 GW	MV	Section 2.2.2
Onshore wind (small)	1.43 GW	MV	Section 2.2.2
Onshore wind (large)	1.83 GW	HV	Section 2.2.2
Offshore wind	0.96 GW	HV	Section 2.2.2
CHP agriculture	3.46 GW	MV	Section 2.2.2
CHP large industry	3.03 GW	HV	Section 2.2.2
Reserve capacity HV	67%	HV	Section 3.2.2
Reserve capacity HV/MV	25%	HV/MV	Section 3.2.2
Reserve capacity MV	25%	MV	Section 3.2.2
Reserve capacity MV/LV	67%	MV/LV	Section 3.2.2
Reserve capacity LV	17.5%	LV	Section 3.2.2

Table A.3.3: Scenario parameters for the climate agreement 2030 scenario (*Klimaatakkoord*, 2019)

Parameter	Value	Voltage level
Ground source heat pump adoption level	5%	LV
Air source heat pump adoption level	5%	LV
EV adoption level	18%	LV – MV
EV charging scenario	Everywhere	LV – MV
Rooftop PV (small)	8.20 GW	LV
Rooftop PV (large)	14.34 GW	MV
PV parks	6.15 GW	MV
Onshore wind (small)	3.43 GW	MV
Onshore wind (large)	1.83 GW	HV
Offshore wind	10.56 GW	HV
CHP agriculture	3.46 GW	MV
CHP large industry	3.03 GW	HV
Reserve capacity	Reference	HV – MV – LV

Substantiation for scenario parameters for the climate agreement 2030 scenario

- 1.5 million houses made more sustainable by 2030 (*Klimaatakkoord*, 2019). This is roughly 20% of building stock, half of these buildings are assumed to adopt heat pumps (50/50 ground vs air source).
- Climate agreement expects 1.5 million EVs in 2030, which is 18% of 8.37 million cars in 2018 (CBS, 2020b; Nijland et al., 2019)
- 7 TWh small rooftop PV in 2030. Using 854 load hours → 8.2 GW (*Klimaatakkoord*, 2019)
- 35 TWh large VRE generation on land in 2030 (*Klimaatakkoord*, 2019). Assumed division wind/PV of 50/50 results in 5.3 GW onshore wind and 20.5 large PV based on 854 load hours for PV and 3327 load hours for onshore wind (*Klimaatakkoord*, 2019)
- Large PV division between roof and park of 70/30 based on current project pipeline (RVO, 2020a)
- Large onshore wind parks are assumed to remain the same as reference due to limited public support. Small onshore wind parks then become 3.43 GW
- Offshore wind increases by 9.6 GW from reference (Rijksoverheid, n.d.)

A4. Coincidence factors and group sizes

Coincidence factors

$$c_{\infty} = \frac{P_{av,1}}{P_{max,1}} \qquad \text{A4.1}$$

Equation A4.1 requires $P_{av,1}$ and $P_{max,1}$ in order to determine the coincidence factor for each consumer type. $P_{av,1}$ is the maximum load of one consumer based on the average load profile. For calculating the $P_{av,1}$, the peak load of each load profile must be divided by the number of consumers for each consumer type. For the consumers with load profiles based data from NEDU (2019), the number of consumers per profile type is available and therefore, $P_{av,1}$ can easily be determined. For the 100 – 300 kW type, the number of consumers has been estimated based on data from grid operator Liander (W. van Westering, Alliander, personal communication, February 5, 2020). For EVs, the number of consumers is set to the number of EVs in the Netherlands (CBS, 2020b) multiplied by the adoption level.

$P_{max,1}$ is the peak load of one consumer. For the NEDU profiles, this is assumed to be equal to the grid connection capacity of each profile type. However, only ranges of grid connection capacities are provided in Table 3.1. The average grid connection capacity of each profile type must lie somewhere within these ranges and is described using a factor between 0 and 1. A value of 0 refers to the lower capacity boundary and 1 the upper capacity boundary. A factor lower than approximately 0.1 seems not to be realistic. In Table A4.1, a value of 0.5 is used for estimating the $P_{max,1}$ per profile type. For EVs the $P_{max,1}$ is equal to the charger capacity of residential chargers (3.7 - 11 kW). Table A4.1 provides an overview of all these inputs and the resulting coincidence factors. For heat pumps, a coincidence factor of 0.53 is adopted directly from a research report about residential heating (van Melle et al., 2015).

Group sizes

To estimate the average size of consumer groups (n_{group}) connected to the same grid asset (cable or transformer), three factors must be taken into account: the number of consumers per type, the number of assets and the distribution of consumer types among these assets. The relation between n_{group} and these factors is expressed in equation A4.2, wherein a distribution factor of 1 signifies a homogeneous distribution of consumers among assets.

$$n_{group} = \frac{number\ of\ consumers}{number\ of\ assets} \cdot distribution\ factor \qquad \text{A4.2}$$

The number of consumer per NEDU profile is shown in Table A4.1. Even though the NEDU profile categories (E1, E2 and E3) each consist of different subcategories (e.g. E1A, E1B & E1C), they are part of the same consumer classes (E1 mainly households, E2 and E3 mainly small service sector). Therefore, the stochastic behavior of consumer loads between different profile subcategories will have similar noncoincidence characteristics. Consequently, the number of consumers are summed per profile category (E1, E2 and E3) instead of per profile subcategory. For heat pumps and EV charging points, the maximum group size is equal to the group sizes of household categories (E1) as they share the same grid connection. Furthermore, the group sizes are linearly dependent on the adoption levels.

The local distribution grid of Liander consists of roughly 140 thousand LV distribution cables connected to 35 thousand distribution transformers (W. van Westering, Alliander, personal communication, February 5, 2020). These numbers are extrapolated to national levels using the ratio between the number of LV consumers in the Liander network and the total number of LV consumers nationwide (Netbeheer Nederland, n.d.). This results in approximately 387 thousand LV distribution cables connected to 97 thousand distribution transformers.

The E1 consumers are mainly households and are assumed to be distributed homogeneously among the LV cables and distribution transformers (distribution factor of 1). For the larger consumers (E2 and E3), a homogeneous distribution is not realistic as these consumers are often clustered (e.g. shopping malls or business parks). To account for this, the assumption is made that the concentration of E2 and E3 consumers is five times higher than if the distribution was homogeneous[8] (distribution factor of 5). The number of consumers per consumer type and the group sizes per LV cable and distribution transformer are listed in Table A4.1.

Table A4.1: Overview of coincidence factors (c_∞), average group sizes (n_{group}) and relevant input parameters.

Consumer type	Grid connection	$P_{max,1}$ [kW]	Number of consumers (*1000)	$P_{av,total}$ [GW]	$P_{av,1}$ [kW]	c_∞	n_{group} Cable	n_{group} Distribution transformer
E1A	<17.3 k	8.6	1496	1.07	0.7	0.08	21	82
E1B	<17.3 kW	8.6	4879	3.23	0.7	0.08	21	82
E1C	<17.3 kW	8.6	1608	1.25	0.8	0.09	21	82
E2A	17.3 – 55.2 kW	35.7	42	0.23	5.4	0.15	4.7	19
E2B	17.3 – 55.2 kW	35.7	323	1.48	4.6	0.13	4.7	19
E3A	55.2 – 100 kW	77.6	14	0.25	17.7	0.23	1	3
E3B	55.2 – 100 kW	77.6	6	0.13	22.0	0.28	1	3
E3C	55.2 – 100 kW	77.6	2	0.07	35.4	0.46	1	3
E3D	55.2 – 100 kW	77.6	0.2	0.01	28.5	0.37	1	3
100 – 300 kW	100 – 300 kW	200	36.6	2.11	57.6	0.29	1	3
EV ‘residential’	3.7 – 11 kW	3.7 – 11	0 – 8373	0 – 7.43	0 – 0.89	0.13 – 0.2	1 – 21	1 – 82
EV ‘everywhere’	3.7 – 11 kW	3.7 - 11	0 – 8373	0 – 5.13	0 – 0.61	0.8 – 0.17	1 – 21	1 – 82
Heat pump	-	-	-	-	-	0.53**	1 – 21	1 – 82

*(W. van Westering, Alliander, personal communication, February 5, 2020)
**(van Melle et al., 2015)

A5. Classes

Industry

Heavy industrial consumers with grid connections larger than 100 MVA are connected to the transmission grid and thus to the HV level in the grid simulation model. Lighter industrial consumers are connected to substations of the regional distribution network and thus to the MV level in the grid simulation model.

Service sector

Service sector consumers larger than 300 kVA are either laced into a MV cable or directly connected to a substation of the regional distribution network and are thus connected to the MV level in the grid simulation model. Smaller consumers are either connected to an LV cable or directly connected to a distribution transformer of the local distribution network and are therefore connected to the LV level in the grid simulation model.

Agriculture

Large agricultural consumers are often greenhouses requiring grid connections up to tens of MVAs (Alfen, n.d.) connected to a substation of the regional distribution network. Most smaller agricultural consumers must be connected to a MV cable of the regional distribution network regardless of their power demand, as the local distribution network only covers urban areas (Liander, n.d.). Therefore, all agricultural consumers are connected to the MV level in the grid simulation model.

[8] The number five is chosen as higher degree of clustering leads to the connected capacity of some consumer types to exceed the standard distribution transformer capacity of 400 kVA.

Households

The large majority of household grid connections range between 1 x 25A and 3 x 25A and are therefore connected to an LV cable of the local distribution network and thus connected to the LV level in the grid simulation model (Liander, 2018).

Heat pumps

In this study, only residential heat pumps are considered. Even though residential heat pumps share the same grid connection as households, they are assigned to a separate class as their power demand is simulated using a different demand profile (section 3.1.3). Like households, heat pumps are also connected to the LV level in the grid simulation model.

Transport

The transport category consists of rail traffic and road traffic. Grid connections for rail traffic are laced into the MV cable of the regional distribution network and thus connected to the MV level in the grid simulation model (Liander, n.d.). For simplicity, rail traffic is added to the (large) service sector class.

Power consumption by road traffic includes power consumption of EVs. In this study, only passenger cars are considered when referring to EVs. Furthermore, the location of charging points is divided into two categories: residential and non-residential. Fast chargers are not included in the grid simulation model in order to limit model complexity. Residential charging points include household EV chargers and public chargers at neighborhood parking spots. These chargers are connected to the LV level in the grid simulation model. Non-residential points are assumed to be located at facilities in the service sector (e.g. offices and shopping centers) connected to the MV level of the grid simulation model.

Conventional power plants

Large conventional power plants (>500 MVA) are connected to the interconnection network, while smaller power plants (<500 MVA) are connected to the transmission network (van Oirsouw, 2012). Therefore, all conventional power plants are connected to the HV level in the grid simulation model.

Combined heat and power (CHP)

CHP generators are used by power consumers and therefore share their grid connections. However, CHP is assigned to separate classes as CHP power generation is simulated using distinct generation profiles (section 3.1.3). The effect of direct self-consumption (without using the power grid) is taken into account in section 3.1.5.

All Dutch CHP capacity is listed in Table 2.2. Industrial consumers using CHP generation include refineries and mining, chemical industry, food and stimulants industry and paper industry. These consumers can be considered as heavy industrial consumers and therefore all industrial CHP capacity is assumed to be connected to the HV level in the grid simulation model. The remaining CHP capacity is used by agricultural and healthcare consumers. Alike agricultural consumers, agricultural CHP capacity is also connected to the MV level of the power grid. Healthcare consumers using CHP generation are often hospitals which are rather large consumers connected to the regional distribution network. Therefore, healthcare CHP generation capacity is also assumed to be connected to the MV level in the grid simulation model.

Wind turbines

Wind turbine generation capacity is divided into two categories: offshore and onshore. Most offshore wind parks are larger than 500 MW and are connected to the interconnection network using marine EHV cables (Rijksoverheid, n.d.). Thus, they are connected to the HV level in the grid simulation model. The large majority of onshore wind parks are larger than 3 MW and some wind parks are larger than 100 MW (Energiekaart, n.d.; RVO, 2020a). Onshore wind parks larger than 100 MW are connected to the transmission network and are thus connected to the HV level in the grid simulation model. Wind parks up to 100 MW are connected substation of the regional distribution network and thus connected to the MV level in the grid simulation model.

Photovoltaics (PV)

PV generation capacity can divided into three categories: residential rooftop PV, service sector rooftop PV and ground bound PV parks (CBS, 2019b). Residential rooftop PV shares its grid connection with households and is

therefore also connected to the LV level in the grid simulation model. Service sector rooftop PV shares its grid connection with buildings from the service sector and its therefore also distributed amongst the LV and MV levels in the grid simulation model. Rooftop PV (connected to LV and MV) are assigned to distinct classes as PV power generation is simulated using distinct generation profiles (section 3.1.3). The effect of direct self-consumption (without using the power grid) is taken into account in section 3.1.5. Ground bound PV parks are often larger than 3 MW and smaller than 100 MW and are therefore connected to a substation of the regional distribution network and thus connected to the MV level in the grid simulation model (RVO, 2020a).

Import/export

Cross-border power import and export flows through EHV cables of the interconnection network and is therefore assigned to the HV level in the grid simulation model (van Oirsouw, 2012).

A6. Self-consumption

The amount of self-consumption depends on the ratio of power generation and demand (Luthander et al., 2015). If the generation is larger than demand, the self-consumption must be equal to the demand. If demand is larger than generation, self-consumption must be equal to generation. However, in the grid simulation model generation and demand is only assessed for consumer classes. One cannot assume that all decentralized generation capacity is evenly spread among consumers or regions and therefore, only a limited fraction of total consumer load can use locally generated power. This connection between self-consumption, consumption, generation and the spread of generation is summarized in equation A6.1.

$$p_{sc} = \begin{cases} p_{load} \cdot d & if \quad p_{load} \cdot d < p_{gen} \\ p_{gen} & if \quad p_{gen} < p_{load} \cdot d \end{cases} \qquad \text{A6.1}$$

In equation A6.1, p_{sc} is the amount of self-consumption, p_{load} the total consumer load, p_{gen} the total decentralized power generation and d the distribution coefficient. If $p_{load} = p_{gen}$ and the distribution coefficient is 1, all decentralized power generation is directly/locally consumed and therefore, distributed generation capacity must be perfectly distributed among consumers. When the distribution coefficient approaches 0, distribution generation capacity must be concentrated in a single point in the power grid and therefore very little decentralized power generation is locally consumed.

For direct self-consumption, power is generated and consumed at a single consumer without using the power grid. The distribution coefficient describes the distribution of generation capacity among individual consumers. For local self-consumption, power is generated and consumer within one distribution network without using parent voltage levels. The distribution coefficient describes the distribution of generation capacity among distribution networks.

6.1.1 Direct self-consumption

For rooftop PV, an increase in capacity will likely be the result of additional consumers installing rooftop PV systems. Following this line of reasoning, the distribution coefficient should be 1 if the annual rooftop PV generation equals the annual consumption of households and small service sector of 168 PJ (appendix A1 and A2). Assuming an annual yield of 1 kWh per Watt of installed PV capacity, this will be at an installed capacity of 4`4 GW. At this rooftop PV capacity, all PV generation can be self-consumed at moments that rooftop PV generation equals the consumer load. If only half of that capacity is installed, only half of the PV generation can be self-consumed and so forth.

For rooftop PV installed at agricultural, large service sector and small industrial consumers (MV), there are less financial incentives to limit the rooftop PV capacity such that annual generation does not exceed the annual consumption. As a result, the distribution coefficient does not have to be 1 if annual rooftop PV generation equals the total annual consumption of 121 PJ (appendix A1 and A2). However, some correlation between PV capacity and distribution factor is still to be expected. The assumption is made that the distribution coefficient is 1 when PV generation is double the annual consumption. Assuming an annual yield of 1 kWh per Watt of installed PV capacity the distribution coefficient will be 1 at an installed capacity of 67 GW.

CHP capacity installed at agricultural consumers (MV) is assumed to be evenly distributed across greenhouses and therefore, the distribution coefficient is close to 1. However, the agricultural load is not known as it is included in the

aggregated residual load profile. Agricultural consumption (35.7 PJ) makes up only 30% of the consumption of the residual load profile (119 PJ) (appendix A1 and A2). If agricultural load is assumed to be linearly correlated on the residual load, the distribution coefficient is adjusted to 0.30. CHP capacity installed at large industrial consumers (HV), mainly resides at the chemical-, food- and paper industries (Table 2.2). Their combined annual electricity consumption is equal to 75.7 PJ (appendix A1), which is 76% of the total heavy industrial consumption (appendix A2). Consequently, a distribution coefficient of 0.76 is assumed.

Note that the amount of direct self-consumption depends on the divisions between large and small service sector/industrial consumers (appendix A2) and is thus changes when these divisions would be altered.

6.1.2 Local self-consumption

Local self-consumption occurs when in a local or regional distribution network, decentralized power generation is consumed in the same area, without needing to be transported via parent voltage levels (rooftop PV, PV parks, CHP and onshore wind). The amount of local self-consumption relative to both the total generation and demand on a voltage level, is determined primarily by the spatial distribution of decentralized generation capacity. If decentralized generation is evenly spread among distribution networks, a higher degree of local self-consumption can be expected than if it were concentrated.

For rooftop PV in local distribution networks (LV), using a similar reasoning as for direct self-consumption, the distribution coefficient is likely to increase as the installed capacity of rooftop PV increases. However, the amount of self-consumption must be higher as the distribution among of small rooftop PV among local distribution networks must be more even than among individuals. Therefore, a distribution coefficient of twice the of the self-consumption is assumed.

For CHP generation, PV parks, rooftop PV and onshore wind turbines connected to the regional distribution networks (MV), one distribution coefficient is used to limit the complexity of the grid simulation model. The distribution coefficient describes the distribution of generation among local or regional distribution networks. Figure 2.12 and Figure 2.15 show that the distribution of generation capacity of onshore wind and larger PV parks is slightly more concentrated in the north of the Netherlands. However, population density is higher in the western coastal regions of the Netherlands (Figure A6.1). Greenhouse horticulture, and therefore CHP generation, is also concentrated in this area (Figure 2.11). Based on these images, it is deemed unlikely that the distribution coefficient is close to 0 or 1. Because it is difficult to get a more accurate sense of the actual distribution coefficient, a range between 0.2 – 0.8

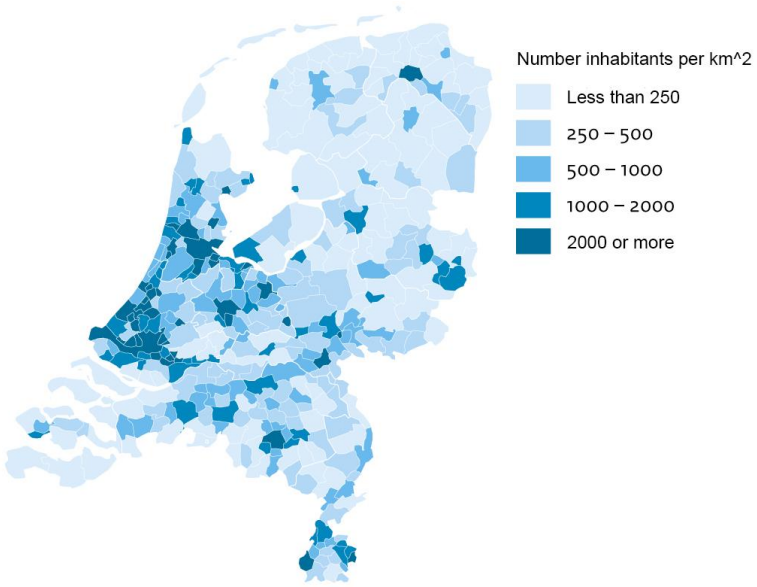

Figure A6.1: Population density per municipality in the Netherlands (CBS, 2016)